Buffer gas collisions effect on electromagnetically induced transparency (EIT) in three level & four level systems

A thesis submitted in partial fulfillment for the award of the Degree of

DOCTOR OF PHILOSOPHY

In

Physics

by

Munipalli Anil Kumar

School of Physics

University of Hyderabad

Hyderabad 500046, India

June 2012

DECLARATION

I here by declare that the work reported in this thesis entitled **"Buffer gas collisions effect on electromagnetically induced transparency (EIT) in three level and four level systems"** has been carried out by me independently in the School of Physics, University of Hyderabad, under the supervision of Dr. Suneel Singh. I also declare that this is my own work and effort, and it has not been submitted at any other University or institution for any degree.

Date: (M. Anil Kumar)

Place

CERTIFICATE

This is certified that the work contained in this thesis entitled "**Buffer gas collisions effect on electromagnetically induced transparency (EIT) in three level and four level systems"** has been carried out by Mr. MUNIPALLI ANIL KUMAR (Reg.No.06PHPH01), under my direct supervision and the same has not been submitted for the award of research degree of any university.

Dr. Suneel Singh

Place: Hyderabad — Thesis Supervisor

Date: — School of Physics

University of Hyderabad

Dean

School of Physics

University of Hyderabad

To My guide

ACKNOWLEDGMENTS

There are many people who influenced, guided, taught, and helped me. Iam thankful to every one of them

First of all, I would like to thank my advisor, Dr. Suneel Singh for his support, advice, and especially for being the perfect role model of a good human being. I am grateful to Dr. Anathalakshmi for teaching Quantum Optics. I want to thank Mr. Sanjeev Kumar and G. Srinivas for their help in computational technique. A Special thanks to wax lab friends (Sudhanirmala and N. shankariah), Optics group friends (K.L.N Deepak, S.K. Ali, M.B.M.Krishna etc) and 2006 batchmates (B. Yugander, Parthasarathi, G.Devaraju, Arun, Vasu etc) last but not least I thank V.Saikiran, P.Satyanarayana, I.Gopalkrishna and Azeem Baig Mirza. Also I want to acknowledge the financial support of University of Hyderabad, U.G.C and C.S.I.R. Finally, I would like to thank all my friends and family, Special thanks to my wife Usha Kiran and my Well wishers (Krishna murthi garu and Venkateshwarao garu) for their support.

Abstract

Electromagnetically induced transparency [EIT] is a phenomenon in which an initially absorbing medium is rendered transparent to a resonant probe (weak) laser when a pump (strong) laser is applied at an adjacent transition. The aim of this dissertation is to develop general theoretical models to study and understand the influence of various broadening and narrowing mechanisms on the phenomenon of EIT and other related processes. These include, i) Doppler broadening arising due thermal motion of atoms (with velocity components v_z) along z (axial) direction as well as in transverse (with velocity components v_x and v_y) directions. ii) velocity changing and dephasing collisions effects a buffer gas in Doppler broadened medium. In chapter 2 we study buffer gas collisions effect on residual broadening (arising due to pump-probe wave vector mismatch along v_z direction) in a ladder (Ξ) system. In chapter 4 we investigate the feasibility of observing EIT phenomena in an inhomogeneous (Doppler) as against a homogeneously broadened media. In Chapter 3 and Chapter 5 deals with a study of transit time (or time of flight) broadening (arising due to thermal motion of atoms across the finite size of the probe beam) and buffer gas collisions effects on the phenomena of EIT, slow light and four wave mixing process in three level lambda (Λ) and four level double lambda systems. Comparison with experiments show that these theoretical models are in good agreement with experiments performed in hot vapor cells containing buffer gas.

TABLE OF CONTENTS

CHAPTER

Chapter 1

1. *Introduction*

1.1 *Review of the study on electromagnetically induced transparency (EIT):*

Electromagnetically Induced Transparency (EIT) [1] describes transparency (nonabsorption) of a weak optical (probe) field at a resonant transition in three level medium due to interference effect induced by a relatively strong (control) field applied at an adjacent transition. The foundations of EIT were laid by Kocharovskaya and Khanin [2] in 1988 and independently by S. Harris in 1991 [3]. Since then numerous experimental and theoretical publications devoted to the study of EIT have appeared and there is considerable activity in this field in recent times.

A physical mechanism underlying the EIT phenomenon is the destructive atomic interference between alternate laser-induced atomic transition amplitudes (or atomic coherences) for a given transition process. The condition behind the EIT is a two-photon (or Raman) resonance. Some other physical explanations for EIT are (i) coherent population trap (CPT) analogy [4] (ii) Dressed state analysis (The CPT analogy and the dressed state explanation for EIT can be related to each other [5] (iii) Multiple routes to excitation, (iv) other alternatives for explaining the EIT process have been proposed such as the use of Feynman diagrams to represent the interfering processes [6], use of a 3D vector model[7] or methods involving stochastic wave function diagrams[8].

Several interaction schemes of atomic levels and laser fields are suggested and experimentally demonstrated the EIT effect, such as a Λ- scheme [3,9] where two lower levels are coupled by two fields with a single upper level, a V- scheme [10], where one ground level is coupled with two higher levels, a ladder Ξ or cascade scheme [11], in which the upper level is coupled with the ground level through an intermediate one, and many others utilizing more than two fields coupling higher numbers of levels. Above proposed three level schemes can be realized in gases or vapors [3, 12], semiconductors [13] and in solid media. [14]

The possibility of controlling the transparency of a medium has a useful application in lasing without inversion [15] and the dispersion property of probe field is also equally interesting

as the steepness of the dispersion function [16] near resonance plays the key role for reduction of group velocity of light pulse (slow light) in the medium and is directly related to the line width of the EIT resonance [17]. EIT can be used as an enhancing non linear optical process including non linear frequency conversion [18]. In addition, EIT can be used in squeezed-light generation [19] and low-light-level photon switching [20]. A very narrow EIT resonances, which is an order of Hz is observed in cell with buffer gas atoms [21] and antirelaxation coating cells [22]. These narrow EIT resonances are used in sensitive magnetometer [23], precision spectroscopy [24] and frequency standards [25]. It is impossible to mention all of the hundreds of papers devoted to the study regarding the EIT and its possible applications. More information about EIT can be found in the review articles on EIT [26, 27] and references therein.

1.2 *Motivation:*

Narrow EIT resonances are being used as the basis for making very sensitive measurements, like sensitive magnetometers [23], precession spectroscopy [24], frequency standards [25], and also in metrology field. Hence the study and identification of various mechanisms that lead to broadening of EIT resonance has attracted considerable attention in recent years. Many broadening mechanisms contribute to the width of the EIT resonance such as, i) time of flight broadening (atoms with a non-zero velocity perpendicular to the direction of propagation of the pump and probe beams will traverse the pump and probe beams in a finite time). ii) Residual Doppler broadening owing to either wave vector mismatch of pump-probe and iii) finite angular separation between the pump-probe beams and power broadening by coupling field intensity [28] etc.. However, no or minimal residual Doppler broadening is observed in EIT experiments performed with the addition of a buffer gas in vapor cells [21, 29]. The measured EIT (or CPT) resonance line widths in these experiments are found to be much narrower, about two orders of magnitude lower than the expected residual Doppler widths. Experimentally very low group velocities and large group delays, via EIT in vapor cells containing buffer gas have also been observed [30]. The existing theoretical treatments of EIT and slow light however do not properly account for various broadening mechanisms mentioned above. It would be of interest and importance to develop a more general treatment of EIT and ultraslow light propagation and related nonlinear optical phenomena including various broadening mechanisms and effects of buffer gas.

Our aim here is to develop a general theory of electromagnetically induced transparency (EIT) and examine various associated phenomena such as slow group velocity, nonlinear generation etc. in inhomogeneously broadened multilevel systems of various types. Different schemes such as ladder system (Ξ), V-system (V), and lambda system (Λ) will be considered for the study of the EIT and other associated phenomena. In gaseous media (such as atomic vapors) comprising the abovementioned multilevel systems, Doppler broadening of various transitions - one photon, two-photon can occur. Collisional effects of a buffer gas (with vapor atoms) such as velocity changing collisions, dephasing collisions and collisional shift of the ground state and optical resonances will also be taken into account. It is expected that velocity changing collisions would cause significant narrowing of EIT line widths which could lead to many interesting and significant effects such as complete transparency and ultraslow light generation at relatively low coupling field intensities and vapor densities. Simultaneously, a four wave mixing (FWM) scheme in a double lambda system using EIT technique will also be studied.

1.3 *EIT*: *Broadening effect*

The term broadening is used to denote the finite spectral width of the resonance of atomic system to electromagnetic fields. Broadening can be classified as two categories 1) homogeneous broadening and 2) inhomogeneous broadening. The cause of homogeneous broadening in EIT is due to spontaneous transitions or nonradiative transitions, broadening due to the interaction with an electromagnetic field (power broadening), phase perturbing (elastic) collisions, laser line *widths etc.* Physically this would correspond to experiments carried out in either a ‘cold’ atomic sample (Bose Einstein condensate, optical trap) or in an atomic beam. An Inhomogeneous broadening occurring in EIT resonance is due to Doppler shift of atomic resonance (Doppler broadening) caused by thermal motion of atoms in a gas medium or impurity ions in a host crystal. For example, if an experiment is carried out in a gas cell, we must also include the effects of Doppler broadening as we would expect that Doppler broadened line shape is much broader than that of the homogeneous line shape. Particularly Doppler broadening affects both EIT resonance and its width in lambda (Λ) and ladder (Ξ) schemes, but EIT can still be observed in these schemes however, it requires a larger coupling field Rabi frequency as compared to cold atomic ensembles.

1.4 *Formulation:*

To study EIT effect it is necessary to understand how coherent fields interact with an atomic system. We followed a semi classical approximation (where electromagnetic fields are treated classically and atom is a quantum object) through which density matrix analysis is considered. This allows us to examine the population of atomic levels and coherence established between levels. The atomic susceptibility is directly related to coherence established between the levels, and thus absorption and dispersion properties are estimated.

a) Interaction Hamilton:

The Hamiltonian in the atom-field interaction can be defined as

$$H = H_0 + V \tag{1.1}$$

Where H_0 is the unperturbed Hamiltonian and V is an interaction term comprised of the electric dipole interactions induced within the atom due to the applied electric field. Thus we can write H as

$$H = H_0 - \vec{\mu}_{ij} \cdot \vec{E} \tag{1.2}$$

Where $\vec{E}$ is the electric field

$$\vec{E} = \sum_a \vec{\varepsilon}_a \exp\left[i\left(\vec{k}_a \cdot \vec{r} - \omega_a t\right)\right] \tag{1.3}$$

and $\vec{\mu}_{ij}$ is the electric dipole matrix element.

$$\vec{\mu}_{ij} = \sum_{i,j} |i\rangle\langle i|\mu\, i\rangle\langle j| \sum_{i,j} \mu_{ij} |i\rangle\langle j| \qquad (i \neq j) \tag{1.4}$$

The Hamiltonian V in the interaction representation is given by

$$V^{int} = e^{\left(\frac{i}{\hbar}\right)H_0 t}(-\vec{\mu}_{ij} \cdot \vec{E})e^{-\left(\frac{i}{\hbar}\right)H_0 t} \tag{1.5}$$

b) *Density matrix equations of motion:*

The time evolution of the density matrix of the system in the interaction representation is

$$\dot{\rho} = \left(\frac{i}{\hbar}\right)\left[\rho, V^{int}\right] \tag{1.6}$$

The equation of motion of ijth element of the density matrix is

$$\dot{\rho}_{ij} = \left(\frac{i}{\hbar}\right)\left[\langle i|\left[\rho, V^{int}\right]|j\rangle\right]$$

$$\dot{\rho}_{ij} = \left(\frac{i}{\hbar}\right)\left[\langle i|\rho V^{int}|j\rangle - \langle i|V^{int}\rho|j\rangle\right] \tag{1.7}$$

Inserting between ρ and V^{int}, and V^{int} and ρ, an orthonormal set of states $|m\rangle$ that obey the completeness property $\sum_m |m\rangle\langle m| = 1$

We get from Eq.(1.7)

$$\dot{\rho}_{ij} = \left(\frac{i}{\hbar}\right)\sum_m \left\{\rho_{im} V^{int}_{mj} - V^{int}_{im}\rho_{mj}\right\} \tag{1.8a}$$

Where $V^{int}_{mn} = \langle m|V^{int}|n\rangle$ and $\rho_{ij} = \langle i|\rho|j\rangle$ (1.8b)

A generalized equation of motion, including the relaxation process $(\rho_{ij})_{relax}$ such as spontaneous decays (γ_{ij} i,j = 1-3), radiative decay of half diagonal elements(γ_{ij} i ≠ j), line width of probe (γ_p) and pump lasers (γ_c), *etc* are incorporated in right hand side of Eq(1.8a). described is as follows

$$\dot{\rho}_{ij} = \left(\frac{i}{\hbar}\right)\sum_m \left\{\rho_{im} V^{int}_{mj} - V^{int}_{im}\rho_{mj}\right\} + (\rho_{ij})_{relax} \tag{1.9}$$

Doppler shift of atomic resonance due to thermal motion of atoms in the medium gives rise to inhomogeneous broadening. To incorporate atomic motion, the derivative $\dot{\rho}_{ij}$ on the left-hand side of Eq.(1.9) can be replaced by the following equation as

$$\dot{\rho}_{ij} \rightarrow \left\{\frac{\partial}{\partial t} + \vec{v}.\vec{\nabla}\right\}\rho_{ij} \tag{1.10}$$

The response of the atom moving with velocity v and relaxation effects with buffer gas collisions terms is illustrated by a density matrix equation can now be written as

$$\left(\frac{\partial}{\partial t} + \vec{v}\cdot\vec{\nabla}\right)\rho_{ij} = -\left(\frac{i}{\hbar}\right)\sum_m \left\{\rho_{im} V^{int}_{mj} - V^{int}_{im}\rho_{mj}\right\} + (\rho_{ij})_{relax} \tag{1.11}$$

1.5 *Buffer gas collisions effect*

In vapors cells atoms are not confined in the interaction region and they are moving in and out of the interaction region. While atoms which are moving out of the interaction region most likely collide with the cell wall, and its quantum state created during the interaction with the laser fields is destroyed. To amend the situation, and prolong the atoms-field interaction time two methods are used i) anti-relaxation wall coating inside the cell, these coatings usually consist of paraffin waxes or silanes with long carbohydrate chains and ii) Addition of buffer gas to the vapor cell, like inert (He and Ne) or diatomic (N_2) gases. Buffer gas is able to prohibit atoms from diffusing rapidly out of the interaction zone by velocity changing collisions, as a result atoms spend a much longer time inside the interaction region, so that the quantum state is still preserved. Collisions with buffer gas atoms can cause dephasing as well result in changes in the velocity of a vapor atom. The effect of such collisions can be incorporated in the density-matrix formalism by including a term [31]

$$\left(\rho_{ij}\right)_{coll} = -\gamma_{ph}\left(1-\delta_{ij}\right)\rho_{ij} - \Gamma_{ij}\rho_{ij} + \int W_{ij}(v' \to v)\rho_{ij}(v',t)d^3v' \qquad (1.12)$$

Here γ_{ph} is the rate of collision-induced dephasing of optical coherences and Γ_{ij} is some average rate of change in velocity v. For simplicity Γ_{ij} is assumed to be independent of v and related to the collisional kernel $W_{ij}(v' \to v)$ by

$$\Gamma_{ij} = \int W_{ij}(v \to v')d^3v' \qquad (1.13)$$

The collision kernel in general is assumed to be of the form

$$W_{ij}(v' \to v) = W_{ij}(v - \alpha v') \qquad (1.14)$$

Where α is a constant, $(1 > \alpha > 0)$. Physically the second term in Eq. (1.12) is the "out term" representing collisional shift of atoms with a velocity *v* to other velocity subclasses at some rate Γ_{ij} and the third term is the "in term" arising due to the collisional shift of atoms from other velocity subclasses into velocity subclass *v*. In this thesis we however restrict our discussion to the case of most prevalent and experimentally relevant strong collision model in which collisions result in rapid thermalization of the velocity distribution of the system. The collision kernel of Eq(1.14) is assumed to be independent of the initial velocity and of the form

$$\lim_{\alpha\to 0} W_{ij}(v' \to v) = \Gamma_{ij} M(v) \quad (1.15)$$

Where $M(v) = \left(\sqrt{\ln 2/(\pi \bar{v}^2)}\right)^3 \exp\left(-\ln 2 \frac{v^2}{\bar{v}^2}\right)$ is the Maxwell velocity distribution of atoms with $\bar{v} = \sqrt{\ln 2}\, v_{th}$ and $v_{th} = \sqrt{2k_B T/m_a}$ is the most probable thermal velocity at a temperature T of an atom of mass m_a and substituting Eq(1.15) in Eq (1.12) yields as

$$\left(\rho_{ij}\right)_{coll} = -\gamma_{ph}(1-\delta_{ij})\rho_{ij} - \Gamma_{ij}\rho_{ij} + \Gamma_{ij} M(v) \int \rho_{ij}(v', t) d^3 v' \quad (1.16)$$

1.6 ***Generalized density matrix equation:***

The generalized density matrix equation can be written as using Eq(1.11) and (1.16) together as

$$\left(\frac{\partial}{\partial t} + \vec{v}\cdot\vec{\nabla}\right)\rho_{ij} = -\left(\frac{i}{\hbar}\right)\sum_m \left\{\rho_{im} V_{mj}^{int} - V_{im}^{int}\rho_{mj}\right\} + (\rho_{ij})_{relax} - \gamma_{ph}(1-\delta_{ij})\rho_{ij} - \Gamma_{ij}\rho_{ij}$$
$$+\Gamma_{ij} M(v) \int \rho_{ij}(v', t) d^3 v' \quad (1.17)$$

Eq (1.17) describes dynamic equation of motion with inclusion of relaxation process & buffer gas collisions effect.

1.7 *References:*

1. K. J. Boller, A. Imamoglu, S. E. Harris, Phys. Rev. Lett. **66**, 2593-2596 (1991).

2. O. A. Kocharovskaya and Y. I. Khanin, Jetp Lett. **48**, 630-634 (1988).

3. J. E. Field, K.H. Han, and S.E. Harris Phys. Rev. Lett. **67**, 3062 (1991);
S. E. Harris, Phys. Today **50** (7) 36 (1997).

4. E. Arimondo, Progress in Optics **35**, 257-354 (1996).

5. J. P. Marangos, Journal of Modern Optics **45**, 471-503 (1998).

6. J. L. Cohen and P. R. Berman, Phys. Rev. A **55**, 3900-3917 (1997).

7. A. Kasapi, J. Opt.Soc. Am. B-Opt. Phys. **13**, 1347-1351 (1996).

8. J. A. Vaccaro, A. V. Durrant, D. Richards, S. A. Hopkins, H. X. Chen and K. E. Hill, J. Mod. Opt. **45**, 315-333 (1998).

9. Y. Q. Li and Min. Xiao Phys. Rev. A **51**, R2703-R2706(1995); S.A. Hopkins, E. Usadi, H. X Chen A. V Durrant, Opt. Commun. **138**, 185-192(1997);
A. Javan, O. Kocharovskaya, H. Lee and M.O. Sully Phys. Rev. A **66**, 013805(1997).

10. J. R. Boon, E. Zekou, D. J. Fulton and M. H. Dunn, Phys. Rev. A **57**, 1323-1328 (1998): G. R. Welch, G. G. Padmabandu, E. S. Fry, M. D. Lukin, D. E. Nikonov, F. Sander, M. O. Scully, A. Weis and F. K. Tittel, Foundations of Physics **28**, 621-638 (1998).

11. M. Xiao, Yong-quing Li, Shao-zheng Jin, and J. Gea-Banacloche, Phys. Rev. Lett. **74**, 666 (1995): Y. Q. Li, S. Z. Jin, and M. Xiao, Phys. Rev. A **51**, R1754 (1995).

12. D. J. Fulton, S. Shepherd, R. R. Moseley, B. D. Sinclair and M. H. Dunn, Phys. Rev. A **52**, 2302-2311 (1995).

13. H. Schmidt, K. L. Campman, A. C. Gossard and A. Imamoglu, Appl. Phys. Lett. **70**, 3455-3457 (1997): H. Schmidt and A. Imamoglu, Opt. Commun **131**, 333-338 (1996): H. Schmidt and R. J. Ram, Appl. Phys. Lett. 76, 3173-3175 (2000).

14. B.E. Ham, M.S. Shahriar, P.R. Hemmer, Opt. Lett. **22**, 1138 (1997): Yang Zhao, Cunkai Wu, Byoung-Seung Ham, M. K. Kim, and Eddie Awad, Phys. Rev. Lett. **79**, 641 (1997).

15. M. O. Scully, S. Y. Zhu, and A. Gavrielides, Phys. Rev. Lett. **62**, 2813 (1989): O. Kocharovskaya, Phys. Rep.-Rev. Sec. Phys. Lett. **219**, 175 (1992): O. A. Kocharovskaya and Y. I. Khanin, Jetp Lett. **48**, 630 (1988): E. S. Fry, X. F. Li, D. Nikonov, G. G. Padmabandu, M. O. Scully, A. V. Smith, F. K. Tittel, C. Wang, S. R. Wilkinson, and S. Y. Zhu, Phys. Rev. Lett. **70**, 3235 (1993).

16. L. V. Hau, S. E. Harris, Z. Dutton, and C. H. Behroozi, Nature (London) **397**, 594 (1999): D. Budker, D. F. Kimball, S. M. Rochester, and V. V. Yashchuk, Phys. Rev. Lett. **83**, 1767 (1999): C. Liu, Z. Dutton, C. H. Behroozi, and L. V. Hau, Nature (London) **409**, 490 (2001).

17. S. E. Harris, J. E. Field, and A. Kasapi, Phys. Rev. A **46**, R29 (1992): O. Schmidt, R. Wynands, Z. Hussein, and D. Meschede, Phys. Rev. A **53**, R27 (1996).

18. K. Hakuta, L. Marmet and B. P. Stoicheff, Phys. Rev. Lett. **66**, 596-599 (1991): R. R. Moseley, S. Shepherd, D. J. Fulton, B. D. Sinclair and M. H. Dunn, Phys. Rev. A **50**, 4339-4349 (1994): M. Jain. H. Xia, G.Y. Yin, A. J Merriam, S.E. Harris Phys. Rev. Lett.**77**, 4326 (1996).

19. M.D Lukin, A.B. Matsko, M. Fleischhauer, M.O Sully Phys. Rev. lett. **82**, 1847 (1999).

20. S.E. Harris, Y. Yamomoto Phys. Rev. lett. **81**, 3611(1998): A. Imamoglu, H. Schmidt, G. Woods, M. Deutsch, Phys. Rev. lett. **79**, 1467 (1997).

21. S. Brandt, A. Nagel, R. Wynands, and D. Meschede, Phys. Rev. A **56**, R1063(1997): M. Erhard and H. Helm, Phys. Rev. A **63**, 043813 (2001).

22. D. Budker, V. Yashchuk, and M. Zolotorev, Phys. Rev. Lett. **81**, 5788 (1998).

23. I. Novikova, A. B. Matsko, and G. R. Welch, Opt. Lett. **26**, 1016 (2001): V. A. Sautenkov, M. D. Lukin, C. J. Bednar, I. Novikova, E. Mikhailov, M. Fleischhauer, V. I. Velichansky,

G. R. Welch, and M. O. Scully, Phys. Rev. A **62**, 023810 (2000).

24. R. Wynands and A. Nagel, Appl. Phys. B **68**, 1 (1998).
25. S. Knappe, R. Wynands, J. Kitching, H. G. Robinson, and L. Hollberg, J. Opt. Soc. Am. B **18**, 1545 (2001).
26. S.E Harris, G.Y. Jain, M. Jain, H. Xia, A.J Merriam, Phil. Trans. R. Soc. London. A **335**, 2291 (1997).
27. M.D Lukin, P. Hemmer, M.O.Scully Adv. At. Mol. Opt. Phys. **42**,347(2000);

A. Joshi, M. Xiao, in E. Wolf, (Ed), progress in Optics, **49** (2006) Elsevier.

28. C. Y. Ye and A. S. Zibrov, Phys. Rev. A **65**, 023806 (2002));

P. R. S. Carvalho, L. E. E. de Araujo, and J. W. R. Tabosa, Phys. Rev. A **70**, 063818 (2004) ;

E. Figueroa, F. Vewinger, J. Appel, and A. I. Lvovsky, Opt. Lett. **31**, 2625 (2006).

29. A. M. Akulshin, A. A. Celikov, and V. L. Velichansky, Opt. Commun. **84**, 139 (1991).
30. M. M. Kash, V. A. Sautenkov, A. S. Zibrov, L. Hollberg, G. R. Welch, M. D. Lukin, Y. Rostovtsev, E. S. Fry, and M. O. Scully, Phys. Rev. Lett. **82**, 5229 (1999).
31. P. R. Berman, J. Opt. Soc. Am. B **3**, 564 (1986).

Chapter 2

In this chapter we will study the phenomena of EIT and slow light in a three level ladder or cascade (Ξ) system. Early studies of EIT considered radiative (homogeneous or cold atomic ensembles) broadening in three level systems. The phenomenon of EIT in a ladder system including Doppler broadening (inhomogeous or hot atomic vapor) was investigated by J Gea-Banacloche [1]. *It is interesting to study by including two photon (residual)Doppler broadening [despite , taking care of proper propagation geometry of pump and probe, the two photon (residual) Doppler broadening is still observed in atomic vapor experiments] and buffer gas collisions effect on EIT and slow light phenomena at lower intensities and vapor densities.*

2.1 *Introduction*

As mentioned earlier EIT is a phenomenon wherein a resonant probe laser is transmitted with highly reduced absorption through a medium coupled by another coherent pump (control) laser. EIT in a Doppler broadened three level ladder or cascade (Ξ) system has been studied by many authors [1-10] and is shown in Figure 2.1(i). In atomic vapors, particularly at low densities, the availability of large mean-free path for thermal motion of atoms can lead to a substantial Doppler broadening of one- and two-photon transitions. The two-photon Doppler broadening can be reduced to a large extent with the use of counter propagating pump and probe geometry as shown in Figure 2.1(ii).

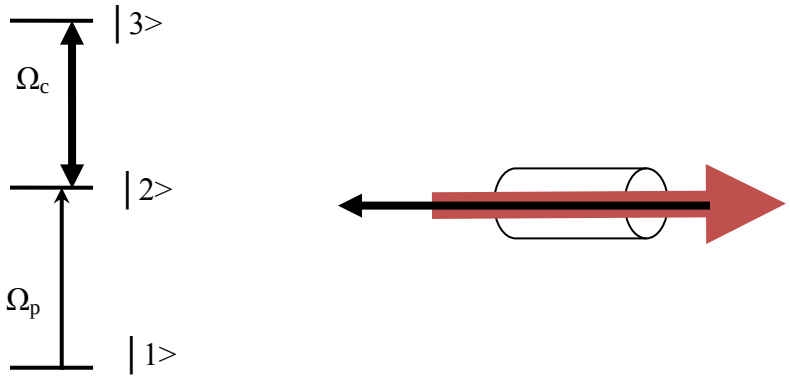

Fig.2.1 *(i) A three level ladder system with Rabi frequencies of probe (Ω_p) and pump (Ω_c)is shown. (ii) Probe (black arrow) and pump (red arrow) counter propagating to each other, to reduce two-photon Doppler broadening effect.*

But as the resonance frequencies of the upper and lower one-photon transitions differ considerably in real atomic systems, there may still remain significant amount of residual broadening on account of the wave-vector mismatch between the coupler and probe beams. Gea-Banacloche *et al.* [1], Shepherd *et al.* [4], and Boon *et al.*[6] theoretically and experimentally studied the role of two-photon residual broadening in EIT in ladder-type inhomogeneously broadened media and identified ways to optimize the absorption reduction effect for various regimes of coupler and probe wavelength (or wave-vector) mismatch. It was found that the nature of EIT in a three-level ladder system depends critically on the sign of the two photon residual Doppler width $\delta k = (k_p - k_c)$ which, depending on the probe and pump (control) field wave-vector mismatch, is either positive ($k_p > k_c$) or negative ($k_p < k_c$) and is markedly dissimilar in these two cases both are shown in Fig 2.2 and the situation can be realized in sodium atom.

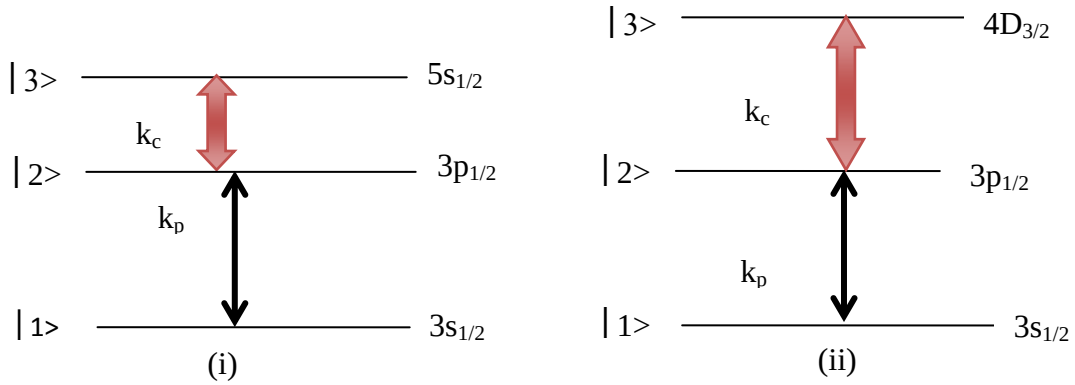

Fig.2.2 : *Two different three level ladder systems of pump and probe laser fields with wave vectors as k_p and k_c. i) Shows positive case of wave vector mismatch (kp > kc) ii) is negative case of wave vector mismatch ($k_p < k_c$).*

Although residual (two photon) Doppler broadening effect can be significant in experiments on EIT in atomic vapors, its influence on slow light in ladder-type systems has been studied theoretically. In addition it would also be of interest to investigate the effect of collisions on the phenomenon of EIT in ladder systems as in many EIT (or coherent population trapping) experiments done in a vapor cell containing an additional (buffer) gas, residual line broadening is not observed [11].

We present a general theory of electromagnetically induced transparency (EIT) in an inhomogeneously broadened ladder-system in which Doppler broadening of both one and two-

photon transitions occurs. The theory is more general in the sense that it takes into account the residual Doppler broadening of the two-photon coherence in different wavevector mismatch regimes and also the collisional effects of an additional (buffer) gas in vapor cell. Both velocity changing and dephasing aspects of collisions with atoms of the buffer gas are considered. The calculations are based on a simple but often applicable collision model which facilitates inclusion of effect of both the velocity changing collisions (VCC) and dephasing collisions on level coherences. It is found that the velocity changing collisions in general cause narrowing of EIT resonance line widths which in a particular wave vector mismatch regime can lead to large transparency and slow light generation at relatively low coupling field intensities. The effect of accompanying collisional dephasing is opposite. It tends to broaden the EIT resonance and washout the transparency.

2.2 *Formulation*

We consider a typical three level ladder (cascade) system as shown Fig.2.1a. The spontaneous emission rate from the upper level |3> to intermediate level |2> is S_{32} and that from level |2> to ground level |1> is S_{21}. A coupling field $\vec{E}_c = (\vec{\varepsilon}_c \exp[i(\vec{k}_c \cdot \vec{r} - \omega_c t)] + c.c)$ of frequency ω_c wave vector $\vec{k}_c$ and Rabi frequency $\Omega_c = (\vec{\mu}_{32} \cdot \vec{\varepsilon}_c)/\hbar$ is driving the |2>↔|3> transition and a weak probe field, $\vec{E}_p = (\vec{\varepsilon}_p \exp[i(\vec{k}_p \cdot \vec{r} - \omega_p t)] + c.c)$ of frequency ω_p wave vector $\vec{k}_p$ and Rabi frequency $\Omega_p = (\vec{\mu}_{21} \cdot \vec{\varepsilon}_p)/\hbar$ is applied to the |1> ↔|2> transition. Here $\vec{\mu}_{32}$and $\vec{\mu}_{21}$ are dipole moment of |3>↔|2> and |2> ↔|1> transition respectively.

2.2 a) *Interaction Hamiltonian:*

Using Eq (1.5) the interaction Hamiltonian in the interaction picture and under rotating wave approximation is given by

$$V^{int} = -\hbar\Omega_p \exp[i(\vec{k}_p \cdot \vec{r} - \Delta_p t)]\,|2\rangle\langle 1| - \hbar\Omega_c \exp[i(\vec{k}_c \cdot \vec{r} - \Delta_c t)]\,|3\rangle\langle 2| + H.c \qquad \textbf{(2.1)}$$

Where $\Delta_p = (\omega_p - \omega_{21})$ and $\Delta_c = (\omega_c - \omega_{32})$ denote detuning of the probe and pump (control) field frequencies from atomic resonance frequencies ω_{21} and ω_{32} respectively and $|i\rangle\langle j| = (i, j = 1 - 3)$ are the atomic raising or lowering operators.

2.2 b) ***Density matrix equation of motions:***

The equations describing time evolution of the slowly varying components of the density-matrix elements $\tilde{\rho}_{ij}$ can now be written using Eq(2.1),(1.8b) and (1.12) in (1,11) and appropriate transformation to eliminate fast oscillating (exponential) terms as

$$\dot{\tilde{\rho}}_{31}(v,t) = -\left[i\left\{\left(\vec{k}_p + \vec{k}_c\right)\cdot\vec{v} - \left(\Delta_p + \Delta_c\right)\right\} + \gamma_{31} + \gamma_p + \gamma_c + \gamma_{ph}\right]\tilde{\rho}_{31}(v,t) + i\Omega_c\tilde{\rho}_{21}(v,t)$$
$$-i\Omega_p\tilde{\rho}_{32}(v,t) - \Gamma_{31}\tilde{\rho}_{31}(v,t) + \int W_{31}(v',t)\,\tilde{\rho}_{31}(v',t)d^3v' \qquad (2.2a)$$

$$\dot{\tilde{\rho}}_{32}(v,t) = -\left[i(\vec{k}_c\cdot\vec{v} - \Delta_c) + \gamma_{32} + \gamma_c + \Gamma_{32} + \gamma_{ph}\right]\tilde{\rho}_{32}(v,t) + i\Omega_c(\rho_{33} - \rho_{22})$$
$$-i\Omega_p^*\tilde{\rho}_{32}(v,t) \qquad (2.2b)$$

$$\dot{\tilde{\rho}}_{21}(v,t) = -\left[i(\vec{k}_p\cdot\vec{v} - \Delta_p) + \gamma_{21} + \gamma_p + \Gamma_{21} + \gamma_{ph}\right]\tilde{\rho}_{21}(v,t) + i\Omega_c^*\tilde{\rho}_{31}(v,t)$$
$$-i\Omega_p(\rho_{22} - \rho_{11}) \qquad (2.2c)$$

$$\dot{\rho}_{33} = -S_{32}\rho_{33}(v,t) + i\Omega_c\tilde{\rho}_{23}(v,t) - i\Omega_c^*\tilde{\rho}_{32}(v,t) - \Gamma_{33}\tilde{\rho}_{33}(v,t)$$
$$+\int W_{33}(v'\to v)\,\tilde{\rho}_{33}(v',t)d^3v' \qquad (2.2d)$$

$$\dot{\rho}_{22} = -S_{21}\rho_{22}(v,t) + S_{32}\rho_{33}(v,t) + i\Omega_p\tilde{\rho}_{12}(v,t) - i\Omega_p^*\tilde{\rho}_{21}(v,t) - \Gamma_{22}\tilde{\rho}_{22}(v,t)$$
$$+\int W_{22}(v'\to v)\,\tilde{\rho}_{22}(v',t)d^3v' \qquad (2.2e)$$

$$\dot{\rho}_{11} = S_{21}\rho_{22}(v,t) + i\Omega_p^*\tilde{\rho}_{21}(v,t) - i\Omega_p\tilde{\rho}_{12}(v,t) - \Gamma_{11}\tilde{\rho}_{11}(v,t)$$
$$+\int W_{11}(v'\to v)\,\tilde{\rho}_{11}(v',t)d^3v' \qquad (2.2f)$$

In this work we, however, restrict our discussion to the case of the most prevalent and experimentally relevant strong collision model in which collisions result in rapid thermalization of the velocity distribution of the system. In this case a single collision on average thermalizes the velocity shift distribution regardless of the initial velocity, i.e., the collision kernel of Eq. (1.14) is assumed to be independent of the initial velocity and of the form

$$\lim_{\alpha\to 0} W_{ij}(v'\to v) = \Gamma_{ij}M(v) \qquad (2.3)$$

Where

$$M(v) = (v_{th}\sqrt{\pi})^{-3}\exp\left(-\vec{v}.\vec{v}/v_{th}^2\right) \qquad (2.4)$$

is the Maxwellian velocity distribution and $v_{th} = (2k_BT/m_A)^{1/2}$ is the most probable thermal velocity at a temperature T of an atom of mass m_A. Using Eqs (2.3) & (2.4) solve the set of

density-matrix Eqs (2.2a-f) in the usual limit of a weak probe and an arbitrarily strong pump (control) fields using the following approach. Initially all the population is in the ground level $|1\rangle$ with a Maxwellian velocity distribution. We assume the probe to be sufficiently weak so as not to induce any population transfer to upper levels. The zero order solutions obtained from Eqs (2.2a-f) in the absence of probe (i.e., putting$\Omega_p = 0$) is

$$\rho_{11}^{(0)} = M(v) \tag{2.5}$$

And the rest of other zeroth-order density matrix elements vanish. The relevant first-order (i.e., to leading order in probe amplitude) density-matrix equations are found as

$$\dot{\tilde{\rho}}_{21}^{(1)}(v,t) = -\{i(\vec{k}_p \cdot \vec{v} - \Delta_p) + \gamma_{21} + \Gamma_{21} + \gamma_{ph} + \gamma_P\}\tilde{\rho}_{21}^{(1)}(v,t) + i\Omega_c^*\tilde{\rho}_{31}^{(1)}(v,t) + i\Omega_p\rho_{11}^{(0)}(v) \tag{2.6a}$$

$$\dot{\tilde{\rho}}_{31}^{(1)}(v,t) = -\left\{i[\left(\vec{k}_p + \vec{k}_c\right) \cdot \vec{v} - (\Delta_p + \Delta_c)] + \gamma_{31} + \Gamma_{31} + \gamma_{ph} + \gamma_c\right\}\tilde{\rho}_{31}^{(1)}(v,t) + i\Omega_c\tilde{\rho}_{21}^{(1)}(v,t) - \Gamma_{31}M(v)\int \tilde{\rho}_{31}^{(1)}(v',t)d^3v' \tag{2.6b}$$

Our aim is to determine the velocity averaged first-order one photon coherence $I_{21}^{(1)} = \int \tilde{\rho}_{21}^{(1)}(v)d^3v$; the imaginary and the real parts of which describes probe absorption and dispersion, respectively, in the three-level ladder system. We solve the above set of density-matrix equations under steady state condition by setting the time derivative to zero on left hand side of Eq (2.6) yields the velocity averaged first order coherence as

$$I_{21}^{(1)} = \int \tilde{\rho}_{21}^{(1)} d^3v$$

$$= i\Omega_p \int \frac{A_{31}M(v)d^3v}{A_{31}A_{21} + |\Omega_c|^2} - i\Omega_p|\Omega_c|^2\Gamma_{31}\left[\int \frac{M(v)d^3v}{A_{31}A_{21} + |\Omega_c|^2}\right]^2$$

$$\times\left[1 - \Gamma_{31}\int \frac{M(v)}{A_{31}}d^3v + \Gamma_{31}\int \frac{|\Omega_c|^2 M(v)d^3v}{A_{21}(A_{31}A_{21} + |\Omega_c|^2)}\right]^{-1} \tag{2.7}$$

Where

$$A_{31} = i\left[\left(\vec{k}_p + \vec{k}_c\right) \cdot \vec{v} - (\Delta_p + \Delta_c)\right] + \gamma_{31} + \Gamma_{31} + \gamma_{ph} + \gamma_c + \gamma_p \tag{2.8a}$$

$$A_{21} = i\left[\left(\vec{k}_p \cdot \vec{v} - \Delta_p\right)\right] + \gamma_{21} + \Gamma_{21} + \gamma_{ph} + \gamma_p \tag{2.8b}$$

2.2 c) ***Analytical Results:***

We now consider the standard collinear geometry employed in most experiments in which the pump (control) and probe fields are counter propagating along the *z* direction. In this case we make the replacements $\vec{k}_p \cdot \vec{v} \to k_p v_z$ and $\vec{k}_c \cdot \vec{v} \to -k_c v_z$ in Eq (2.8) and henceforth for brevity, denote *v*(= v_z) as the velocity component along the *z* axis and also $\delta k = (k_p - k_c)$. Of particular interest here is the regime of large collisions in which the detunings, residual Doppler width, etc. are very small compared to the Doppler width, i'e $\delta k v_{th}$, $|\Omega_c|^2$,$\Delta_p \ll \Gamma_{31} \ll \gamma_D$. It is then possible to derive analytic forms for velocity averaged one photon coherence and from it expressions for the absorption coefficient and the group index in this regime of interest. In this limit we can make in Eq. (2.8) an expansion of the term

$$\frac{1}{A_{31}(v)} = \frac{1}{-i(\Delta_p + \Delta_c) + \gamma_{31} + \Gamma_{31} + \gamma_p + \gamma_c + \gamma_{ph}} \times \left[1 - \frac{i\delta k v}{(-i(\Delta_p + \Delta_c) + \gamma_{31} + \Gamma_{31} + \gamma_p + \gamma_c + \gamma_{ph})} + \frac{(i\delta k v)^2}{(-i(\Delta_p + \Delta_c) + \gamma_{31} + \Gamma_{31} + \gamma_p + \gamma_c + \gamma_{ph})^2} + \cdots\right] \quad (2.9)$$

Substituting Eq. (2.9) in Eq. (2.7) and retaining only the leading terms we ge

$$\frac{I_{21}^{(1)}}{\Omega_p} = i \int \frac{M(v)dv}{A_{21}} \left[1 - \frac{|\Omega_c|^2 \int \frac{M(v)dv}{A_{21}}}{-i(\Delta_p + \Delta_c) + \gamma_{31} + \gamma_p + \gamma_c + \gamma_{ph} + \frac{(\delta k v_{th})^2}{2\Gamma_{31}} + |\Omega_c|^2 \int \frac{M(v)dv}{A_{21}}}\right] \quad (2.10)$$

As all the parameters are assumed very small compared to the Doppler width, it is possible to evaluate the integral in Eq. (2.10) in the standard Doppler limit as $\int \frac{M(v)dv}{A_{21}(v)} \approx \frac{\sqrt{\pi}}{\gamma_D}$. Substituting $\frac{\sqrt{\pi}}{\gamma_D}$ for the integral in Eq (2.10) real & imaginary parts of the velocity averaged first order coherence under Doppler limit as

$$Re\left(\frac{I_{21}^{(1)}}{\Omega_p}\right)=\frac{(\Delta_p+\Delta_c)|\Omega_c|^2\left(\frac{\sqrt{\pi}}{\gamma_D}\right)^2}{\left(\Delta_p+\Delta_c\right)^2+\left(\gamma_{31}+\gamma_p+\gamma_c+\gamma_{ph}+\frac{(\delta k v_{th})^2}{2\Gamma_{31}}+|\Omega_c|^2\frac{\sqrt{\pi}}{\gamma_D}\right)^2}\ , \tag{2.11a}$$

$$Im\left(\frac{I_{21}^{(1)}}{\Omega_p}\right)=\frac{\sqrt{\pi}}{\gamma_D}\left\{-\frac{|\Omega_c|^2\frac{\sqrt{\pi}}{\gamma_D}\left\{\gamma_{31}+\gamma_p+\gamma_c+\gamma_{ph}+\frac{(\delta k v_{th})^2}{\Gamma_{21}}+|\Omega_c|^2\frac{\sqrt{\pi}}{\gamma_D}\right\}}{\left(\Delta_p+\Delta_c\right)^2+\left(\gamma_{31}+\gamma_p+\gamma_c+\gamma_{ph}+\frac{(\delta k v_{th})^2}{2\Gamma_{31}}+|\Omega_c|^2\frac{\sqrt{\pi}}{\gamma_D}\right)^2}\right\}. \tag{2.11b}$$

The susceptibility of the medium is related to the velocity averaged one-photon coherence as follows:

$$\chi^{(1)}(\omega_p)=N\frac{|\mu_{21}|^2}{\hbar}\frac{I_{21}^{(1)}}{\Omega_p} \tag{2.12}$$

Where *N is* the atomic density of the vapor. The probe wave vector in the medium is given by

$$k(\omega_p)=\frac{\omega_p}{c}n(\omega_p) \tag{2.13}$$

Where $n(\omega_P)$ is the (complex) linear refractive index of the medium that is related (at low atomic vapor densities) to the linear susceptibility as

$$n(\omega_p)=[1+4\pi\chi^{(1)}(\omega_p)]^{1/2}\cong[1+2\pi\chi^{(1)}(\omega_p)]=(1+2\pi\chi_{re})+i2\pi\chi_{im} \tag{2.14}$$

Here χ_{re} and χ_{im} are real and imaginary parts, respectively, of$\chi^{(1)}(\omega_p)$. Substituting Eq. (2.14) in Eq. (2.13) and from Eq. (2.12) we obtain the probe *intensity* absorption coefficient [twice the imaginary part of k_p] and dispersion coefficient as

$$\alpha=\frac{\omega_p}{c}\ 4\pi N\frac{|\mu_{21}|^2}{\hbar}\ Im\left(\frac{I_{21}^{(1)}}{\Omega_p}\right) \tag{2.15}$$

$$\beta=\frac{\omega_p}{c}\left[1+2\pi N\frac{|\mu_{21}|^2}{\hbar}Re\left(\frac{I_{21}^{(1)}}{\Omega_p}\right)\right] \tag{2.16}$$

2.3 ***Estimation of probe absorption coefficient (α) and group index (n_g):***

Probe absorption coefficient* (α) *:

Using Eq (2.11b) and Eq(2.15) we obtained absorption coefficient **(α)** as

$$\alpha = \alpha_0 \left\{ 1 - \frac{|\Omega_c|^2 \frac{\sqrt{\pi}}{\gamma_D} \left\{ \gamma_{31} + \gamma_p + \gamma_c + \gamma_{ph} + \frac{(kv_{th})^2}{2\Gamma_{31}} + |\Omega_c|^2 \frac{\sqrt{\pi}}{\gamma_D} \right\}}{(\Delta_p + \Delta_c)^2 + \left(\gamma_{31} + \gamma_p + \gamma_c + \gamma_{ph} + \frac{(kv_{th})^2}{2\Gamma_{31}} + |\Omega_c|^2 \frac{\sqrt{\pi}}{\gamma_D} \right)^2} \right\} \quad (2.17)$$

Here $\alpha_0 = 4\pi N \frac{|\mu_{21}|^2}{\hbar} \frac{\sqrt{\pi}}{\gamma_D}$ is the Doppler limit absorption coefficient in the absence of the pump (control) field, i.e., $\Omega_c = 0$. We first consider the case in which **($k_p > k_c$)** or **($\lambda_p < \lambda_c$)** so that the sign of the residual Doppler width is positive. This situation can be realized, for example, in the ladder-type $3S_{1/2} \rightarrow 3P_{1/2} \rightarrow 5S_{1/2}$ transition in sodium atom. Comparison of these transitions with the three-level system of Figure 2.2(i) gives the level separation of wave length λ_{21} = 5890 A^0 and λ_{32} = 6154 A^0, spontaneous emission rates: $2\gamma_{21} = S_{21} = 2\pi$(10MHz) and $2\gamma_{32} = S_{32} = 2\pi$(0.4MHz). Additional contributions to the line widths arising from the line widths of probe γ_p[~2π(1MHz)] and pump γ_c[~2π(1MHz)] lasers [4] are also included in the numerical calculations. Thus we take the effective homogeneous width of the two-photon and one-photon coherences as $\gamma_{31}^t = \gamma_{31} + \Gamma_{31} + \gamma_p + \gamma_c + \gamma_{ph}$ and $\gamma_{21}^t = \gamma_{21} + \Gamma_{21} + \gamma_p + \gamma_{ph}$, respectively. The one-photon Doppler (half) width at (half Maximum) for sodium D1 transition is typically γ_D =2π(1 GHz). For simplicity and without loss of generality we assume equal velocity-changing rates, i.e., Γ_{31}=Γ_{21}. On the other hand if we choose the case in which **($k_p < k_c$)** or **($\lambda_p > \lambda_c$)** the sign of residual Doppler width is negative and is shown in Figure 2.2(ii). We choose the $3S_{1/2} \rightarrow 3P_{1/2} \rightarrow 4D_{3/2}$ transition in sodium atoms, the levels separation of wavelengths are λ_{21} = 5896 A^0 and λ_{32} = 5683 A^0 with spontaneous emission rates: $2\gamma_{21} = S_{21} = 2\pi$(10MHz) and $2\gamma_{32} = S_{32} = 2\pi$(1.6MHz). The advantage of choosing the sodium-type atom is that in addition to the other parameters, the residual Doppler width in either of the above two regimes is nearly the same, i.e., $(\delta k v_{th}/\vec{k} v_{th}) \cong \pm 0.04$ where $\vec{k} = (k_p + k_c)/2$ and $\gamma_D = \vec{k} v_{th}$.

Since a three-level ladder system is more general and can also be formally reduced to a type configuration [1,4,6] in which dephasing of two-photon coherence is negligible, we choose values for the dephasing parameter γ_{ph} ranging from zero to Γ_{31} in numerical calculations.

Figure 2.3 displays the effect of collisions on probe absorption [calculated numerically using the exact result Eqs. (2.15)], plotted as a function of the probe detuning for various dephasing rates γ_{ph}. It is clear that for lower dephasing rates, absorption at the line center is reduced considerably compared with the no collision case in the regime where $\boldsymbol{k_p} > \boldsymbol{k_c}$ and the EIT resonance exhibits sub (residual) Doppler narrowing as the velocity-changing parameter Γ_{31} increases beyond the value of residual Doppler width. As the dephasing rate increases, the broadening of the EIT resonance occurs and the line center transparency reduces somewhat but absorption is still lower than that in the absence of collision in the regime where $\boldsymbol{k_p} > \boldsymbol{k_c}$. These results indicate that velocity-changing collisions enhance EIT and cause narrowing of the resonance, whereas the effect of the dephasing collisions is quite the reverse.

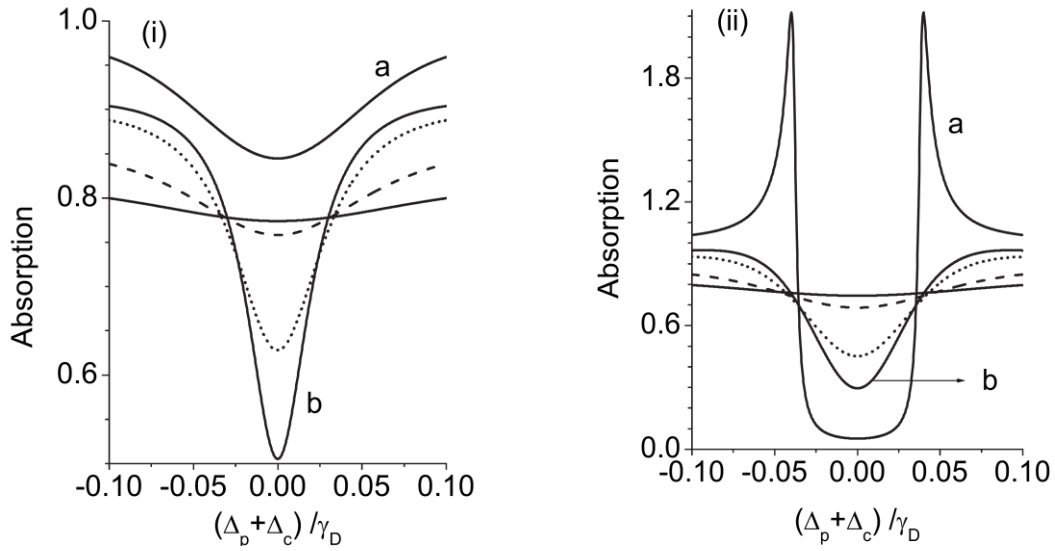

Fig.2.3 *Probe absorption (α/ 0.83αo) as a function of the two photon detuning at a fixed pump (control) field amplitude Ωc /γ_D=0.1 and velocity-changing collisions rate Γ_{31}/γ_D=0.1 and for various collisional dephasing rate γ_{ph}. The value of the residual Doppler broadening is (i) kv_{th}/γ_D=+0.04 and (ii) kv_{th}/γ_D = −0.04. Curves a are the absorption profiles in the absence of buffer gas when Γ_{31}= γ_{ph}= 0, for which the origin and nature of EIT in the* $\boldsymbol{k_p} < \boldsymbol{k_c}$ *regime (kv_{th}/γ_D = −0.04) are explained in many earlier works [1,4,6]. Curves b, dotted, dashed, and solid lines, correspond to the dephasing rates, γ_{ph}= 0, Γ_{31}/ 10, Γ_{31}/2, and Γ_{31}, respectively.*

Figure 2.3 displays the effect of collisions on probe absorption [calculated numerically using the exact result Eqs. (2.15)], plotted as a function of the probe detuning for various

dephasing rates γ_{ph}. It is clear that for lower dephasing rates, absorption at the line center is reduced considerably compared with the no collision case in the regime where $\boldsymbol{k_p > k_c}$ and the EIT resonance exhibits sub (residual) Doppler narrowing as the velocity-changing parameter Γ_{31} increases beyond the value of residual Doppler width. As the dephasing rate increases, the broadening of the EIT resonance occurs and the line center transparency reduces somewhat but absorption is still lower than that in the absence of collision in the regime where $\boldsymbol{k_p > k_c}$**.** These results indicate that velocity-changing collisions enhance EIT and cause narrowing of the resonance, whereas the effect of the dephasing collisions is quite the reverse.

To understand this behavior and to elucidate the role of various narrowing or broadening mechanisms in EIT, let us consider the Doppler limit expression for probe absorption coefficient Eq. (2.17). In the absence of the pump (control) field (Ω_c=0) the absorption profile, which otherwise should be a Doppler broadened line shape, appears (in Doppler limit) as a constant α_o. The pump (control) field intensity-dependent second term in Eq. (2.17) leads to the appearance of a dip at the line center ($\Delta_p+\Delta_c$=0) in the one-photon probe absorption profile (given by the first term α_o). The width of this dip is given by

$$\gamma_{31}^{t} = \gamma_{31} + \gamma_p + \gamma_c + \gamma_{ph} + \frac{\left(k_p - k_c\right)^2 v_{th}^2}{\Gamma_{31}} + |\Omega_c|^2 \frac{\sqrt{\pi}}{\gamma_D} \quad . \tag{2.18}$$

That is, the EIT width is the sum of the homogeneous width γ_{31} of the two-photon coherence, laser line widths γ_p, γ_c, collisional dephasing γ_{ph}, residual Doppler width, and a power broadening term dependent on the intensity (proportional to $|\Omega_c|^2$) of the pump (control) field. Thus the width of the resonance will increase at higher pump (control) field intensities. The absorption value at line center $\Delta_p + \Delta_c = 0$ is

$$\frac{\alpha}{\alpha_0} = \frac{\left(\gamma_{31} + \gamma_p + \gamma_c + \gamma_{ph} + \frac{\left(k_p - k_c\right)^2 v_{th}^2}{2\Gamma_{31}}\right)}{\left(\gamma_{31} + \gamma_p + \gamma_c + \gamma_{ph} + \frac{\left(k_p - k_c\right)^2 v_{th}^2}{2\Gamma_{31}} + |\Omega_c|^2 \frac{\sqrt{\pi}}{\gamma_D}\right)} \quad . \tag{2.19}$$

The above expressions show that the sign of the residual Doppler broadening does not matter in the limit of large velocity-changing collisions. It is also apparent from the above results that the

residual Doppler width term is rendered negligible when $(k_p - k_c)^2 v_{th}^2/2 \ll \Gamma_{31}$ and now the condition for reduced absorption at the line center is that

$$\gamma_{31} + \gamma_p + \gamma_c + \gamma_{ph} \ll |\Omega_c|^2 \frac{\sqrt{\pi}}{\gamma_D} \quad . \tag{2.20}$$

Therefore for a particular value of Ω_c and depending on the value of the dephasing parameter γ_{ph}, absorption at the line center can be considerably lower in the presence of buffer gas as compared to that in the absence of a buffer gas. Under these conditions the width of the EIT resonance (transparency dip) as given by Eq. (2.18) is also nearly independent of the residual Doppler width and, hence, is much narrower for small dephasing rates. Further it is evident from Eqs. (2.18) and (2.19) that the transparency at the line center decreases and the broadening of EIT resonance occurs as the collisional dephasing of two-photon coherence γ_{ph} increases.

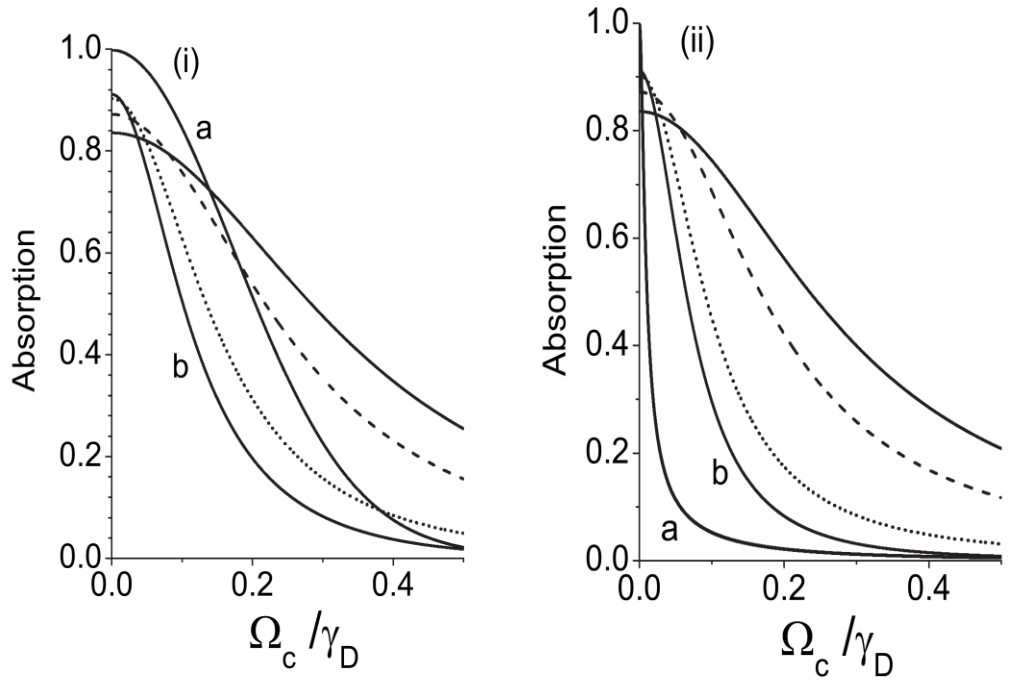

Fig.2.4 *Peak absorption (α/ 0.83αo) at two-photon resonance [Δ_p=Δ_c= 0] as a function of the pump (control) field amplitude Ω_c /γ_D for (i) kv_{th} /γ_D = + 0.04 and (ii) kv_{th} /γ_D = − 0.04. Curves a are the results in the absence of buffer gas. Curves b, dotted, dashed, and solid lines, correspond to the dephasing rates, γ_{ph}=0, Γ_{31}/ 10, Γ_{31}/2, and Γ_{31} respectively. The velocity-changing collision parameter Γ_{31}/γ_D=0.1.*

In this case the condition given by Eq. (2.20) reveals that for large collisional dephasing, higher probe pump intensities are required for achieving complete transparency at the line center. This behavior is shown in Fig.2.4 where the peak absorption value at two-photon resonance as a function of pump (control) field amplitudes is plotted for various collisional dephasing rates. In the regime, $\boldsymbol{k_p > k_c}$, we observe that compared to the no collisions case, the reduction in peak (line center) absorption occurs at much lower pump (control) field amplitudes in the presence of velocity-changing collisions and for low dephasing. In contrast, in the other regime where $\boldsymbol{k_p < k_c}$ peak (line center) absorption is very small for much lower pump (control) field amplitudes than those in the presence of collisions.

Group index (n_g):

The real part of $[I_{21}^{(1)}/\Omega_p]$ is related to the dispersion coefficient (β) (real part of the probe wave vector in the medium) is given by Eq (2.16). The group velocity of the probe field in the medium is given by

$$v_g = [dk(\omega_p)/d\omega_p]^{-1} = \frac{c}{n + \omega_p\,(dn/d\omega_p)} \tag{2.21}$$

When both pump and probe are on resonance ($\Delta_p = \Delta_c = 0$) the probe absorption is extremum so that $[d[\left(\frac{Im(I_{21}^{(1)}}{\Omega_p}\right)]/d\omega_p] = 0$ and further under EIT conditions $n \ll \omega_p(\frac{dn}{d\omega_p})$, the group velocity of probe is

$$v_g = \frac{c}{\omega_p 2\pi N \frac{|\mu_{21}|^2}{\hbar} \frac{d}{d\omega_p}[Re\left(\frac{I_{21}^{(1)}}{\Omega_p}\right)]} = \frac{c}{n_g}\ , \tag{2.22}$$

where n_g is the group index. Thus in addition to absorption characteristics, dispersion spectrum is also of importance since n_g is directly proportional to the derivative (slope) of the dispersion curve. A very steep dispersion profile would result in a high value for n_g which means a very low group velocity. From Eq.(2.11a) and (2.22) the group index at exact two photon detuning $\Delta_p + \Delta_c = 0$ is found as

$$n_g = \frac{c\alpha_0}{2} \frac{|\Omega_c|^2 \frac{\sqrt{\pi}}{\gamma_D}}{\left\{\gamma_{31} + \gamma_p + \gamma_c + \gamma_{ph} + \frac{(\delta k v_{th})^2}{2\Gamma_{31}} + |\Omega_c|^2 \frac{\sqrt{\pi}}{\gamma_D}\right\}^2} . \qquad (2.23)$$

Figure 2.5 shows the group index n_g calculated numerically [using Eqs. (2.3i)] as a function of the pump (control) field amplitude Ω_c for various values of the dephasing rate γ_{ph}. Once again we find that the case when $\boldsymbol{k_p} > \boldsymbol{k_c}$, the peak (maximum) group index value occurs at lower pump (control) field amplitude values in the presence of velocity-changing collisions and for low dephasing rates. In the other regime where $\boldsymbol{k_p} < \boldsymbol{k_c}$ group index values, however, are much higher at still lower pump (control) field amplitudes than those for the case when collisions are present. In the latter regime the group velocity $v_g(=c/n_g)$ obtained is slower by more than 3 orders of magnitude at pump (control) field intensities (proportional to $|\Omega_c|^2$) that are lower by more than 1 order of magnitude compared with those in the case when collisions are present.

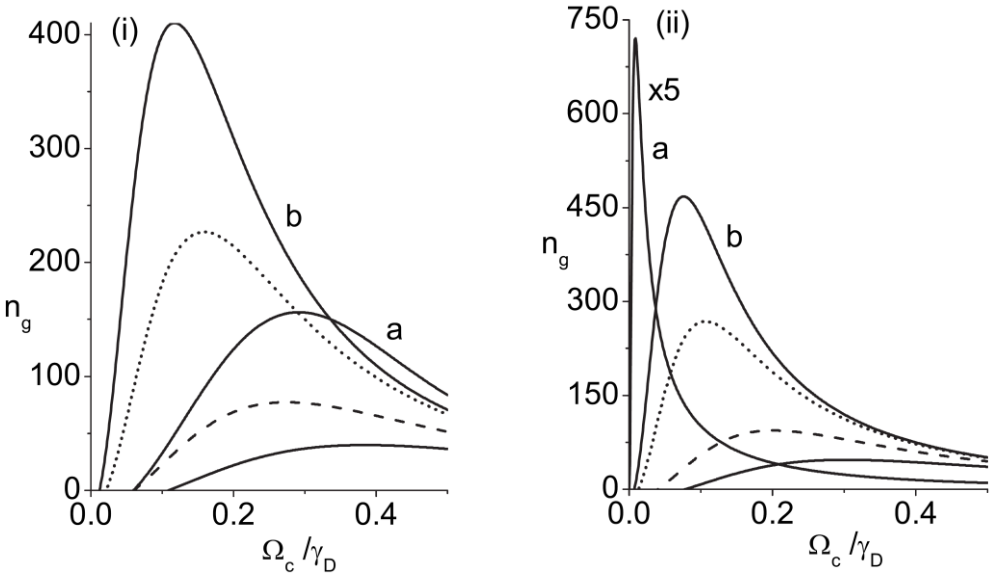

Fig.2.5 *Group index n_g as a function of the pump (control) field amplitude (Ω_c/γ_D) for (i) kv_{th}/γ_D = +0.04 and (ii) kv_{th}/γ_D= −0.04. Curves a are the results in the absence of buffer gas. Curves b, dotted, dashed, and solid lines, correspond to the dephasing rates, γ_{ph}=0, Γ_{31}/ 10, Γ_{31}/2, and Γ_{31}, respectively. The velocity-changing collision parameter is Γ_{31}/γ_D=0.1. The vapor density is $N=2\times(10^{12})$ atoms/cm^3.*

2.4 *Summary and Conclusions:*

We have studied the effect of residual Doppler broadening and velocity-changing and dephasing collisions on electromagnetically induced transparency and slow light propagation in a vapor. A strong collision model is considered for velocity-changing collisions. Earlier studies have shown that residual Doppler broadening affects both linewidth and the absorption dip of the EIT resonance in a markedly dissimilar way depending on the wave-vector mismatch regime. Velocity-changing collisions eliminate this asymmetric behavior of EIT associated with the sign of the residual Doppler width in both regimes of wave-vector mismatch. Though in this work we have only considered collinear propagation of pump (control) and probe light, the theory is as well applicable to noncollinear geometry situations in hot vapors in which the probe light can propagate in an arbitrary direction with respect to the pump (control) light wave vector [7], giving rise to a residual Doppler width of the order of a few megahertz.

Probe wave vector greater than coupler wave vector ($k_p > k_c$):

At low dephasing collisions rates and at higher velocity-changing collision rates, the EIT resonance exhibits narrowing and absorption at the line center decreases. The width γ_{31}^{T} of the EIT resonance narrows considerably and, for velocity-changing collision rates very large relative to the residual Doppler width, is limited by power broadening. Moreover velocity-changing collisions also affect the dispersion properties of the system. In the regime ***(kp > kc)*** the narrowing and steepening of the dispersion curves in the presence of velocity-changing collisions leads to the enhancement of the group index n_g due to which the reduction in the group velocity occurs at much lower pump (control) field intensities. At higher dephasing collisions rates absorption increases at line center & the group index is also decreases. To nullify dephasing collisions effect on absorption higher coupling fields are required.

Probe wave vector lesser than coupler wave vector ($k_p < k_c$):

In this case however in the absence of buffer gas absorption is still lower as compared to the regime ***kp > kc*** with lower dephasing collision rates. The nature of absorption profile has been explained by earlier workers [1, 4, 6]. The peak (line center) absorption is very small for much lower pump (control) field amplitudes than those in the presence of collisions. The group index values are much higher and the slowing of group velocity $v_g(=c/n_g)$ by more than 3 orders

of magnitude is predicted at lower values of pump (control) field intensities (proportional to $|\Omega_c|^2$)compared with those in the case when collisions are present.

In conclusion we have studied EIT in a Doppler broadened ladder system in which buffer gas velocity changing and dephasing collisions are considered. It is found that the velocity-changing collisions in general cause narrowing of EIT resonance linewidths which, in a particular wave-vector mismatch regime, can lead to large transparency and slow light generation at relatively low pump (control) field intensities. Large collisional dephasing of two-photon coherence in a ladder system, however, tends to mask these effects and higher pump (control) field amplitudes are required for observation of EIT. Therefore an addition of buffer gas will broaden the EIT resonance and increase the width of the resonance at high pressure in a Doppler broadened ladder system.

2.5 ***References:***

1. J. Gea-Banacloche, Y. Q. Li, S. Z. Jin, and M. Xiao, Phys. Rev. A **51**, 576 (1995).

2. M. Xiao, Yong-quing Li, Shao-zheng Jin, and J. Gea-Banacloche, Phys. Rev. Lett. **74**, 666 (1995): Y. Q. Li, S. Z.Jin, and M. Xiao, Phys. Rev. A **51**, R1754 (1995).

3. D. J. Fulton, S. Shepherd, R. R. Moseley, B. D. Sinclair, and M. H. Dunn, Phys. Rev. A **52**, 2302 (1995).

4. S. Shepherd, D. J. Fulton, and M. H. Dunn, Phys. Rev. A **54**, 5394 (1996).

5. R. R. Moseley, S. Shepherd, D. J. Fulton, B. D. Sinclair, and M. H. Dunn, Opt. Commun. **119**, 61 (1995).

6. J. R. Boon, E. Zekou, D. McGloin, and M. H. Dunn, Phys.Rev. A **59**, 4675 (1999).

7. S. D. Badger, I. G. Hughes, and C. S. Adams, J. Phys. B **34**, L749 (2001).

8. H. S. Moon, L. Lee, and J. B. Kim, J. Opt. Soc. Am. B **22**, 2529 (2005).

9. Y. Wu and X. Yang, Phys. Rev. A **71**, 053806 (2005).

10. H. S. Moon, L. Lee, and J. B. Kim, Opt. Express **16**, 12163 (2008).

11. S. Brandt, A. Nagel, R. Wynands, and D. Meschede, Phys. Rev. A **56**, R1063 (1997).

Chapter 3

In this chapter we consider a typical three level lambda (Λ) system. The probe is applied on the transition connecting the ground level |1> and excited state |3> whereas pump is connects the state |2> and |3>. In a lambda system the two fields (probe and pump) share a common excited state |3>. The two lower levels |1> and |2> usually are sublevels (hyperfine or Zeeman states) of a ground state and thus are not connected by dipole transition. Hence dephasing between these two lower levels is mainly due to spin exchange self-collisions and is of the order of a few Hz to 1KHz. The buffer gas collisional dephasing between these ground levels is found to be negligible. On the other hand in the ladder system, dephasing rate is typically larger than lambda (Λ) system due to the spontaneous decay of level |3>, otherwise, lambda (Λ) and ladder systems are similar to one another. In chapter 2 we studied the effect of a buffer gas on the phenomenon of EIT in an inhomogeneously (Doppler) broadened ladder system and it was found that the buffer gas velocity changing collisions caused narrowing of EIT resonances whereas buffer gas dephasing collisions broadened EIT resonances. In this chapter we study the effect of buffer gas collisions on EIT and associated slow light propagation in a Doppler broadened medium comprising three-level lambda (Λ) systems. In addition to the Doppler shifts caused by longitudinal motion of atoms along the direction of propagation of (probe and pump) fields we also take into account the time of flight (or transit time) broadening effects arising from the transverse motion of atoms across the finite intensity spread of the probe (and pump) field. A theoretical formulation is developed through which the narrowing of EIT resonance and its width can be explained in lambda systems.

3.1 *Introduction:*

Electromagnetically induced transparency (EIT) [1] describes transparency (nonabsorption) of a weak optical (probe) field at a resonant transition in three level medium due to interference effect induced by a relatively strong (pump) field applied at an adjacent transition. The dispersion property of probe field is equally interesting as the steepness of the dispersion function near resonance plays the key role for reduction of group velocity of light pulse [2,3,4] and is directly related to the linewidth of the EIT resonance [5]. Hence study and identification of various mechanisms that lead to broadening of EIT resonance has attracted considerable attention in

recent years. The width of the EIT resonance depends upon the decay rate of the two photon coherence created between of a ground-state doublet coupled to a common excited state by two coherent light fields in a Λ type three-level atomic system. Several other broadening mechanisms may also contribute to the width of the EIT resonance such as residual Doppler broadening owing to either wave vector mismatch between the pump and the probe beams due to large frequency separation between the ground state doublet [6] or finite angular separation between the pump and the probe beams [7] and power broadening by pump field intensity. For probe and pump beams of *finite size*, the EIT spectrum is also subjected to transit time (or time of flight) broadening [8]. Ye and Zibrov [9] and Carvalho et. al. [10] studied linewidth dependence on angular separation between the pump and probe beams and estimated a residual Doppler broadening of a few MHz of EIT resonance in Cs vapor. However, no or minimal residual Doppler broadening was observed in experiments performed with the addition of a buffer gas in vapor cells. The measured EIT (or CPT) resonance linewidths in these experiments were found to be much narrower, about two orders of magnitude lower than the expected residual Doppler widths. Akulshin et. al. [11] for instance, measured a narrow full width at half maximum of 70 kHz in ^{87}Rb vapor as against an expected residual Doppler width of about 600 kHz arising from 1 mradian angular deviation between pump and probe lasers. Brandt et. al. [6] studied effects of buffer gas on residual Doppler broadening of Cs ground states with a hyperfine splitting of 9.2 GHz and found linewidth reductions by three orders of magnitude to values below 50 Hz. In Ref. [12] a numerical model was used to calculate the CPT line shape, introducing discrete velocity groups, and indeed demonstrating the expected narrowing. Firstenberg et. al. [13] derived an analytic expression that demonstrated both Doppler broadening and collisions-induced Dicke type narrowing of the line shape of CPT resonances. Shuker et. al. [14] recently have studied experimentally the properties of EIT resonances as a function of the angular deviation between the pump and the probe fields. Their measurements show that, in a buffer-gas cell, Doppler broadening due to the angular deviation is strongly suppressed, and moreover it depends quadratically on the angle as opposed to the linear dependence for regular Doppler broadening. Comparison of the results with the analytic theory of Ref. [13], for Dicke-like narrowing in EIT showed a very good quantitative agreement between the measurements and the theoretical model. The analytical results derived in Ref. [13] are valid only in the limit of very weak pump field intensities that is much less compared to the product of homogeneous and

collision widths of the ground state coherence. M. M. Kash. et. al. [3] experimentally observed small group velocities and large group delays, via EIT in a cell containing Ne buffer gas and ^{87}Rb vapor of density 2×10^{12} (atoms/cm^3). For this case Kash et. al. demonstrated theoretically that under their experimental conditions, a reduction of γ_{21} upto 40 Hz allows the possibility of reaching much lower group velocities, near 10 m/s. Their theoretical treatment of slow light however ignores residual Doppler broadening of around 6 kHz arising from the frequency separation between the ground state doublet. More recently Firstenberg et. al. [15] have also presented a more general theory extending their previous low pump field results of Ref. [13] to incorporate power broadening and *finite size* probe beam for collinear probe pump propagation. Numerical results for EIT transmission spectra in low power broadening limit and collinear and degenerate (equal) probe – pump wave vectors case were computed from the density matrix elements in which velocity changing collisions were incorporated using essentially the strong collision model. It is however desirable to have analytical expressions for a better understanding of various processes such as the residual Doppler shifts, power broadening, buffer gas collisions (velocity changing, dephasing collisions, resonance shift) affecting EIT and the associated slow light characteristics. Moreover, as mentioned above, in most EIT experiments probe and pump wave vectors are not equal (nondegenerate) due to large frequency separation between the ground state doublet. Even for the degenerate case, angular deviation (or divergence) between probe and pump is unavoidable in several potential applications of EIT which include slowing and storing of images [16] solitons [17, 18] and strong confinement [19]. Hence it is also important to include residual Doppler broadening occurring due to transit time broadening nondegenerate wave vectors and angular deviation in the theory.

In this chapter we present a theoretical treatment of EIT and slow light in a Doppler broadened lambda system in presence of a buffer gas. The theory is more general as it includes transit time broadening, finite angular separation between the probe and pump and two photon residual Doppler broadening occurring due to wave vector mismatch of pump and probe. Using a strong collision model, the effects of velocity changing collisions with atoms of a buffer gas is incorporated into density matrix formalism. Dephasing collisions and collisional shift of the ground state and optical resonances are also taken into account [9, 12, 14]. A generalized nonlinear envelope (NEE) describing propagation of an ultrashort probe pulse through a resonance medium whose linear (complex) susceptibility (or refractive index) can be modified

(controlled) by an arbitrarily intense pump field, is derived. Various limiting forms of the NEE are considered and contact with the exisiting theories is established. Analytical results are obtained in the intermediate Doppler Dike and low pump field intensities limit. Comparison is made with the existing theories. Using experimental parameters, we show analytically and numerically that significant narrowing of EIT line widths caused by velocity changing collisions can lead to complete transparency and ultraslow light generation at relatively low pump field intensities and vapor densities.

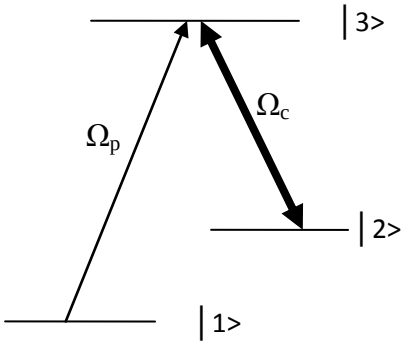

Fig.3.1 *The interaction scheme of a three level lambda system with a probe and a pump field of Rabi frequency respectively, Ω_p and Ω_c.*

3.2 ***Formulation:***

We consider typical Λ type three-level atomic system depicted in Fig. 1. The spontaneous emission rates from the upper level |3> to lower (ground) levels |2> and |1> is S_{32} and S_{31} respectively. A coupler filed $\vec{E}_c = \vec{\varepsilon}_c \exp\left[i\left(\vec{k}_c \cdot \vec{r} - \omega_c t\right)\right] + c.c$ of frequency ω_c and wave vector $\vec{k}_c$ and Rabi frequency $\Omega_c = (\vec{\mu}_{32} \cdot \vec{\varepsilon}_c)/\hbar$ drives |2>↔|3> transition and a weak probe field, $\vec{E}_p = \vec{\varepsilon}_p \exp\left[i\left(\vec{k}_p \cdot \vec{r} - \omega_p t\right)\right] + c.c$ of frequency ω_p and wave vector $\vec{k}_p$ and Rabi frequency $\Omega_p = (\vec{\mu}_{31} \cdot \vec{\varepsilon}_p)/\hbar$ is applied to the |1> ↔|3> transition. Here $\vec{\mu}_{32}$ and $\vec{\mu}_{31}$ respectively, are dipole moments of the |2>↔|3> and |1> ↔|3> transitions. The probe and the coupler fields may in general be non-collinear with a very small angular separation θ between them.

3.2 a) ***Interaction Hamiltonian:***

The interaction picture Hamiltonian V^{int} under near resonant conditions and rotating wave approximation is

$$V^{int} = -\hbar[\Omega_p \exp\left[i\left(\vec{k}_p \cdot \vec{r} + \Delta_p t\right)\right]|3\rangle\langle 1| + \Omega_c \exp\left[i\left(\vec{k}_c \cdot \vec{r} + \Delta_c t\right)\right]|3\rangle\langle 2|] + H.C \quad (3.1)$$

Where $\Delta_p = (\omega_{31} - \omega_p)$ and $\Delta_c = (\omega_{32} - \omega_c)$ denote detuning of the probe and control field frequencies from atomic resonance frequencies ω_{31}andω_{32} respectively and $|i\rangle\langle j|$ (i ,j =1- 3) are the atomic raising or lowering operators.

3.2 b) ***Density matrix equation of motions:***

To describe time evolution of the slowly varying components of the density matrix elements $\tilde{\rho}_{ij}(v,t)$can be obtained, by using Eq (3.1), (1.8b), and (1.16) in Eq (1.11) and appropriate transformations to eliminate fast oscillating (exponential) terms as

$$\dot{\tilde{\rho}}_{31}(v,t) = -\left[i\left(\Delta_p + \vec{k}_p \cdot \vec{v}\right) + \gamma + \gamma_{ph}\right]\tilde{\rho}_{31}(v.t) - i\Omega_p(\rho_{33} - \rho_{11}) + i\Omega_c\tilde{\rho}_{21}(v.t) \quad (3.2a)$$

$$\dot{\tilde{\rho}}_{23}(v,t) = -\left[-i\left(\Delta_c + \vec{k}_c \cdot \vec{v}\right) + \gamma + \gamma_{ph}\right]\tilde{\rho}_{23}(v.t) + i\Omega_c(\rho_{33} - \rho_{22}) - i\Omega_p\tilde{\rho}_{21}(v.t) \quad (3.2b)$$

$$\dot{\tilde{\rho}}_{21}(v,t) = -\left[-i\delta_T + i((\vec{k}_p - \vec{k}_c) \cdot \vec{v}) + \gamma_{21}\right]\tilde{\rho}_{21}(v.t) + i\Omega_c\tilde{\rho}_{31}(v.t) - i\Omega_p\tilde{\rho}_{23}(v.t)$$

$$-\Gamma_{21}\tilde{\rho}_{21}(v.t) + \int W_{21}(v' \to v)\tilde{\rho}_{21}(v.t)d^3v' \quad (3.2c)$$

$$\dot{\rho}_{33}(v,t) = -[S_{31} + S_{32}]\rho_{33}(v.t) + i\Omega_p(\tilde{\rho}_{13} - \tilde{\rho}_{31}) + i\Omega_c(\tilde{\rho}_{23} - \tilde{\rho}_{32})$$

$$-\Gamma_{33}\rho_{33}(v.t) + \int W_{33}(v' \to v)\rho_{33}(v',t)d^3v' \quad (3.2d)$$

$$\dot{\rho}_{22}(v,t) = S_{32}\rho_{33}(v.t) + i\Omega_c(\tilde{\rho}_{32} - \tilde{\rho}_{23}) - \Gamma_{22}\rho_{22}(v.t) + \int W_{22}(v' \to v)\rho_{22}(v',t)d^3v' \quad (3.2e)$$

$$\dot{\rho}_{11}(v,t) = S_{31}\rho_{33}(v.t) + ip(\tilde{\rho}_{31} - \tilde{\rho}_{13}) - \Gamma_{11}\rho_{11}(v.t) + \int W_{11}(v' \to v)\rho_{11}(v',t)d^3v' \quad (3.2f)$$

Here $\delta_T = \Delta_c - \Delta_p$ denotes two photon detuning of the probe and pump fields. In addition, collisions also shift the optical resonance towards lower frequency [9, 13, 14] which can be incorporated by replacing probe detuning Δ_p by $\Delta'_p(= \Delta_p + \delta_p)$ and pump field detuning Δ_c by $\Delta'_c(= \Delta_c + \delta_c)$ in Eq.(3.2) where δ_p (δ_c) is collisional shift of the one-photon optical transition.

In most studies of EIT in vapor cell containing a few Torr of buffer gas , the one photon (optical) coherence $\tilde{\rho}_{23}(v.t)$ and $\tilde{\rho}_{31}(v.t)$are predominantly Doppler broadened and for optical transitions the collisional dephasing is very large compared with the velocity changing collisions effects. We can thus ignore the effect of velocity changing collisions on one-photon coherence in E.q(3.2a) and (3.2b). Furthermore we have ignored collisional dephasing γ_{ph} on two photon coherence $\tilde{\rho}_{21}(v.t)$ in E.q(3.2c), as for a closely spaced ground levels or for levels belonging to the same electronic manifold, the interaction potential experienced is similar and collisional dephasing effects are negligible. In strong collision mode, collisions, result in rapid thermalization of the velocity distribution of the system regardless of the initial velocity i'e., the collision kernel of Eq.(1.14) is assumed to be independent of initial velocity and of the form

$$Lt_{\alpha\to 0}\, W_{ij}(v' \to v) = \Gamma_{ij} M(v) \qquad (3.3a)$$

Where $M(v) = M(v_x)M(v_y)M(v_z)$ (3.3b)

and

$$M(v_j) = [\ln 2/(\pi\bar{v}^2)]^{3/2} \exp\left(-\ln 2 \frac{v_j^2}{\bar{v}^2}\right), j = x, y, z\,, \qquad (3.3c)$$

is the Maxwellian velocity distribution of atoms with $\bar{v} = \sqrt{\ln 2}\, v_{th}$ and $v_{th} = (\frac{2k_B T}{m_A})^{1/2}$ is the most probable thermal velocity at a temperature T of an atom of mass m_a. Our aim is to calculate the velocity averaged slowly varying component of the first order one-photon coherence $R_{31} = \int \tilde{\rho}_{31}^{1}(v)\, dv'$ in steady-state, the imaginary and real parts of which describes probe absorption and dispersion respectively in the three level Λ system. For this purpose we consider the standard weak probe case in which one makes perturbation expansion of the density matrix elements as $\tilde{\rho}_{ij}(v)$ as follows:

$$\tilde{\rho}_{ij} = \tilde{\rho}_{ij}^{0}(v,t) + \lambda_p \tilde{\rho}_{ij}^{1}(v,t) \qquad (3.4)$$

where λ_p is a perturbation parameter proportional to the probe amplitude Ω_p. The zero order solutions (in probe amplitude Ω_p) $\tilde{\rho}_{ij}^{0}(v)$ are valid to all orders in pump field amplitude Ω_c and the first order solutions $\tilde{\rho}_{ij}^{1}$ are valid to all orders in Ω_c and up to first order in (weak) probe field amplitude Ω_p. The zeoth order solution are obtained under the assumption that the probe is so

weak as not to cause any population transfer to other levels i.e., from Eq (3.2) we get the zeroth order solution as

$$\tilde{\rho}_{11}^{0}(v,t) = M(v) \ , \tag{3.5}$$

and all other zero order matrix elements vanish. Using Eq (3.5) and from Eq.(3.2) the relevant density matrix elements equations for first order matrix elements are found as:

$$\dot{\tilde{\rho}}_{21}^{1}(v,t) = -\left[i\left(\Delta\vec{k}\cdot\vec{v} - \delta_T'\right) + (\gamma_{21} + \Gamma_{21})\right]\tilde{\rho}_{21}^{1}(v,t) + i\Omega_c\tilde{\rho}_{31}^{1}(v,t) + \Gamma_{21}M(v)\int \tilde{\rho}_{21}^{1}(v,t)d^3v', \tag{3.6a}$$

$$\dot{\tilde{\rho}}_{31}^{1}(v,t) = -\left[\left(ik_p v_z + \Delta_p'\right) + \gamma + \gamma_{ph}\right]\tilde{\rho}_{31}^{1}(v,t) + i\Omega_p M(v) + i\Omega_c\tilde{\rho}_{21}^{1}(v,t) \ . \tag{3.6b}$$

Here δ_T' (= δ_T + δ_r) where δ_r is collisional shift of the two-photon transition and $\delta_T = \Delta_c - \Delta_p$ denotes two-photon detuning of the probe and pump fields. Eq(3.3a) is used in Eq.(3.6a). The term $\Delta\vec{k}\cdot\vec{v} = \left(\vec{k}_p - \vec{k}_c\right)\cdot\vec{v}$ appearing in Eq.(3.6a) contains in general, the residual Doppler broadening arising due to both probe and pump wave vector mismatch (non-degenerate case) and finite angular separation between the probe and probe.

The above density matrix equations for slowly varying atomic variables are written in plane-wave approximation for the probe and coupler fields. The plane-wave approximation is valid and is utilized in most studies of EIT and slow light conducted using well collimated and sufficiently large probe beam diameter. For if laser beam diameters are sufficiently large [9] transit time broadening effects arising from finite beam width in the transverse plane can be ignored. Eqs.(3.6a) and (3.6b) can be further generalized to the case of a non-planar (finite size) probe beam by replacing Ω_p with a space-time dependent probe amplitude $\Omega_p(\vec{r},t)$. Consequently including space dependence in the slowly varying quantities $\tilde{\rho}_{21}^{1}(\vec{r},t,v)$ and $\tilde{\rho}_{31}^{1}(\vec{r},t,v)$ introducing the Fourier transformation of a function as

$$f(\vec{r},t,v) = \int_{-\infty}^{\infty}\frac{d^3q}{(2\pi)^3}e^{i\vec{q}_\perp\cdot\vec{r}}\int_{-\infty}^{\infty}\frac{d\omega}{2\pi}e^{-i\omega t}f(\vec{q},\omega,t) \ , \tag{3.7}$$

and using Eq.(1.10) and (3.8) in Eqs.(3.6a) and (3.6b) we get

$$\left[i(\vec{q}_\perp\cdot\vec{v} - \omega) + i\left(\Delta\vec{k}\cdot\vec{v} - \delta_T'\right) + \gamma_{21}\right]\tilde{\rho}_{21}^{1}(\vec{q},\omega,v) = i\Omega_c\tilde{\rho}_{31}^{1}(\vec{q},\omega,v) - \Gamma_{21}\tilde{\rho}_{21}^{1}(\vec{q},\omega,v) + \Gamma_{21}M(v)\int \tilde{\rho}_{21}^{1}(\vec{q},\omega,v)\,d^3v' \ , \tag{3.8a}$$

$$\left[i(\vec{q}_\perp \cdot \vec{v} - \omega) + i\left(\Delta'_p + k_p v_z\right) + \gamma + \gamma_{ph}\right]\tilde{\rho}^1_{31}(\vec{q}, \omega, v) = i\Omega_p(\vec{q}, \omega)M(v) + i\Omega_c\tilde{\rho}^1_{21}(\vec{q}, \omega, v)\ .$$

(3.8b)

Solving Eqs. (3.8a) and (3.8b) we obtain the velocity averaged, solution for the first order coherence in the strong collision model as

$$R^s_{31}(\vec{q}, \omega) = \int \tilde{\rho}^1_{31}\,(\vec{q}, \omega, v)d^3v$$

$$= i\Omega_p(\vec{q}, \omega)\int_{-\infty}^{\infty} \frac{d^3v\ M(v)\ [\gamma^t_{21} - i(\delta'_T + \omega) + i\left(\Delta\vec{k}\cdot\vec{v} + \vec{q}\cdot\vec{v}\right)]}{\left[\gamma^t_{21} - i(\delta'_T + \omega) + i\left(\Delta\vec{k}\cdot\vec{v} + \vec{q}\cdot\vec{v}\right)\right]\left[\gamma^t + i\left(\Delta'_p - \omega\right) + i\left(k_p v_z + \vec{q}\cdot\vec{v}\right)\right] + |\Omega_c|^2}$$

$$- i\Gamma_{21}\Omega_p|\Omega_c|^2$$

$$\times \int_{-\infty}^{\infty}\left[\frac{d^3v\ M(v)}{\left[\gamma^t_{21} - i(\delta'_T + \omega) + i\left(\Delta\vec{k}\cdot\vec{v} + \vec{q}\cdot\vec{v}\right)\right]\left[\gamma^t + i\left(\Delta'_p - \omega\right) + i\left(k_p v_z + \vec{q}\cdot\vec{v}\right)\right] + |\Omega_c|^2}\right]^2$$

$$\times\left\{1 - \Gamma_{21}\int_{-\infty}^{\infty}\frac{M(v)d^3(v)}{\left[\gamma^t_{21} - i(\delta'_T + \omega) + i\left(\Delta\vec{k}\cdot\vec{v} + \vec{q}\cdot\vec{v}\right)\right]}\right.$$

$$\left. + \Gamma_{21}|\Omega_c|^2\int_{-\infty}^{\infty}\frac{M(v)d^3(v)\left[\gamma^t_{21} - i(\delta'_T + \omega) + i\left(\Delta\vec{k}\cdot\vec{v} + \vec{q}\cdot\vec{v}\right)\right]^{-1}}{\left[\gamma^t_{21} - i(\delta'_T + \omega) + i\left(\Delta\vec{k}\cdot\vec{v} + \vec{q}\cdot\vec{v}\right)\right]\left[\gamma^t + i\left(\Delta'_p - \omega\right) + i\left(k_p v_z + \vec{q}\cdot\vec{v}\right)\right] + |\Omega_c|^2}\right\}^{-1}$$

(3.9)

where $\gamma^t = \gamma + \gamma_p$ and $\gamma^t_{21} = \gamma_{21} + \Gamma_{21}$. The above analytic solution for strong collision model is an exact result valid for arbitrary coupling field intensities, residual Doppler shifts due to wave vector mismatch arising from: (i) the frequency difference between the coupler and probe beams (ii) angular separation between the probe and coupling beams and (iii) finite width (transit time or time of flight broadening) of probe beam. The usual result for the Doppler broadened case in the absence of buffer gas can be obtained from Eq.(3.9) by setting $\Gamma_{21} = 0$ and neglecting all collision induced optical dephasing and resonance shifts, as

$$R^0_{31}(\vec{q}, \omega) =$$

$$= i\Omega_p(\vec{q}, \omega)\int_{-\infty}^{\infty} \frac{d^3vM(v)[\gamma^t_{21} - i(\delta'_T + \omega) + i\left(\Delta\vec{k}\cdot\vec{v} + \vec{q}\cdot\vec{v}\right)]}{\left[\gamma^t_{21} - i(\delta'_T + \omega) + i\left(\Delta\vec{k}\cdot\vec{v} + \vec{q}\cdot\vec{v}\right)\right]\left[\gamma^t + i\left(\Delta'_p - \omega\right) + i\left(k_p v_z + \vec{q}\cdot\vec{v}\right)\right] + |\Omega_c|^2}$$

(3.10)

For very large pump field amplitudes when $|\Omega_c|^2 >> \Delta\vec{k}\cdot\vec{v}, \vec{q}\cdot\vec{v}, kv_0, \Gamma_{21}$ the velocity changing collisions effect , of course are not important. This can be seen by replacing $\left[\gamma_{21}^t - i(\delta_T' + \omega) + i\left(\Delta\vec{k}\cdot\vec{v} + \vec{q}\cdot\vec{v}\right)\right]\left[\gamma^t + i\left(\Delta_p' - \omega\right) + i\left(k_p v_z + \vec{q}\cdot\vec{v}\right)\right] + |\Omega_c|^2 \approx |\Omega_c|^2$ in Eq.(3.10).

The term $\Delta\vec{k}\cdot\vec{v} = \left(\vec{k}_p - \vec{k}_c\right)\cdot\vec{v}$ appearing in Eq.(3.9) contains in general, the residual Doppler broadening arising due to both probe and pump wave vector mismatch (non-degenerate case) and finite angular separation between the probe and probe. It can be evaluated in the present case as follows: The probe field wave vector is directed along z direction, $\vec{k}_p\cdot\vec{v} = k_p v_z$ and the pump wave vector, for a small angular separation θ from probe beam can be expressed as $\vec{k}_c\cdot\vec{v} = k_c v_z\cos\theta + k_c v_x \sin\theta \cong k_c v_z + k_c v_x\theta$ such that $k_p v_z \gg k_p v_x\theta$. Thus we can write for residual Doppler broadening

$$\Delta\vec{k}\cdot\vec{v} = \left(\vec{k}_p - \vec{k}_c\right)\cdot\vec{v} = \left(k_p - k_c\right)v_z - k_c v_x\theta \qquad (3.11)$$

The first term in Eq. (3.11) is the (longitudinal) residual Doppler shift due to wave vector mismatch arising from the frequency difference between the pump and probe beams and is significant for large ground level doublet separation. For instance, a ground state hyperfine splitting frequency of 6.834 GHz in rubidium [14] or 9.2 GHz in cesium [6] gives rise to a residual Doppler broadening $((\omega_{hf}/c)\bar{v}/2\pi)$ of the order of 6 kHz – 9 kHz. The second term in Eq.(3.11) is the residual Doppler shift due to angular separation between the probe and pump beams and for an angle θ = 0.5 mrad gives rise to a residual Doppler broadening $k_p v_x\theta/2\pi$ of the order of 0.1MHz. For a beam diameter d (of probe or pump) and assuming ($q_x \approx q_y$ =) q = 2π/d , the transit time (or time of flight) broadening term $\vec{q}\cdot\vec{v}$ appearing in Eq.(3.9) can be written as

$$q\bar{v} \approx (2\pi/d)\,\bar{v}\,. \qquad (3.12)$$

3.2 c) ***Analytical Results:***

To facilitate a clear understanding of the role of velocity changing collisions on various possible broadening mechanisms arising from the thermal motion of atoms we will now derive an analytical form for the velocity averaged, first order coherence $R_{31}^s(\vec{q},\omega)$ in the limiting cases of Doppler-Dicke and low coupling field intensities. The regime is of interest in most studies of EIT and CPT in vapor cell containing buffer gas, in the Doppler–Dicke (intermediate) regime, in

which the one-photon Doppler width $\gamma_D = (k_p\bar{v} \approx k_c\bar{v})$ exceeds all relevant frequencies (usual one photon Doppler limit) and the velocity changing collisions rate Γ_{21} is large compared with the residual Doppler width of the two photon transition (two photon Dicke limit)

$$\gamma_D \gg \gamma_{ph}, \Gamma_{21} \gg \Delta\vec{k}\cdot\vec{v}, \vec{q}\cdot\vec{v}, \gamma_{21}. \tag{3.13}$$

Furthermore we restrict our analysis to low coupling field amplitudes such that

$$|\Omega_c|^2 \ll \gamma_D, \Gamma_{21} \quad . \tag{3.14}$$

In these limits we can make in Eq. (3.9) an expansion of the term

$$\frac{1}{\left[\gamma_{21}^t - i\left(\delta_T^{'} + \omega\right) + i\left(\Delta\vec{k}\cdot\vec{v} + \vec{q}\cdot\vec{v}\right)\right]} \approx \frac{1}{\gamma_{21}^t - i\left(\delta_T^{'} + \omega\right)}\left[1 - \frac{i\left(\Delta\vec{k}\cdot\vec{v} + \vec{q}\cdot\vec{v}\right)}{\gamma_{21}^t - i\left(\delta_T^{'} + \omega\right)} - \frac{\left(\Delta\vec{k}\cdot\vec{v} + \vec{q}\cdot\vec{v}\right)^2}{\gamma_{21}^t - i\left(\delta_T^{'} + \omega\right)^2} + \cdots\right], \tag{3.15}$$

and retain only terms to leading orders in $\left(\Delta\vec{k}\cdot\vec{v} + \vec{q}\cdot\vec{v}\right)^2$ and $|\Omega_c|^2$ in view of the conditions specified by Eqs.(3.13) and(3.14), assuming near two-photon resonance conditions and small bandwidth of the probe pulse such that, $\Gamma_{21} \approx \gamma_{21}^t \gg \left(\delta_T^{'} + \omega\right)$ to obtain the expression

$$R_{31}^s(\vec{q},\omega) = i\Omega_p(\vec{q},\omega)K \times \left[1 - \frac{|\Omega_c|^2\Gamma_{21}K}{-i\left(\delta_T^{'} + \omega\right) + \gamma_{21} + |\Omega_c|^2K + \frac{\langle\left(\Delta\vec{k}\cdot\vec{v} + \vec{q}\cdot\vec{v}\right)^2\rangle}{\Gamma_{21}}}\right], \tag{3.16}$$

with

$$K = \int_{-\infty}^{\infty} \frac{M(v_z)dv_z}{\gamma^t + i\left(\Delta_p^{'} - \omega\right) + ik_pv_z + \frac{|\Omega_c|^2}{\Gamma_{21}}} \tag{3.17}$$

Using Eq.(3.11) for $\Delta\vec{k}\cdot\vec{v}$ the velocity averaging in Eq.(3.14)can be performed as follows:

$$\langle\left(\Delta\vec{k}\cdot\vec{v} + \vec{q}\cdot\vec{v}\right)^2\rangle = \int_{-\infty}^{\infty} dv_x M(v_x) \int_{-\infty}^{\infty} dv_y M\left(v_y\right) \int_{-\infty}^{\infty} dv_z M(v_z)\,(\Delta\vec{k}\cdot\vec{v} + \vec{q}\cdot\vec{v})^2$$

$$= \langle(\Delta\vec{k}\cdot\vec{v})^2\rangle + \langle(\vec{q}\cdot\vec{v})^2\rangle + 2\langle\left(\Delta\vec{k}\cdot\vec{v}\right)(\vec{q}\cdot\vec{v})\rangle$$

$$= [(q_x^2 + q_y^2) + (k_p - k_c)^2 + (k_c\theta)^2 - 2q_x(k_c\theta)]\frac{\bar{v}^2}{2} \ . \qquad (3.18)$$

We have thus derived a simple analytical result which demonstrates explicitly the mechanism by which the velocity changing collisions cause narrowing of EIT resonance by eliminating the various broadening effects. Eq.(3.16) (along with Eqs.(3.17) and (3.18)) is a general result as it includes all possible broadening processes affecting the phenomenon of EIT in hot atomic vapors, such as residual Doppler broadening (see Eq.(3.18)) due to wave vector mismatch arising from: (i) the frequency difference between the pump and probe beams (ii) angular separation between the probe and pump beams and (iii) transit time (or time of flight broadening) due to finite width of the probe beam. In addition it also incorporates collisional depahsing and resonance frequency shifts. Eq(3.16) is similar to the results of Firstenberg et. al., [15] derived using diffusion like equations for the slowly varying atomic variables. Eq.(3.16) presented here however is more general as it incorporates collisions and broadenings effects as mentioned above.

3.2 d) ***One photon coherence: (Doppler limit):***

We notice that under the conditions of one photon Doppler limit specified by Eq.(3.12) in which the one photon Doppler width γ_D exceeds all relevant frequencies, the v_z integral in Eq.(3.19a) can be evaluated as

$$K = \int_{-\infty}^{\infty} \frac{M(v_z)dv_z}{\gamma^t + |\Omega_c|^2/\Gamma_{21} + i(\Delta_p' - \omega) + ik_p v_z} = \frac{\sqrt{\pi}}{\gamma_D} e^{[\gamma^t + |\Omega_c|^2/\Gamma_{21} + i(\Delta_p' - \omega)/\gamma_D^2]} \ . \qquad (3.19a)$$

When the pump field is on resonance i.e., Δ_p' and since $\gamma^t + |\Omega_c|^2/\Gamma_{21} + i(\Delta_p' - \omega)/\gamma_D^2 \ll 1$ we can further approximate the term $e^{[\gamma^t + |\Omega_c|^2/\Gamma_{21} + i(\Delta_p' - \omega)/\gamma_D^2]}$ by unity in Eq.(3.20). Therefore the result for velocity averaged one photon coherence of the probe transition for the strong collision model in the Doppler limit can be obtained by substituting

$$K \approx \frac{\sqrt{\pi \ln 2}}{\gamma_D}, \qquad (3.19b)$$

in Eq.(3.16).

3.3 *Probe pulse propagation equation*:

We now derive an envelope equation that describes propagation of a short probe pulse through a resonant medium rendered transparent via EIT i.e., whose linear (complex) refractive index is modified (controlled) by an arbitrarily intense coupling field. Our derivation of the envelope equation starts with the three-dimensional wave equation for the probe field given by

$$\left[(\nabla_{\perp}^2 + \partial_z^2) - \frac{1}{c^2}\partial_t^2\right]\vec{E}_p(\vec{r},t) = \frac{4\pi}{c^2}\partial_t^2\vec{P}_{31}(\vec{r},t)\ . \tag{3.20}$$

Here $\nabla_{\perp}^2 = \partial_x^2 + \partial_y^2$ with $\partial_u^2 = \frac{\partial}{\partial_u^2}$ and $\partial_u = \frac{\partial}{\partial_u}$ where u = x, y, z, t. Assuming negligible changes in the pulse envelope along z direction compared to those in the transverse plane we express the field and polarization in terms of their Fourier transforms as

$$f(\vec{r}_{\perp},z,t) = \int_{-\infty}^{\infty}\frac{d^3q_{\perp}}{(2\pi)^3}e^{i\vec{q}\cdot\vec{r}}\int_{-\infty}^{\infty}\frac{d\omega}{2\pi}e^{-i\omega t}f(\vec{q}_{\perp},z,t)\ , \tag{3.21}$$

the function $f(\vec{r}_{\perp},z,t)$ being either $\vec{E}_p$ or $\vec{P}_{31}$. Introducing these forms in Eq (3.20) we obtain

$$\left[(-q_{\perp}^2 + \partial_z^2) + \frac{\omega^2}{c^2}\right]\vec{E}_p(\vec{q}_{\perp},z,\omega) = -\frac{4\pi}{c^2}\vec{P}_{31}(\vec{q}_{\perp},z,\omega)\ . \tag{3.22}$$

The induced polarization can be decomposed into linear, $\vec{P}_{31}^{L}$ and $\vec{P}_{31}^{NL}$ contribution as

$$\vec{P}_{31}(\vec{q}_{\perp},z,\omega) = \vec{P}_{31}^{L}(\vec{q}_{\perp},z,\omega) + \vec{P}_{31}^{NL}(\vec{q}_{\perp},z,\omega)\ . \tag{3.23}$$

The probe field and linear component of polarization can be expressed in terms of the slowly varying amplitudes $\vec{\varepsilon}_p(\vec{r},t)$ and $\vec{p}_{31}(\vec{r},t)$ as

$$\vec{E}_p(\vec{r}_{\perp},z,t) \quad = \vec{\varepsilon}_p(\vec{r},z,t)\exp\left[ik_pz - i\omega_pt\right] + c.c.\ , \tag{3.24a}$$

$$\vec{P}_{31}^{L}(\vec{q}_{\perp},z,\omega) = \vec{p}_{31}(\vec{r},z,t)\exp\left[ik_pz - i\omega_pt\right] + c.c.\ , \tag{3.24b}$$

where ω_p is the carrier frequency of the probe pulse and $k_p = \frac{\omega_p}{c}$. Representation of the slowly varying amplitude $\vec{\varepsilon}_p(\vec{r},t)$ in terms of its spectral component is

$$\vec{\varepsilon}_p(\vec{q},z,\omega) = \int_{-\infty}^{\infty}d^2r_{\perp}e^{-i\vec{q}_{\perp}\cdot\vec{r}_{\perp}}\int_{-\infty}^{\infty}dt\ e^{i\omega t}\,\vec{\varepsilon}_p(\vec{r}_{\perp},z,t)\ . \tag{3.25}$$

Consequently $\vec{E}_p(\vec{q},z,\omega)$ and $\vec{\varepsilon}_p(\vec{q},z,\omega)$ are related by

$$\vec{E}_p(\vec{q}_\perp,z,\omega)=\int_{-\infty}^{\infty}d^2r_\perp e^{-i\vec{q}_\perp.\vec{r}_\perp}\int_{-\infty}^{\infty}dt\ e^{i\omega t}[\vec{\varepsilon}_p(\vec{r}_\perp,z,t)e^{ik_pz}\,e^{-i\omega_p t}+c.c.] \quad (3.26a)$$

$$\cong \vec{\varepsilon}_p(\vec{q}_\perp,z,\omega-\omega_p)e^{ik_pz}\,. \quad (3.26b)$$

Similarly $\vec{P}_{31}^{L}(\vec{q}_\perp,z,\omega-\omega_p)=\vec{p}_{31}(\vec{q},z,\omega-\omega_p)e^{ik_pz}$. (3.27)

If we now express the nonlinear polarization component generated at some wave vector k_{nl} and frequency ω_p as,

$$\vec{P}_{31}^{NL}(\vec{r}_\perp,z,t)=\vec{\wp}_{31}(\vec{r}_\perp,z,t)\exp[ik_{nl}\,z-i\omega_p t]+c.c \quad (3.28)$$

We then have the relation

$$\vec{P}_{31}^{NL}(\vec{q},z,\omega)=\int_{-\infty}^{\infty}d^2r_\perp e^{-i\vec{q}_\perp.\vec{r}_\perp}\int_{-\infty}^{\infty}dt\ e^{i\omega t}[\vec{\wp}(\vec{r}_\perp,z,t)e^{ik_pz}\,e^{-i\omega_p t}+c.c] \quad (3.29a)$$

$$\cong \vec{\wp}_{31}(\vec{q}_\perp,z,\omega-\omega_p)e^{ik_pz} \quad (3.29b)$$

Inserting Eq (3.23) and the relations defined by Eq (3.26b) and (3.27) and (3.29b) in (3.22) we obtain

$$\left[(-q_\perp^2+\partial_z^2)+2ik_p\,\partial_z+\frac{\omega^2}{c^2}-k_p^2\right]\vec{\varepsilon}_p(\vec{q}_\perp,z,\omega-\omega_p)=-\frac{4\pi}{c^2}\omega^2\vec{p}_{31}(\vec{q}_\perp,z,\omega-\omega_p)$$

$$-\tfrac{4\pi}{c^2}\omega^2\vec{\wp}_{31}(\vec{q}_\perp,z,\omega-\omega_p)e^{-i(k_{nl}-k_p)z}\ . \quad (3.30)$$

Using the usual relation between the linear polarization and linear susceptibility $\chi^{(1)}$

$$\vec{P}_{31}(\vec{q}_\perp,z,\omega')=\chi^{(1)}(\vec{q}_\perp,\omega')\vec{\varepsilon}_p(\vec{q}_\perp,z,\omega')\,. \quad (3.31)$$

Eq.(3.30) reduces to the form

$$[-q_\perp^2+\partial_z^2+2ik_p\,\partial_z+k^2(\omega)-k_p^2]\vec{\varepsilon}_p(\vec{q}_\perp,z,\omega-\omega_p)$$

$$=-\tfrac{4\pi}{c^2}\omega^2\vec{\wp}_{31}(\vec{q}_\perp,z,\omega-\omega_p)e^{-i(k_{nl}-k_p)z}\,, \quad (3.32)$$

where

$$k^2(\omega)=\tfrac{\omega^2}{c^2}[1+4\pi\chi^{(1)}(\vec{q}_\perp,\omega-\omega_p)] \quad (3.33)$$

We now expand k(ω) defined by Eq.(3.33) in a power series about the carrier frequency ω_p as

$$k(\omega) = k(\omega_p) + (\omega - \omega_p)k_1 + D \tag{3.34}$$

Where $k_1 = \left(\frac{d}{d\omega}k(\omega)\right)_{\omega=\omega_p} = \frac{1}{V_g(\omega_p)}$ is reciprocal of the group velocity $V_g(\omega_p)$ and $D = \sum_{n=2}^{\infty}\frac{1}{n!}(\omega-\omega_p)^n k_n$ contains the high order group velocity dispersion terms, $k_n = \left(\frac{d^n}{d\omega^n}k(\omega)\right)_{\omega=\omega_p}$. We also note from Eq.(3.33) that the carrier wave vector in the medium is given in terms of the linear susceptibility $\chi^{(1)}$ of the medium by

$$k(\omega_p) = k(\omega)_{\omega=\omega_p} = \frac{\omega_p}{c}[1 + 4\pi\chi^{(1)}(\vec{q}_\perp, \omega-\omega_p)_{\omega=\omega_p}]^{\frac{1}{2}} \approx \frac{\omega_p}{c}n\,, \tag{3.35}$$

where the complex refractive index n of the medium is defined as

$$n = [1 + 4\pi\chi^{(1)}(\vec{q}_\perp, \omega-\omega_p)_{\omega=\omega_p}]^{\frac{1}{2}} \approx \left[1 + 2\pi\chi^{(1)}(\vec{q}_\perp, \omega-\omega_p)_{\omega=\omega_p}\right]. \tag{3.36}$$

From Eq.(3.34) we obtain

$$k^2(\omega) = k^2(\omega_p) + 2(\omega-\omega_p)k_1k(\omega_p) + 2k(\omega_p)D + 2(\omega-\omega_p)k_1D + (\omega-\omega_p)^2k_1^2 + D^2\,. \tag{3.37}$$

Moreover we can express the term ω^2 occurring on the right of Eq.(3.34) as $\omega^2 = (\omega-\omega_p+\omega_p)^2 = (\omega-\omega_p)^2 + 2\omega_p(\omega-\omega_p) + \omega_p^2$. There after introducing Eq.(3.37) in Eq.(3.32) and taking transform with respect to the frequency variable $(\omega-\omega_p)$ as defined by Eq (3.21) yields in the time domain, the expression

$$\left[-q_\perp^2 + \partial_z^2 + 2ik_p(\partial_z + nk_1\partial_t) + 2ik_1\tilde{D}\,\partial_t + 2nk_p\tilde{D} - k_1^2\partial_t^2 + 2k_p^2(n-1) + \tilde{D}\right]\vec{\varepsilon}_p(\vec{q}_\perp, z, t)$$
$$= -\frac{4\pi}{c^2}\omega_p^2 e^{-i(k_{n1}-k_p)z}(1 + \frac{i}{\omega_p}\partial_t)^2\vec{\wp}_{31}(\vec{q}_\perp, z, t) \tag{3.38}$$

Where $\tilde{D}$ represents differential operator $\tilde{D} = \sum_{n=2}^{\infty}\frac{k_n}{n!}(i\,\partial_t)^n = -\frac{k_2}{2}\partial_t^2 + \cdots$ and Eq.(3.38) can be converted to a retarded time frame, specified by the coordinates defined by $\tau = t - k_1 v$ and $\xi = z$ so that $\partial_z = \partial_\xi - k_1\,\partial_t$ and $\partial_t = \partial_\tau$. Using these transformations the envelope equation Eq.(3.38) becomes

$$\left[-q_\perp^2 + 2ik_p(\partial_\xi + (n-1)k_1\,\partial_\tau) + 2nk_p\tilde{D} + 2ik_1\tilde{D}\,\partial_\tau + 2k_p^2(n-1)p - 2k_1\,\partial_\xi\,\partial_\tau + \partial_\xi^2 + \tilde{D}^2\right]\vec{\varepsilon}_p(\vec{q}_\perp,\xi,\tau) = -\frac{4\pi}{c^2}\omega_p^2 e^{-i(k_{nl}-k_p)z}(1+\frac{i}{\omega_p}\partial_\tau)^2\vec{\wp}_{31}(\vec{q}_\perp,\xi,\tau)\,. \quad (3.39)$$

This can be rearranged in the form

$$\left[-q_\perp^2 + 2k_p^2(n-1)[1+\frac{1}{k_p}\sum_{l=1}^{\infty}\frac{k_l}{l!}(i\,\partial_\tau)^l + 2ik_p(\partial_\xi - i\tilde{D})(1+i\frac{k_1}{k_p}\partial_\tau) + \partial_\xi^2 + \tilde{D}^2\right]\vec{\varepsilon}_p(\vec{q}_\perp,\xi,\tau)$$
$$= -\frac{4\pi}{c^2}\omega_p^2 e^{-i(k_{nl}-k_p)z}(1+\frac{i}{\omega_p}\partial_\tau)^2\vec{\wp}_{31}(\vec{q}_\perp,z,t)\,. \quad (3.40)$$

Ignoring higher order terms compared to the linear ∂_τ (l = 1) term in the series, dropping the very small $\tilde{D}^2$ term and under slowly varying envelope approximation neglecting the higher order space derivatives ∂_ξ^2 in Eq.(3.40) and using Eq.(3.36) we obtain the envelope equation as

$$\left[\frac{i}{2k_p}(1+i\frac{k_1}{k_p}\partial_\tau)^{-1}q_\perp^2 + (\partial_\xi - i\tilde{D})\right]\vec{\varepsilon}_p(\vec{q}_\perp,\xi,\tau) = 2\pi ik_p\chi^{(1)}(\vec{q}_\perp,\omega-\omega_p)_{\omega=\omega_p}\vec{\varepsilon}_p(\vec{q}_\perp,\xi,\tau)$$
$$+2\pi ik_p e^{-i(k_{nl}-k_p)z}(1+i\frac{k_1}{k_p}\partial_\tau)^{-1}(1+\frac{i}{\omega_p}\partial_\tau)^2\vec{\wp}_{31}(\vec{q}_\perp,\xi,t) \quad (3.41)$$

The above expression describes propagation of a short pulse in a resonant, Doppler broadened nonlinear medium whose absorption and dispersion properties governed by (the imaginary and real parts respectively of the refractive index n, are modified (controlled) by an arbitrarily intense coupling field. The (complex) refractive index n of the resonant medium can be expressed, through Eq.(3.36), in terms of the linear susceptibility that is related to the velocity averaged one photon coherence $R_{31}^s$by

$$\chi^{(1)}(\vec{q}_\perp,\omega-\omega_p)_{\omega=\omega_p} = N\frac{|\mu_{31}|^2}{\hbar}\frac{R_{31}^s(\vec{q}_\perp,\omega-\omega_p)_{\omega=\omega_p}}{\Omega_p} \quad (3.42)$$

Where N is the atomic density of the vapor and $R_{31}^s(\vec{q}_\perp,\omega-\omega_p)_{\omega=\omega_p}$ is given by Eq (3.9) or its limiting form of Eq (3.16) (along with Eq.(3.19b) and Eq.(3.18)). We note from Eq.(3.42) that in a Doppler broadened vapor the linear susceptibility and thereby the linear refractive index in general is a function of the transverse wave vector $\vec{q}_\perp$ owing to thermal motion of atoms across the finite size beams, which gives rise to time of flight broadening (see Eq.(3.12)). As is usually done in literature by performing an inverse Fourier transform Eq.(3.42) is reverted to the space-

time domain. This however may lead to a complicated form for the linear and (nonlinear) susceptibilities due to $\vec{q}_\perp$ dependence of the susceptibility. This we emphasize is the situation in reality since most experiments involving EIT use very narrow diameter laser beams. In the following section we show that by adding to the medium, a buffer gas which through velocity changing collisions suppresses the transit time broadening, it is possible to eliminate the transverse wave vector $\vec{q}_\perp$ dependence from the susceptibility and thereby perform the inverse Fourier transform analogous to a homogeneously broadened medium.

3.4 *Results and discussion:*

It is thus important to study the nature of the imaginary and real parts of the linear susceptibility as these essentially determine the absorption and dispersion of the probe in the medium The latter governs the group index and thereby the speed of the light in the medium. In this section we will study in detail the effect of buffer gas collisions on the EIT resonance and slow light propagation using experimental parameters for ^{87}Rb. Numerical results for EIT and slow light propagation using the exact result Eq.(3.9) through (3.42) obtained for strong collision model Eq.(3.3a) for large velocity changing collisions parameter (intermediate regime) will be presented and discussed in light of analytical solutions derived in the Dicke-Doppler intermediate regime in previous sections. The experimental parameters [3, 12, 24] chosen for numerical calculations shown in the Figures below are given (in Table I) for D1 transition of ^{87}Rb vapor with Ne as buffer gas at pressure p (Torr). The most probable thermal velocity of a ^{87}Rb atom at temperature T is given by $v_{th} = 13.83\ T^{1/2}$ and T = 360 ^{o}K . The decoherence rate, γ_{21} of the two-photon coherence (between unlinked transition) does not depend on the buffer gas pressure. It is mainly influenced by spin-exchanging self-collisions among the active-atom (rubidium) and $\gamma_{21}/2\pi$ increases linearly as a function of the density N of rubidium vapor with a slope of about 10^{-10} Hz-cm^3[25].

Table I. **Atomic and collisional parameters of ^{87}Rb atom at pressure p (Torr) of Ne buffer gas**

$\gamma_{21}/2\pi$ (Hz)	$\Gamma_{21}/2\pi$ (MHz)	$\gamma_c/2\pi$ (MHz)	$\delta_r/2\pi$ (kHz)	$\delta_p/2\pi$ (MHz)	λ_{31} (nm)	$\gamma_{31}/2\pi = \gamma_{32}/2\pi$ (MHz)
10^3	2 p	5.4 p	0.4 p	3.7 p	795 (D1)	3

The probe wave vector in the medium given by (3.35) can be related through Eq (3.36) to the real and imaginary parts respectively of the linear susceptibility $\chi^{(1)}\left(\vec{q}_\perp, \omega - \omega_p\right)_{\omega=\omega_p}$ as

$$k \approx \frac{\omega_p}{c}\left[1 + 2\pi\chi^{(1)}_{rel}\left(\vec{q}_\perp, \omega - \omega_p\right)_{\omega=\omega_p}\right] + i\frac{\omega_p}{c}2\pi\chi^{(1)}_{im}\left(\vec{q}_\perp, \omega - \omega_p\right)_{\omega=\omega_p}] = \beta + i\frac{\alpha}{2} \quad . \tag{3.43}$$

The probe intensity absorption coefficient α and the dispersion coefficient β using Eq.(3.43) and Eq.(3.42) are evaluated as

$$\alpha = \frac{\omega_p}{c} 4\pi N \frac{|\mu_{31}|^2}{\hbar} \operatorname{Im}\left(R^{(s)}_{31}\left(\vec{q}_\perp, \omega - \omega_p\right)_{\omega=\omega_p} / \Omega_p\right) \quad , \tag{3.44}$$

and

$$\beta = \frac{\omega_p}{c} + \frac{\omega_p}{c} 2\pi N \frac{|\mu_{31}|^2}{\hbar} \operatorname{Re}\left(R^{(s)}_{31}\left(\vec{q}_\perp, \omega - \omega_p\right)_{\omega=\omega_p} / \Omega_p\right) . \tag{3.45}$$

The form of group velocity of the probe field in the medium is obtained from $k_1 = \left(\frac{d}{d\omega}k(\omega)\right)_{\omega=\omega_p} = \frac{1}{v_g(\omega_p)}$ and Eq.(3.43) is

$$v_g = \left[\frac{dk(\omega_p)}{d\omega_p}\right]^{-1} \approx \frac{c}{\omega_p 2\pi N \frac{|\mu_{31}|^2}{\hbar}\left[\frac{d}{d\omega}\operatorname{Re}\left(R^{(s)}_{31}\left(\vec{q}_\perp, \omega - \omega_p\right)_{\omega=\omega_p} / \Omega_p\right)\right]_{\delta'_T=0}} = \frac{c}{n_g} \quad , \tag{3.46}$$

where n_g is the group index. Thus in addition to absorption characteristics, dispersion spectrum is also of importance since v_g (n_g) is inversely (directly) proportional to derivative (slope) of the dispersion curve. A very steep dispersion profile would result in a high value of n_g which means a very low group velocity.

We now present analytical results for EIT and slow light propagation using results obtained in previous sections in the Dike-Doppler limit for strong collision model. Substituting Eq.(3.19b) in Eq.(3.42) and from Eq.(3.43) we get the Doppler limit velocity averaged absorption coefficient α for the probe *intensity* [25] as

$$\frac{\alpha}{\alpha_0} = 1 - \frac{|\Omega_c|^2 \frac{\sqrt{\pi \ln 2}}{\gamma_D}\left[\gamma_{21} + \frac{\left\langle\left(\Delta\vec{k}\cdot\vec{v} + \vec{q}_\perp\cdot\vec{v}\right)^2\right\rangle}{\Gamma_{21}} + |\Omega_c|^2 \frac{\sqrt{\pi \ln 2}}{\gamma_D}\right]}{\left(\delta'_T\right)^2 + \left[\gamma_{21} + \frac{\left\langle\left(\Delta\vec{k}\cdot\vec{v} + \vec{q}_\perp\cdot\vec{v}\right)^2\right\rangle}{\Gamma_{21}} + |\Omega_c|^2 \frac{\sqrt{\pi \ln 2}}{\gamma_D}\right]^2} \quad . \tag{3.47}$$

Here $\alpha_0 = 4\pi N \frac{\omega_p}{c} \frac{|\mu_{31}|^2}{\hbar} \frac{\sqrt{\pi \ln 2}}{\gamma_D}$ can be identified with the Doppler limit result for probe *intensity* absorption coefficient for one photon transition in the absence of the control field, $\Omega_c = 0$.

Eq.(3.47) shows that pump field (Rabi frequency) dependent second term will give rise to an interference dip in the probe absorption around the two photon resonance. Using the relation $I_c = \frac{c}{2\pi} |\varepsilon_c|^2 \times 10^{-7} (J/sec - cm^2)$ [23] the halfwidth of this EIT resonance can be inferred, in the Dicke-Doppler limit, from Eq.(3.47) as

$$\gamma_{21}^w = \gamma_{21} + \langle (\Delta\vec{k} \cdot \vec{v} + \vec{q}_\perp \cdot \vec{v})^2 \rangle / \Gamma_{21} + \eta I_c \ , \qquad (3.48)$$

where the parameter

$$\eta/2\pi = 3|\mu_{32}|^2 (\sqrt{\pi \ln 2}/\gamma_D) \times 10^{47} \ (\text{Hz-cm}^2/\text{mW}) \ . \qquad (3.49)$$

can be regarded as the slope of the EIT resonance linewidth as a function of the *average* pump field intensity I_c (in mW/cm^2) obtained for a Gaussian pump laser by dividing the total power P_c by the area A ($= \pi d^2/4$) within the radius d/2.

Eq.(3.48) shows that the EIT resonance (half) linewidth γ_{21}^w has contributions from the homogeneous γ_{21} and residual Doppler widths of the two photon coherence and power broadening arising from the pump field *average intensity* I_c. Consequently the EIT resonance halfwidth $\gamma_{21}^w/2\pi$ increases linearly as a function of the pump laser intensity I_c with a slope of $\eta/2\pi$ (Hz-cm^2/mW). The value of halfwidth slope of 7.5 kHz-cm^2/mW obtained using experimental parameters in Table I is within the range of experimentally observed values for D1 [3] and D2 transitions of ^{87}Rb vapor with Ne as buffer gas [12].

The value of the electromagnetically induced dip in the probe absorption profile at exact two photon resonance ($\delta'_T = 0$) is found from Eq.(3.47) to be

$$\alpha/\alpha_0 = 1 - \eta I_c/\gamma_{21}^w \ . \qquad (3.50)$$

It is clear from above results that the residual Doppler broadening arising due to thermal motion of atoms affects the width and consequently the on-resonance value of the probe transparency (absorption) dip. The effect of buffer gas collisions on the phenomenon of EIT now can be elucidated as follows: Eqs.(3.50) and (3.48) reveal that complete on (two-photon) resonance

transparency ($\alpha = 0$) is obtained as γ_{21}^{w} approaches the value of ηI_c which would occur when the pump intensity is much large compared to the other broadening contributions i.e.,

$$\eta I_c >> \gamma_{21} + \langle\left(\Delta\vec{k}\cdot\vec{v} + \vec{q}_\perp\cdot\vec{v}\right)^2\rangle/\Gamma_{21} . \quad (3.51)$$

Since the residual Doppler width term in Eq.(3.48) is inversely proportional to the velocity changing collision parameter Γ_{21} (in the Dicke-Doppler limit) it decreases with increasing Γ_{21}. Consequently the width γ_{21}^{w} of the EIT resonance narrows considerably as Γ_{21} increases and at sufficiently high buffer gas pressures when $\Gamma_{21} \gg \langle\left(\Delta\vec{k}\cdot\vec{v} + \vec{q}_\perp\cdot\vec{v}\right)^2\rangle$, it tends to an almost Doppler free value

$$\gamma_{21}^{w} = \gamma_{21} + \eta I_c \quad . \quad (3.52)$$

As seen from Eq.(3.51), under these circumstances the required intensity for nearly complete on (two-photon) resonance transparency is also reduced significantly to a value given by the condition

$$I_c >> \gamma_{21}/\eta . \quad (3.53)$$

Substituting Eq.(3.52) in (3.50) and under the condition stipulated by Eq.(3.53) we find that the value of the probe absorption dip at exact two-photon resonance is given simply by the expression

$$\alpha / \alpha_o = \gamma_{21} / (\eta I_c) . \quad (3.54)$$

Thus the pump intensity required for observation of EIT is much lower in systems possessing intrinsically very small γ_{21}.

Figure 2 (i) and (ii) show respectively the numerical results for probe absorption as a function of the two photon detuning δ'_T and line center ($\delta'_T = 0$) probe absorption values for various velocity changing collision parameter Γ_{21} computed from Eq.(3.44) along with Eqs.(3.9) and (3.11) with $\theta = 0$ and using parameters in Table I. It is observed from these Figs., in accordance with analytical results presented above, that reduction of the residual Doppler width with increasing Γ_{21} causes narrowing of EIT resonances and reduces absorption drastically so

that very large transparency can be achieved at even very low pump field amplitudes such that, $|\Omega_c|^2 \ll \gamma_D \Gamma_{21}$, a condition assumed earlier in Eq.(3.15) for analytical calculations. These results also reveal that collisional effects are optimum around 11 Torr of buffer pressure wherein saturation sets in and thereafter a slight increase in absorption increases as the pressure increases.

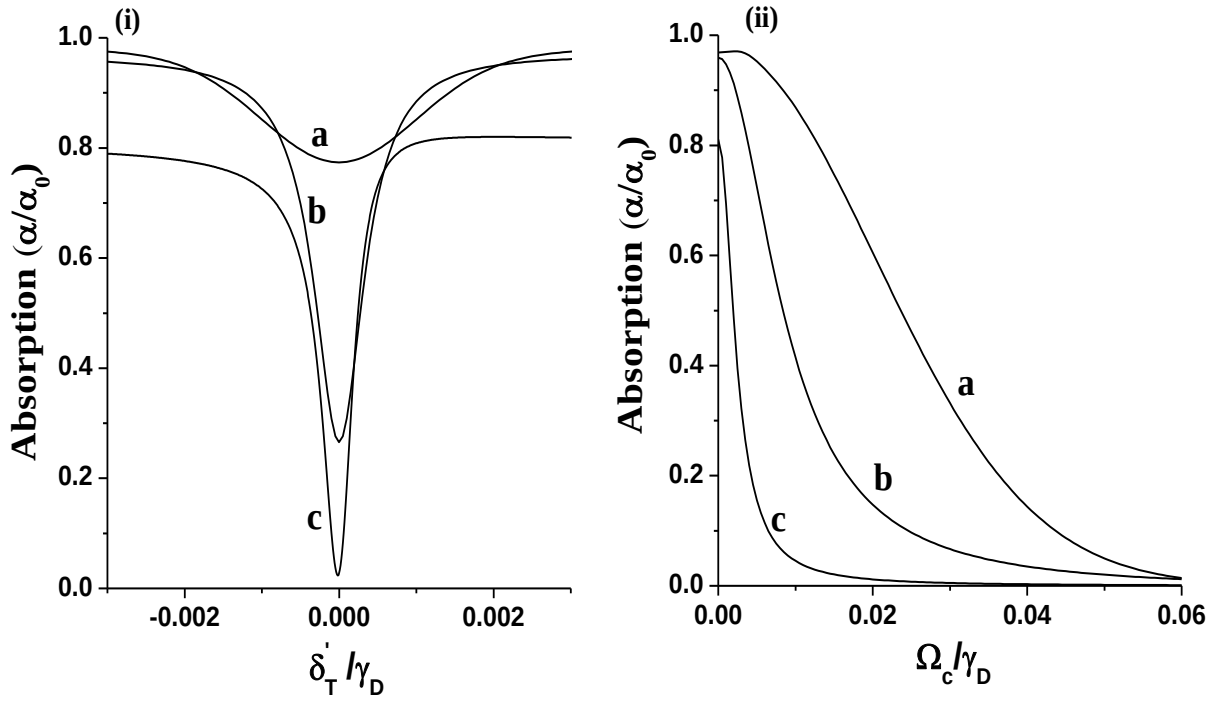

Fig.2 *(i) Shows probe absorption as function of two photon detuning (δ_T'/γ_D) at a fixed value of pump field amplitude $\Omega_c/\gamma_D = 0.014$. (ii) Peak absorption values at two photon ($\delta_T'/\gamma_D = 0$) resonance as function of pump field amplitude Ω_c/γ_D. Curve **a** is the absorption profile in the absence of buffer gas ($\Gamma_{21} = 0$) whereas curves **b** and **c** are those in the presence of a buffer gas corresponding respectively, to the velocity changing collision parameter $\Gamma_{21} = 0.008\gamma_D$ and $0.08\,\gamma_D$. The collisional dephasing collision rate is $\gamma_p = 2.7\Gamma_{21}$. The transit time broadening for a 2 mm diameter probe beam is, $\vec{q}_\perp \cdot \vec{v} = 2\pi \times 216$ kHz and the dephasing between the unlinked transition is, $\gamma_{21} = 2\pi \times 1000$ Hz.*

We now proceed to examine the role of velocity changing collisions on slow light propagation in the medium. The real part of the susceptibility is obtained as

$$\mathrm{Re}\left(\frac{R_{31}^{(s)}}{\Omega_p}\right)_{\omega=\omega_p} = \delta_T' \frac{|\Omega_c|^2 \left(\frac{\sqrt{\ln 2\,\pi}}{\gamma_D}\right)^2}{\left(\delta_T'\right)^2 + \left(\gamma_{21} + \frac{\langle\left(\Delta\vec{k}\cdot\vec{v} + \vec{q}_\perp\cdot\vec{v}\right)^2\rangle}{\Gamma_{21}} + |\Omega_c|^2 \frac{\sqrt{\pi \ln 2}}{\gamma_D}\right)^2}, \tag{3.55}$$

The group velocity of a probe pulse with a carrier frequency ω_p propagating through a resonant medium consisting of three level Λ type systems, can be evaluated using Eqs.(3.46) and (3.55) as

$$v_g = \frac{2}{\alpha_o} \frac{\left[\gamma_{21} + \langle\left(\Delta\vec{k}\cdot\vec{v} + \vec{q}_\perp\cdot\vec{v}\right)^2\rangle/\Gamma_{21} + \eta\, I_c\right]^2}{\eta\, I_c} = \frac{2}{\alpha_o} \frac{\left[\gamma_{21}^w\right]^2}{\eta\, I_c}\ , \tag{3.56}$$

The above result indicates quadratic dependence of the group velocity of the probe pulse on the EIT resonance linewidth. It is also clear that at sufficiently high buffer gas pressures when γ_{21}^w attains an almost Doppler free value given by Eq.(3.52) and furthermore when $I_c >> \gamma_{21}/\eta$, Eq.(3.56) reduces to the form:

$$v_g = \frac{2\eta}{\alpha_o} I_c\,, \tag{3.57}$$

which shows that the group velocity increases linearly with increase in pump intensity with a slope $2\eta/\alpha_o$. Further simplification of Eq.(3.56) leads to following form for the group velocity

$$v_g = \frac{100}{\hbar\omega_{31}} \frac{I_c}{N}\ (\mathrm{m/sec})\,. \tag{3.58}$$

Therefore as discussed above, linewidth narrowing effects of velocity changing collision will not only cause reduced absorption at lower pump intensities but also can result in much slower group velocity in the medium. This effect is shown in Fig.3(i) and (ii) where the group velocity v_g calculated numerically from Eqs.(3.46) along with Eqs.(3.9), (3.11) and (3.12) (for D1 transition of ^{87}Rb atom) is plotted as a function of the pump Rabi frequency Ω_c in the absence of buffer gas, $\Gamma_{21} = 0$ (see Fig. 3(i)) and in the presence of buffer gas, $\Gamma_{21} = 0.08\gamma_D$ (Fig. 3(ii)) which corresponds a buffer gas pressure of 11 Torr. A pump beam diameter of 2 mm and two-

photon decoherence rate $\gamma_{21} = 2\pi\times1000$ Hz (is chosen in order to facilitate comparison with a few existing experimental results of Kash et. al. [3] and Mikhailov and coworkers [4].

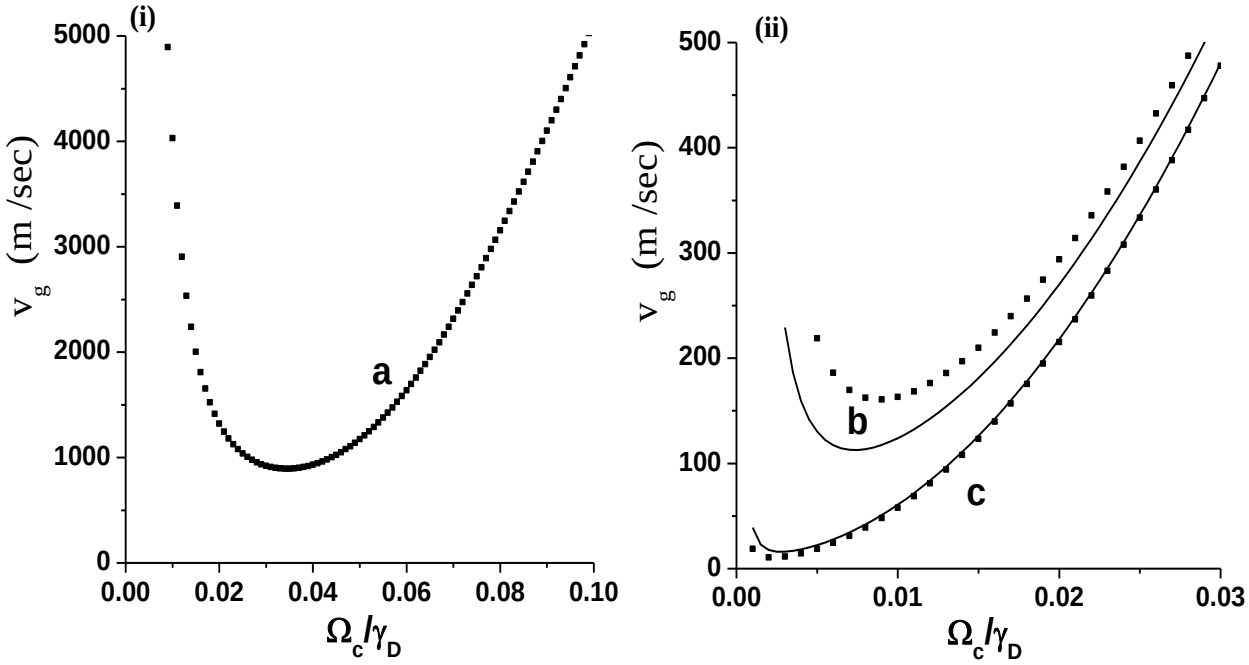

Fig.3 *(i) and (ii): Group velocity v_g (m/sec) as a function of the pump field Rabi frequency Ω_c/γ_D at exact two photon ($\delta_T'/\gamma_D = 0$) resonance. (i) Curve **a** shows the values of the group velocity in the absence of buffer gas ($\Gamma_{21} = 0$). (ii) Curves **b** and **c** are show the group velocity values in the presence of a buffer gas and correspond respectively, to the velocity changing collision parameter $\Gamma_{21} = 0.008\,\gamma_D$ and $0.08\ \gamma_D$. Dotted curves show the numerically evaluated full expression Eq.(3.9) and Eq.(3.36) whereas the solid curves are the numerical results obtained using analytical expression Eq.(3.55) and Eq.(3.46). A good agreement is found between the exact and analytical results for higher value of Γ_{21} (= $0.08\gamma_D$). The collisional dephasing rate is $\gamma_p = 2.7\Gamma_{21}$. The transit time broadening for a 2 mm diameter probe beam is, $\vec{q}_\perp \cdot \vec{v} = 2\pi\times$ 216 kHz and the dephasing between the unlinked transition is, $\gamma_{21} = 2\pi\times1000$ Hz.*

Kash et. al. [3] using a **Ne** buffer pressure (of 30 Torr) have experimentally observed minimum average group velocity of 90 m/sec in hot ^{87}Rb vapor of atomic density N = 2×10^{12} (atoms/cm^3) at pump power of around 0.3 which corresponds to pump Rabi frequency Ω_c/γ_D =

0.014. We find that the theoretical values of group velocity shown in Fig.3(ii) are in good agreement with experimental observation of M. M. Kash et. al. [3] even for 11 Torr Ne buffer pressure as we have seen above the collisional effects of the buffer gas saturate around this pressure beyond which there is no significant change in EIT lineshape.

It is clear from Eqs.(3.57) and (3.58) and Fig.3 that the group velocity increases with increasing pump intensity. Furthermore Eq.(3.58) shows that under EIT conditions (when $I_c >> \gamma_{21}/\eta$) the group velocity in a Λ system is inversely proportional to the atomic density N Therefore further reduction of the group velocity may be possible by increasing N as was demonstrated experimentally by Mikhailov and coworkers [4] in hot ^{87}Rb vapor using 3 torr of $\mathbf{N_2}$ buffer gas. They have observed EIT transmission linewidth of only a few kiloHertz and group velocities below 100 m/sec using higher ^{87}Rb vapor densities ranging from (N =) 1.18×10^{12} to 3.05×10^{12} (atoms/cm^3)**.** It was also seen in their experiment that increasing the laser beam diameter increases the dispersion and reduces the group velocity. This is expected since increasing the beam diameter reduces the transit time broadening since atoms take longer time to traverse the width of the beam in the transverse direction. Thus we find that our results are in good qualitative and quantitative agreement with experimental results for group velocity and EIT in hot ^{87}Rb vapor in buffer gas environment.

3.5 ***Summary and Conclusion:***

In conclusion we have studied the effect of velocity changing (and dephasing) collisions on electromagnetically induced transparency and the associated slow light propagation in a vapor. A generalized nonlinear envelope equation (NEE) describing propagation of an ultrashort (probe) pulse of finite transverse extent through a *resonant* Λ type medium which yields known results in various limiting cases. The aim here was mainly to investigate the nature of the linear susceptibility under these conditions which in general is found to be a function of the transverse wave vector $\vec{q}_\perp$ owing to thermal motion of atoms across the finite size (probe) beam. It however reduces to the usual plane wave form of the linear refractive index in nearly plane wave approximation. Considering strong collisions models for inclusion of velocity changing collisions simple analytical expressions are provided using which can be used to explain and evaluate the EIT linewidth, absorption value at exact two photon resonance and group velocities in a three level system of type Λ in the presence of buffer gas. It is found that the residual

Doppler broadening affects both the width and the absorption dip of the EIT resonance. We show that for higher collision rates the EIT resonance shifts its position and experiences a narrowing ; effect of which on EIT resonance is twofold: first, with increasing velocity changing collisions rate parameter Γ_{21} (or buffer gas pressure p), absorption at the (collisionally shifted) line center decreases and second, the width γ_{21}^{w} of the EIT resonance narrows considerably and for Γ_{21} very large compared to the residual Doppler width is limited by power broadening. This Dicke-type narrowing can be explained by an averaging process of the Doppler effect that is induced by frequent changes of velocities due to collisions. In the presence of velocity changing collisions, huge reduction of the group velocity at much lower pump field intensities occurs due to the narrowing of the residual Doppler width with increasing Γ_{21}. These theoretical results are consistent with earlier experimental studies involving buffer gas, which clearly demonstrated line narrowing, power broadening aspects of EIT resonances and the feasibility of attaining very slow group velocities for small pump fields strengths and lower density atomic vapors in the presence of a buffer gas. Although in the present work we have considered Rb vapor with Ne as buffer gas for illustration purposes, the theory is well applicable to other vapors such as Cs with Ne as buffer gas [6].

3.6 ***References:***

1. K. J. Boller, A. Imamoglu, and S. E. Harris, Phys. Rev. Lett. 66, 2593 (1991); for review see S. E. Harris, Phys. Today **50**, No. 7, 36 (1997).

2. L. V. Hau, S. E. Harris, Z. Dutton, and C. H. Behroozi, Nature (London) **397**, 594 (1999) ; D. Budker, D. F. Kimball, S. M. Rochester, and V. V. Yashchuk, Phys. Rev. Lett. **83**, 1767 (1999); C. Liu, Z. Dutton, C. H. Behroozi, and L. V. Hau, Nature (London) **409**, 490 (2001).

3. M. M. Kash, V. A. Sautenkov, A. S. Zibrov, L. Hollberg, G. R. Welch, M. D. Lukin, Y. Rostovtsev, E. S. Fry, and M. O. Scully, Phys. Rev. Lett. **82**, 5229 (1999))

4. E. E. Mikhailov, Y. V. Rostovtsev and G. R. Welch, J. Mod. Opt. **50**, 2645 (2003).

5. S. E. Harris, J. E. Field, and A. Kasapi, Phys. Rev. A **46**, R29 (1992); O. Schmidt, R. Wynands, Z. Hussein, and D. Meschede, Phys. Rev. A **53**, R27 (1996).

6. S. Brandt, A. Nagel, R. Wynands, and D. Meschede, Phys. Rev. A **56**, R1063 (1997).

7. C. Bolkart, D. Rostohar, and M. Weitz, Phys. Rev. A **71**, 043816 (2005).

8. E. Pfleghaar, J. Wurster, and S. I. Kanorsky, and A. Weis, Opt.Commun. **99**, 303 (1993)).

9. C. Y. Ye and A. S. Zibrov, Phys. Rev. A **65**, 023806 (2002.

10. P. R. S. Carvalho, L. E. E. de Araujo, and J. W. R. Tabosa, Phys. Rev. A **70**, 063818 (2004).

11. A. M. Akulshin, A. A. Celikov, and V. L. Velichansky, Opt. Commun. **84**, 139 (1991)).

12. M. Erhard and H. Helm, Phys. Rev. A **63**, 043813 (2001).

13. O. Firstenberg, M. Shuker, A. Ben-Kish, D. R. Fredkin, N. Davidson, and A. Ron, Phys. Rev.A **76**, 013818 (2007).

14. M. Shuker, O. Firstenberg, R. Pugatch, A. Ben-Kish, A. Ron, and N. Davidson, Rev.A **76**, 023813 (2007).

15. O. Firstenberg, M. Shuker, R. Pugatch, D. R. Fredkin, N. Davidson, and A. Ron, Phys. Rev A **77**, 043830 (2008).

16. R. M. Camacho, C. J. Broadbent, I. Ali-Khan, and J. C. Howell, Phys. Rev. Lett. **98**, 043902 (2007).

17. T. Hong, Phys. Rev. Lett. **90**, 183901 (2003).

18. I. Friedler, G. Kurizki, O. Cohen, and M. Segev, Opt. Lett. **30**, 3374 (2005).

19. A. Andre, M. Bajcsy, A. S. Zibrov, and M. D. Lukin, Phys. Rev. Lett. **94**, 063902 (2005).

20. P. R. Berman, J. Opt. Soc. Am. B **3**, 572 (1986).

21. T. Brabec and F. Krausz, Phys. Rev. Lett. 78, 3282 (1997).

22. A. L. Gaeta, Phys. Rev. Lett. **84**, 3582 (2000).

23. R. W. Boyd, Nonlinear Optics (Academic Press 2003).

24. W. Happer, Rev. Mod. Phys. **44**, 169 (1972).

25. M. Shuker, O. Firstenberg, Y. Sagi, A. Ben-kish, N. Davidson and A. Ron, Phys. Rev. A **78**, 063818 (2008), Figure 7.

Chapter 4

The Vee (V) scheme is different from the lambda (Λ) and ladder (Ξ) schemes. In V-system both probe and pump are connected to the ground state. The fact that the strong pump field interact directly with the ground state |1> cause depletion of population to higher excited state |2> therefore Vee scheme suffers optical pumping and simultaneously probe and pump decay rates (spontaneous decay rates), contribute dephasing on unlinked transition between /2> - |3> which is much larger compared to lambda (Λ) and ladder (Ξ) dephasing rate. Recently there is an ambiguity has arisen on absorption dip in EIT phenomena in a V-system. This is similar to that of Autler-Townes (AT) splitting and saturation effect at exact resonance. In order to reslove the ambiguity and understand these phenomenon (EIT, AT splitting and saturation) in a V system, it is necessary that, a comprehensive study is needed on homogeneous and inhomogeneous (Doppler broaden) medium.

4.1 *Introduction*

Quantum coherence and interference among atomic states coupled by laser field provide EIT in a V-type atomic system. It can be engineered by the action of two fields, one weak field (thin line) called the probe and one stronger field (thick line) called the pump, on two different atomic transitions which share a common ground level shown in Figure 4.1(a). The combined effect of the two fields is to excite only that combination of the two upper levels that enhances stimulated emission by the interference of the two paths [1] and the interference of two excitation paths is shown in Figure 4.1(b). It is of special interest to demonstrate EIT via quantum interference because no population trapping is involved in V-type atomic system. One of the most potential applications of the atomic coherence is to extend the conventional laser sources to ultra-violet and possibly X-rays and even Gamma-ray spectral range, where the conventional methods based on population inversion are not available or difficult to implement. Mismatched (unequal probe and pump field frequency) V-type system with coupling field frequency lower than the probe field frequency are the ideal candidates for the high-frequency inversionless laser systems [2]. On that account, the study of electromagnetically induced transparency in such systems represents the first step in a high frequency inversionless lasers realization. EIT creates the reduction (dip) in absorption upon which the lasing without inversion (LWI) is realized.

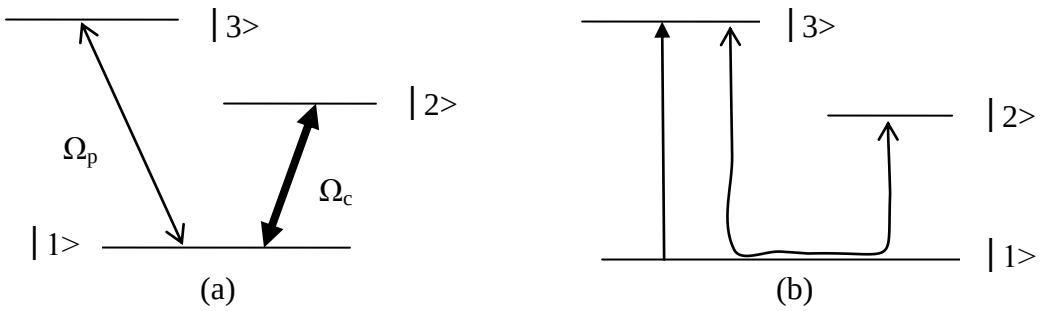

Fig.4.1 (a) : *Schematic diagram of a three-level V-type atomic system driven by a weak probe field of Rabi frequency (Ω_p) and strong pump field of Rabi frequency (Ω_c).(b) Shows the interference of two excitation paths of pump and probe.*

The reduced (dip) absorption in EIT is due to destructive interference between two competing excitation pathways. In optical regime, some cases where the Autler-Townes (AT) splitting (ac equivalent of the dc stark effect) [3] effect is mistaken for EIT because the features of AT splitting caused by a strong field also look very similar to that of EIT at the line center. Both phenomena display a reduction (dip) in absorption at line center. An explicit study on AT effect conducted by Cohen-Tannoudji [4,5] showed that the absorption line is made up of two Lorentzian like lines that are located next to each other. Thus in a V-system the reduction (dip) in absorption can be interpreted as either EIT or a gap between two resonances known as AT splitting. Although reduction (dips) in the absorption lines has been experimentally reported in a three-level V–system [2, 6-11], still a certain ambiguity remains as to whether these results are consequences of EIT or AT splitting effect. Along with this ambiguity the strong field connected to ground state |1> leads to saturation effect in a V- system. As a result reduced (dip) absorption appears in probe absorption profile. These three effects (EIT, AT splitting and saturation) look similar to each other and work in tandem to make the medium transparent at exact resonance by monitoring the standard probe absorption profile and gave a miss interpretation about each other.

In this chapter we investigate the possibility of EIT phenomena occurring and the observed reduced (dip) absorption can be differentiated from EIT and that consequence of saturation, AT splitting effects, by considering a homogenous and an inhomogeneous Doppler broaden medium through a V- type interaction scheme. We solve the steady-state density-matrix

equations for this system and perform a Doppler average over atomic velocity distribution. Atomic susceptibility and expressions for probe absorption, dispersion and group index are numerically estimated and we demonstrate that with the use of EIT it is possible to control the speed of the light at line center (on resonance) in an inhomogeneous Doppler broadened medium, whereas it is not possible to observe an EIT & the associated slow light effect in a homogenous medium at lower Rabi frequency (Ω_c).

4.2 *Formulation*

We consider typical V type three-level atomic system depicted in Fig. 1(a). The spontaneous emission rates from the upper level |3> (|2>) to ground level |1> is $2\gamma_{31}$ ($2\gamma_{21}$). A coupling field $\vec{E}_c = \vec{\varepsilon}_c \exp\left[i\left(\vec{k}_c \cdot \vec{r} - \omega_c t\right)\right] + c.c.$, of frequency ω_c, wave vector $\vec{k}_c$ and Rabi frequency $\Omega_c = (\vec{\mu}_{21} \cdot \vec{\varepsilon}_c)/\hbar$ is driving the |2>↔|1> transition and a weak probe field $\vec{E}_p = \vec{\varepsilon}_p \exp\left[i\left(\vec{k}_p \cdot \vec{r} - \omega_p t\right)\right] + c.c.$, of frequency ω_p, wave vector $\vec{k}_p$ and Rabi frequency $\Omega_p = (\vec{\mu}_{31} \cdot \vec{\varepsilon}_p)/\hbar$, is applied on the transition |3> ↔|1>. Here $\vec{\mu}_{31}$ and $\vec{\mu}_{21}$ are respectively, the dipole moment of |2>↔|1> and |3> ↔|1> transitions. The probe and the pump fields may in general be collinear.

4.2. a) Interaction Hamiltonian

Using Eq. (1.15) the interaction picture Hamiltonian V^{int} under near resonant conditions and rotating wave approximation is

$$V^{int} = -\hbar[\Omega_p \exp\left[i\left(\vec{k}_p \cdot \vec{r} + \Delta_p t\right)\right]|3\rangle\langle 1| + \Omega_c \exp\left[i\left(\vec{k}_c \cdot \vec{r} + \Delta_c t\right)\right]|2\rangle\langle 1| + H.C] \qquad (4.1)$$

Where $\Delta_p = (\omega_{31} - \omega_p)$ and $\Delta_c = (\omega_{21} - \omega_c)$ denote detuning of the probe and control filed frequencies ω_{31} and ω_{21} respectively and $|i\rangle\langle j|$ (i,j=1-3) are the atomic raising or lowering operators.

4.2. b) Density matrix equation of motions:

(i) Inhomogeneous medium:

Thermal motion atoms in hot vapor produce significant Doppler broadening on optical transitions because of non-zero velocity distribution of atoms. The density matrix equations for a V-scheme can be derived using the interaction picture Hamiltonian V^{int} given by Eq.(4.1) substituting in Eq.(1.9) and Doppler broadening effect can be incorporated by Eq.(1.10).

Thereafter using appropriate transformations in these equations to eliminate fast oscillating (exponential) terms, equations describing time evolution of the slowly varying components of the density matrix elements $\tilde{\rho}_{jk}(v,t)$ can be obtained as

$$\dot{\tilde{\rho}}_{31} = -A_{31}\tilde{\rho}_{31} + i\Omega_p(\rho_{11} - \rho_{33}) - i\Omega_c\tilde{\rho}_{32} \ , \tag{4.2a}$$

$$\dot{\tilde{\rho}}_{21} = -A_{21}\tilde{\rho}_{21} + i\Omega_c(\rho_{11} - \rho_{22}) - i\Omega_p\tilde{\rho}_{23}, \tag{4.2b}$$

$$\dot{\tilde{\rho}}_{32} = -A_{32}\tilde{\rho}_{32} - i\Omega_c^*\tilde{\rho}_{31} + i\Omega_p\tilde{\rho}_{12}, \tag{4.2c}$$

$$\dot{\rho}_{11} = i\Omega_p\tilde{\rho}_{31} - i\Omega_p^*\tilde{\rho}_{13} + i\Omega_c\tilde{\rho}_{21} - i\Omega_c^*\tilde{\rho}_{12} + 2\gamma_{31}\rho_{33} + 2\gamma_{21}\rho_{22} \ , \tag{4.2d}$$

$$\dot{\rho}_{22} = i\Omega_c\tilde{\rho}_{21} - i\Omega_c^*\tilde{\rho}_{12} - 2\gamma_{21}\rho_{22}, \tag{4.2e}$$

$$\dot{\rho}_{33} = i\Omega_p\tilde{\rho}_{13} - i\Omega_p^*\tilde{\rho}_{31} - 2\gamma_{31}\rho_{33}. \tag{4.2f}$$

where

$$A_{21} = \gamma_{21} + i(\Delta_c + k_c v_z), \tag{4.3a}$$

$$A_{31} = \gamma_{31} + i(\Delta_p + k_p v_z), \tag{4.3b}$$

$$A_{32} = \gamma_{32} + i(\Delta_p - \Delta_c), \tag{4.3c}$$

and

$$\gamma_{32} = \gamma_{21} + \gamma_{31}. \tag{4.3d}$$

We solve the set of density-matrix equations in the usual limit of a weak probe and an arbitrarily strong control fields using the following approach. Initially all the population is in the ground level $|1\rangle$ and exited level $|2\rangle$ with Maxwell velocity distribution as

$$\rho_{11}^{(0)} + \rho_{22}^{(0)} = M(v), \tag{4.4a}$$

Where

$$M(v) = \left(\frac{1}{\bar{v}}\sqrt{\frac{\ln 2}{\pi}}\right)\exp\left(-\ln 2\,\frac{\vec{v}\cdot\vec{v}}{\bar{v}^2}\right). \tag{4.4b}$$

is the Maxwell velocity distribution of atoms with $\bar{v} = \sqrt{\ln 2}\, v_{th}$ and $v_{th} = (2k_BT/m_A)^{1/2}$ is the most probable thermal velocity at a temperature T of an atom of mass m_A. We assume the probe to be sufficiently weak so as not to induce any population transfer to upper levels $|3\rangle$. For this purpose we consider the standard weak probe case in which one makes perturbation expansion of the density matrix elements as follows:

$$\tilde{\rho}_{ij} = \tilde{\rho}_{ij}^{0}(v,t) + \lambda_p \tilde{\rho}_{ij}^{1}(v,t) \tag{4.5}$$

The zero order solutions obtained from Eqs (4.2) in the absence of probe (i.e., putting$\Omega_p = 0$) is

$$\rho_{11}^{(0)} = \frac{\left[\Omega_c^2\left[\frac{1}{A_{12}} + \frac{1}{A_{21}}\right] + 2\gamma_{21}\right]}{\left[2\Omega_c^2\left[\frac{1}{A_{12}} + \frac{1}{A_{21}}\right] + 2\gamma_{21}\right]} M(v), \tag{4.6a}$$

$$\rho_{22}^{(0)} = \frac{\left[\Omega_c^2\left[\frac{1}{A_{12}} + \frac{1}{A_{21}}\right]\right]}{\left[2\Omega_c^2\left[\frac{1}{A_{12}} + \frac{1}{A_{21}}\right] + 2\gamma_{21}\right]} M(v), \tag{4.6b}$$

$$\tilde{\rho}_{12}^{(0)} = \frac{i\Omega_C^*\left[\rho_{22}^{(0)} - \rho_{11}^{(0)}\right]}{A_{12}}. \tag{4.6c}$$

And the rest of other zeroth-order density matrix elements vanish. The relevant first-order (i.e., to leading order in probe amplitude) density-matrix equations are found as

$$\dot{\tilde{\rho}}_{31}^{(1)} = -A_{31}\tilde{\rho}_{31}^{(1)} + i\Omega_p\rho_{11}^{(0)} - i\Omega_c\tilde{\rho}_{32}^{(1)}, \tag{4.7a}$$

$$\dot{\tilde{\rho}}_{32}^{(1)} = -A_{32}\tilde{\rho}_{32}^{(1)} - i\Omega_c^*\tilde{\rho}_{31}^{(1)} + i\Omega_p\tilde{\rho}_{12}^{(0)}. \tag{4.7b}$$

We solve the above set of density-matrix equations under steady state condition by setting the time derivative to zero on left hand side of Eq.(4.7). The one photon coherence in a inhomogeneously broaden medium $\left(I_{31}^{(1)}\right)_{inh}$ is obtained as

$$\left(I_{31}^{(1)}\right)_{Inh} = \int \tilde{\rho}_{31}^{(1)} M(v)dv = i\Omega_p \int \frac{A_{32}M(v)dv}{(A_{32}A_{31} + |\Omega_c|^2)} - i\Omega_p|\Omega_c|^2 \int \frac{(A_{32} + A_{21})M(v)dv}{(A_{32}A_{31} + |\Omega_c|^2)(2|\Omega_c|^2 + A_{21}A_{12})} \tag{4.8}$$

The imaginary and the real parts of $\left(I_{31}^{(1)}\right)_{inh}$ describe probe absorption and dispersion, respectively, in an inhomogeneously (Doppler) broadened three-level V- system. The susceptibility of the medium is related to the one-photon coherence of medium (consider velocity averaged coherence of an inhomogeous Doppler broadened medium) as follows:

$$\chi^{(1)}(\omega_p) = N\frac{|\mu_{31}|^2}{\hbar}\left(\frac{I_{31}^{(1)}}{\Omega_p}\right)_{inh} \quad (4.9)$$

Where N is the atomic density of the vapor. From Chapter 2 using Eq (2.14), (2.13) and from Eq. (4.9) we obtain probe intensity absorption coefficient [twice the imaginary part of k_p] and dispersion coefficient as

$$\alpha_{inh} = \frac{\omega_p}{c}\, 4\pi N\frac{|\mu_{31}|^2}{\hbar}\, \mathrm{Im}\left(\frac{I_{31}^{(1)}}{\Omega_p}\right)_{inh}, \quad (4.10a)$$

$$\beta_{inh} = \frac{\omega_p}{c}\left[1 + 2\pi N\frac{|\mu_{31}|^2}{\hbar}\mathrm{Re}\left(\frac{I_{31}^{(1)}}{\Omega_p}\right)_{inh}\right]. \quad (4.10b)$$

Thus in addition to absorption characteristics, dispersion spectrum is also of importance since n_g is directly proportional to the derivative (slope) of the dispersion curve (estimation is given in chapter 2) described as

$$(n_g)_{inh} = 2\pi N\frac{\omega_p}{c}\frac{|\mu_{31}|^2}{\hbar}\frac{d}{d\omega_p}\mathrm{Re}\left(\frac{I_{31}^{(1)}}{\Omega_p}\right)_{inh}, \quad (4.11a)$$

$$(n_g)_{inh} = -2\pi N\frac{\omega_p}{c}\frac{|\mu_{31}|^2}{\hbar}\left[\int \frac{(A_{32}^2 - |\Omega_c|^2)(|\Omega_c|^2 + A_{21}A_{12}) - |\Omega_c|^2 A_{21}(A_{32} + A_{31})}{(A_{32}A_{31} + |\Omega_c|^2)^2(2|\Omega_c|^2 + A_{21}A_{12})}\, M(v)dv\right]. \quad (4.11b)$$

***(ii) Homogeneous medium*:**

In this standard stationary atom case the expression for the one photon coherence $\left(I_{31}^{(1)}\right)_h$ is obtained from Eq.(4.8) by putting velocity (v □□0) as

$$\left(I_{31}^{(1)}\right)_h = \tilde{\rho}_{31}^{(1)} = i\Omega_p\frac{[\gamma_{32} + i(\Delta_p - \Delta_c)]}{[(\gamma_{32} + i(\Delta_p - \Delta_c)(\gamma_{31} + i\Delta_p) + |\Omega_c|^2]} - |\Omega_c|^2\frac{\left[[\gamma_{32} + i(\Delta_p - \Delta_c)] + [(\gamma_{21} + i\Delta_c)]\right]}{[(\gamma_{32} + i(\Delta_p - \Delta_c)(\gamma_{31} + i\Delta_p) + |\Omega_c|^2][2|\Omega_c|^2 + \gamma_{21}^2 + \Delta_c^2]} \quad (4.12a)$$

Therefore the probe absorption (dispersion) coefficient α (β) at exact resonance of pump field $(\Delta_c = 0)$ as

$$\alpha_h = \frac{\omega_p}{c}\, 4\pi N \frac{|\mu_{31}|^2}{\hbar}\, \mathrm{Im}\left(\frac{I_{31}^{(1)}}{\Omega_p}\right)_h , \qquad (4.12b)$$

$$\beta_h = \frac{\omega_p}{c}\left[1 + 2\pi N \frac{|\mu_{31}|^2}{\hbar}\, \mathrm{Re}\left(\frac{I_{31}^{(1)}}{\Omega_p}\right)_h\right]. \qquad (4.12c)$$

The group index $(n_g)_h$ can be estimated in a homogenous medium at on resonance ($\Delta_p = \Delta_c = 0$) from Eq.(4.13) as

$$\left(n_g\right)_h = 2\pi N \frac{\omega_p}{c} \frac{|\mu_{31}|^2}{\hbar} \frac{d}{d\omega_p} \mathrm{Re}\left(\frac{I_{31}^{(1)}}{\Omega_p}\right)_h , \qquad (4.13a)$$

$$\left(n_g\right)_h = -2\pi N \frac{\omega_p}{c} \frac{|\mu_{31}|^2}{\hbar} \left[\frac{\left(\gamma_{32}^2 - |\Omega_c|^2\right)\left(|\Omega_c|^2 + \gamma_{21}^2\right) - |\Omega_c|^2 \gamma_{21}(\gamma_{32} + \gamma_{31})}{(\gamma_{32}\gamma_{31} + |\Omega_c|^2)^2 (2|\Omega_c|^2 + \gamma_{21}^2)}\right]. \qquad (4.13b)$$

4.3 *Results and Discussion:*

There are three phenomena called EIT, saturation and AT splitting effects which have a remarkable effect on probe absorption & dispersion. These effects look similar to each other if one observes the probe absorption profiles. Usually the probe absorption profile has a dip under EIT condition (quantum mechanical destructive interference of transition probabilities) at exact resonance; which indicates a reduction in probe absorption. Along with reduction in probe absorption, EIT resonances are extremely narrow. But the absorption profile under saturation and AT splitting effects will also look very similar to that of EIT absorption profile. We now present numerical results for probe absorption and dispersion in a homogenous and inhomogeous (Doppler broadened) medium. We first consider the case of homogeneous broadening. The typical V-scheme is realized in Na^{23} where pump & probe both fields are applied to same transition $3S_{1/2}$ -$3P_{1/2}$. The transition wave length and spontaneous emission rates are 5896 Å and $2\gamma_{21}=2\gamma_{31}=2\pi$ (10 MHz) respectively. The effective width (half width at half maximum) in a homogenous medium $\gamma = 2\pi$ (5 MHz) and for in an inhomogeneous medium as $\gamma_D = 2\pi$ (1000MHz)

Figure 4.2(i)&(ii) shows probe absorption (dispersion) (calculated numerically using Eqs (4.12)) plotted as a function of the probe detuning for various pump field Rabi frequencies (Ω_c/γ) in a homogenous medium. From figure, it is clear that probe (curve a) is totally absorbed at lower pump Rabi frequency ($\Omega_c < \gamma$). The dispersion (curve a) corresponds to normal dispersion which is exactly replica of a two level system, if the pump Rabi frequency $\Omega_c \approx \gamma$ (curve b) absorption is lowered and absorption profile is broader than previous curve **a**. The reduction in absorption is due to population transfer from lower level $|1\rangle$ to upper level $|2\rangle$. The dispersion curve b still remains as a normal dispersion. Slightly higher pump Rabi frequency ($\Omega_c > \gamma$) probe absorption profile (curve c) has a dip and the dispersion deviates from normal dispersion. This behavior is mainly due to saturation effect where population is almost equally distributed between the two levels $|1\rangle$ & $|2\rangle$ shown in figure (iii). At higher pump Rabi frequency ($\Omega_c >> \gamma$) probe absorption (curve d) has two separately distinct resonances which is a clear signature of AT splitting effect, absorption vanishes at line center (on resonance). The probe dispersion (curve d) has two separate normal dispersion curves which are well separated, but at line center dispersion curve slope is positive (very small).

To understand the behavior of probe dispersion at line center, we numerically estimated group index n_g at exact resonance. Figure 4. 2(iv) display the effect of group index n_g at exact resonance (calculated numerically using Eqs (4.13)) plotted as function of pump Rabi frequency (Ω_c/γ). From figure at lower pump Rabi frequency ($\Omega_c \leq \gamma$) the group index n_g sign is negative whereas at higher pump Rabi frequency ($\Omega_c > \gamma$) group index n_g sign remains as positive but very small. The probe group velocity v_g (= c/-n_g) initially suffers superluminal (fast) light effect, but compared to group velocity v_g absorption is much more dominant, so initially probe is absorbed in the medium at lower pump Rabi frequency ($\Omega_c \leq \gamma$). At higher Rabi frequency ($\Omega_c > \gamma$) the group velocity v_g (= c/+n_g) suffers subluminal (slow) light effect, whereas probe is transparent due saturation and AT splitting effect at line center (on resonance).

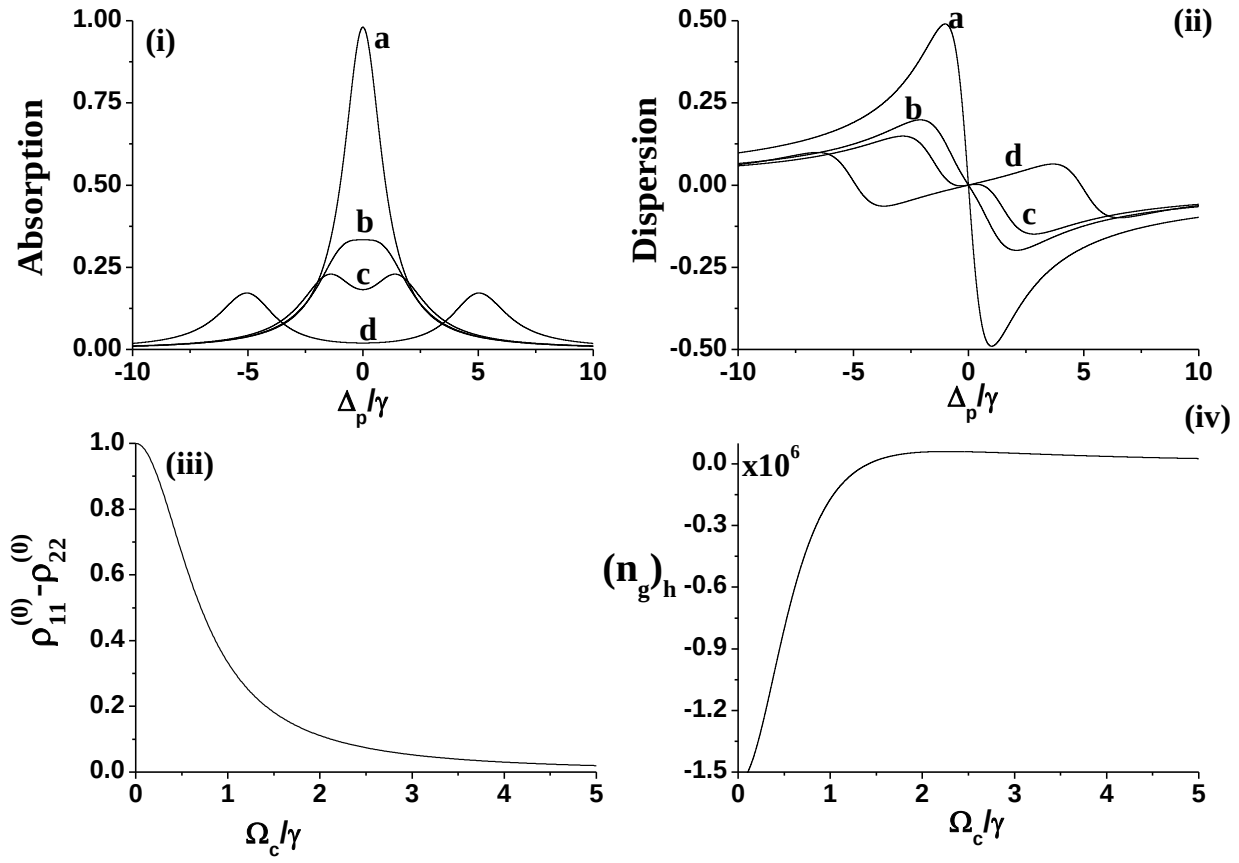

Fig.4.2 *(i) & (ii) Shows probe absorption and dispersion as a function of probe detuning (Δ_p/γ). (iii) & (iv) Shows population difference and group index* $\boldsymbol{n_g}$ *as a function of pump field Rabi frequency (Ω_c/γ) in a homogeneous medium. Curves* ***a, b, c*** *and* ***d*** *corresponds to pump Rabi frequency values 0.1γ, 1γ, 1.5 γ, and 5γ respectively, and N=2x10^{12} atoms/cm^3.*

It is clear evidence that in a homogenous medium the probe nonabsorption (dip) behavior at line center (on resonance) is mainly due to saturation and AT splitting effects. In a homogenous medium a large two photon dephasing (γ_{32}) between the levels $|2\rangle$ & $|3\rangle$ is of an order of spontaneous decay rate ($\gamma_{32}=2\gamma$) mask EIT effect on probe.

To beat two photon dephasing (γ_{32}) effect we considered inhomogeneous Doppler broadened medium where two photon dephasing (γ_{32}) effect can be minimized. Figure 4.3 (i) &(ii) shows probe absorption (dispersion) (calculated numerically using Eqs (4.10)) plotted as a function of the probe detuning for various pump field Rabi frequencies (Ω_c/γ_D) in an inhomogeneous Doppler broadened medium. At lower pump Rabi frequency ($\Omega_c \ll \gamma_D$) Curves

a, b, c are depicted as probe absorption (dip) & dispersion due to EIT effect. It is confirmed from Figure (vi) where the group index n_g (calculated numerically using Eqs (4.11)) is plotted as function of pump field Rabi frequency (Ω_c/γ_D) that the group index n_g has a positive sign and the corresponding group velocity v_g (= c/+n_g) of probe, initially suffers subluminal (slow) light effect. If pump Rabi frequency ($\Omega_c << \gamma_D$) probe absorption (dip) & dispersion is still due to EIT effect, simultaneously population is transfer takes place from lower level $|1\rangle$ to upper level $|2\rangle$ (where population is not equally distributed in the levels shown in Figure 4.3(v)). At higher pump Rabi frequency ($\Omega_c \leq \gamma_D$) it is very difficult to distinguish between EIT & saturation effect on probe absorption (dip), but a qualitative analysis from population difference and group index n_g. provides distinction between EIT and saturation effect. Figure 4.3 (iii) & (iv) the curves a′, b′ are probe absorption (dispersion) at $\Omega_c \leq \gamma_D$. The population is distributed between the levels $|1\rangle$ & $|2\rangle$ and group index n_g has positive and very small shown in Figure 4.3 (v) & (vi). From this indirect evidence, we can conclude that EIT and saturation effect both are indistinguishable and the dominant mechanism on probe absorption (dip) is mainly due to saturation effect. If the pump Rabi frequency is further increased beyond γ_D ($\Omega_c \gg \gamma_D$) then AT splitting effect will take place and the probe absorption (dispersion) has two resonance peaks which are well separated as shown in Figure 4.3 (iii) & (iv) by curve c′. Therefore higher pump Rabi frequency probe absorption (dip) at exact resonance is mainly due to AT splitting effect.

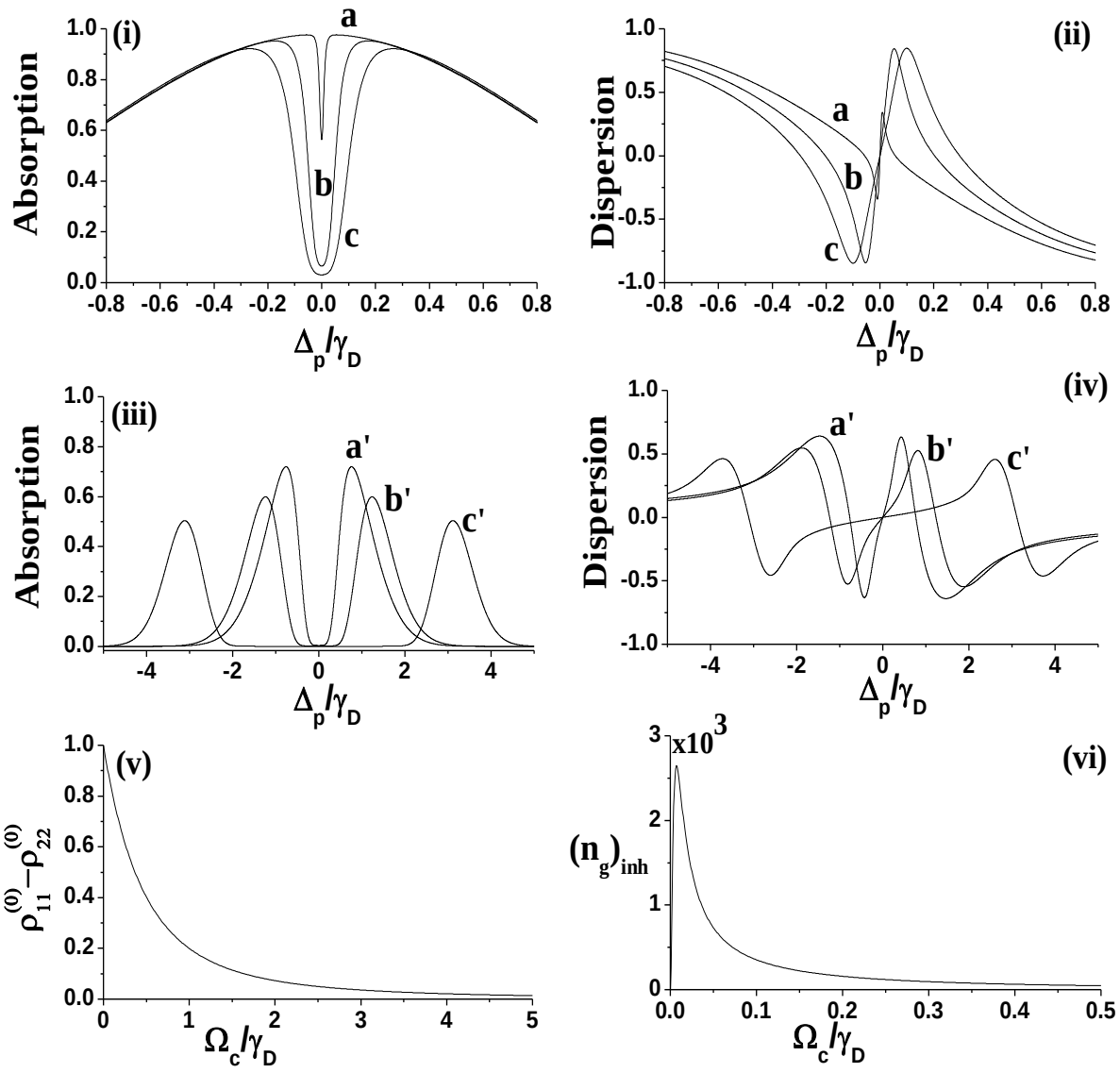

Fig. 4.3 *(i- iv)) Shows probe absorption (dispersion) as a function of probe detuning (Δ_p/γ_D). (v)-(vi) shows population difference and group index n_g as function of pump field Rabi frequency (Ω_c/γ_D) in a Doppler broadened medium. Curves a, b, c and a′, b′,c′ corresponds to pump Rabi frequency (Ω_c) values are as $0.005\gamma_D$, $0.05\gamma_D$, $0.1\gamma_D$ and $0.5\gamma_D$, $1\gamma_D$,$3\gamma_D$ respectively and $N=2x10^{12}$ atoms/cm^3.*

4.4 *Conclusions:*

To summarize, we have studied the effect of homogenous and inhomogeneous Doppler broadening medium influence on probe absorption (dispersion) and slow light phenomena in a V-type atomic system on closely spaced levels. In homogenous medium the reduction of probe absorption (dip) is mainly due to saturation and AT splitting effect at exact resonance, where a large two photon dephasing (γ_{32}) mask EIT process. To overcome the effect of two photon dephasing (γ_{32}) introduce inhomogeneous Doppler broadening effect (by heating cell), then under EIT condition it is possible to observe slow light effect at very small pump Rabi frequency Ω_c in a simple three level V-system. Finally we conclude that in an inhomogeneous Doppler broadened medium it is feasible to observe EIT effect under lower pump Rabi frequency whereas in a homogenous medium it is impossible to observe EIT effect. At higher pump Rabi frequency the probe absorption (dip) at line center (on resonance) is mainly due to AT splitting effect in both homogeneous and inhomogeneous Doppler broaden medium.

4.5 ***References:***

1. M. Fleischhauer et al., Phys. Rev. A **46**, 1468 (1992).

2. J. R. Boon, E. Zekou, D. J. Fulton, and M. H. Dunn, Phys. Rev. A **57**, 1323 (1998).

3. S. H. Autler and C. H. Townes, Phys. Rev. **100**, 703 (1955).

4. C. Cohen-Tannoudji and S.Reynaud, J. Phys. B **10**, 2311 (1997).

5. C. Cohen-Tannoudji, Amazing light (springer, Berlin,1996), Chap. **11**, pp. 109-123.

6. D. J. Fulton, S. Shepherd, R. R. Moseley, B. D. Sinclair, and M. H. Dunn, Phys. Rev. A **52**, 2302 (1995).

7. Y. Zhao, C. Wu, B.-S. Ham, M. K. Kim, and E. Awad, Phys. Rev. Lett. **79**, 641 (1997).

8. J. Zhao, L. Wang, L. Xiao, Y. Zhao, W. Yin, and S. Jia, Opt. Commun. **206**, 341 (2002).

9. S. Vdovic, T. Ban, D. Aumiler, and G. Pichler, Opt. Commun. **272**, 407 (2007).

10 L. Li, W. Tang, and H. Guo, Phys. Rev. A **76**, 053837 (2007).

11. P. S. Light, F. Benabid, G. J. Pearce, F. Couny, and D. M. Bird, Appl. Phys. Lett. **94**, 141103 (2009).

Chapter 5

Until now we studied the modification of absorption and dispersion properties of a (weak) probe light in three level atomic systems (of lambda, ladder or Vee type interaction scheme) due to presence of another strong (pump) light. The phenomenon of electromagnetically induced transparency (EIT) in such systems is seen to originate from a destructive interference between two distinct quantum mechanical paths leading to the excitation of the same upper level. However studies involving modification of EIT and its applications with inclusion of an additional fourth level have also been of considerable interest in recent times and are widely reported in literature. Such studies however are carried out mostly in closed-loop four-level systems of double Lambda (Λ), double ladder or diamond (◊) *configuration etc. In this chapter we discuss four wave mixing (FWM) using EIT scheme in a Doppler broadened medium comprising double lambda (Λ) systems with inclusion of buffer gas. The results obtained are shown to be analogous to observed experimental results in more complex and costly setups like cold atomic ensembles or atomic beams.*

5.1 *Introduction*

Suppression of linear absorption and modification of dispersion properties by electromagnetically induced transparency (EIT) also initiated various novel interaction schemes for enhancing nonlinear optical phenomena in absorbing media. One of these interesting nonlinear optical phenomena is the process of four-wave mixing. Harris *et al*. proposed using EIT to suppress absorption of the short-wavelength light generated in a four- wave mixing (FWM) scheme and showed that the FWM efficiency can be greatly enhanced [1]. Since then various groups [2-6] have studied FWM in four level systems using EIT [7]. Nonlinear optical phenomenon may also be observed at low light intensities approaching single photon energy levels [8]. Using EIT technique it is possible to explore quantum nonlinear optics and quantum information processes [9]. While studying double lambda-Λ systems one usually utilizes the continuous (CW) and plused lasers [10-13]. Korsunsky et. al. have studied the phase dependent *nonlinear optics* in double-lambda system [14]. The time dependent analysis of Ref [4,15] in forward FWM is limited by three photon destructive interference, in an ultraslow-propagation regime in an optically dense medium. Experimental studies of H. Kang *et al.* [16] in cold atomic

^{87}Rb, D1 transition (double-Λ system) using continuous-wave (cw) lasers shows slow light propagation and 10% efficiency for (backward) FWM scheme despite destructive interference of three photon and one photon excitation.

However, EIT and the FWM process in a vapor cell or solids at room temperature is affected by inhomogeneous broadening [13, 17, 18] arising due to thermal motion (in vapors) or local field fluctuations (in solids). For instance thermal motion of atoms in an atomic vapor can cause inhomogeneous broadening of distinct forms viz.(i) the transit time (or time of flight) broadening caused by movement of the atoms across the finite extent of the pump-probe beams in a transverse plane (to the z axis) [19], (ii) residual Doppler broadening owing to wave vector mismatch between pump and probe beams [20] propagating along z axis, and(iii) a small finite angular separation between pump-probe beams [21]. As we have mentioned earlier most studies of EIT and the associated nonlinear processes ignore the finite transit time (or time of flight) broadening that is of the order of γ_t ($\approx v_{th}k_{\perp} \approx v_{th}\, 2\pi/d$) where $v_{th} = (2k_BT/m_A)^{1/2}$ is the most probable thermal velocity of an atom of mass m_A at absolute temperature T and k_B is the Boltzmann constant. Therefore even in a room temperature atomic vapor, the transit time broadening, γ_t ($> 2\pi \times 0.1$ MHz) is much greater than the residual Doppler widths (of the order of a few KHz) induced by velocity component along z axis,

In this work we present a detailed theoretical study of EIT and the associated FWM process in a Doppler broadened medium comprising double lambda systems, including the effect of a buffer gas. The theory is more general as it includes various forms of Doppler broadening and other broadening (mentioned above) effects in presence of buffer gas in a vapor cell. In our study we consider cw laser fields (pump, coupler, probe, FWM signal), all the fields are coplanar and probe and FWM signals are weak compared with pump-coupler fields. An interaction scheme is considered in which all the applied field frequencies are on resonance. We utilize density matrix formalism and a strong collision model to incorporate dephasing and velocity changing collisions aspects of buffer gas into the theory.

5.2 *Formulation:*

We consider a typical four-level double Λ –type system shown in Figure 5.1. A strong laser (called pump) field given by $\vec{E}_c = \vec{\varepsilon}_c \exp\left[i\left(\vec{k}_c \cdot \vec{r} - \omega_c t\right)\right] + c.c.$, drives the transition $|2\rangle \leftrightarrow |3\rangle$

and a weak probe laser field, $\vec{E}_p = \varepsilon_p \exp[i(\vec{k}_p \cdot \vec{r} - \omega_p t)] + c.c.$ acts on the transition $|1> \leftrightarrow |3>$ forming a standard Λ type configuration. The spontaneous decay rates from level $|3>$ to levels $|2>$ and $|1>$ are γ_{32} and γ_{31} respectively. Another coupling (or control) laser field $\vec{E}_s = \vec{\varepsilon}_s \exp[i(\vec{k}_s \cdot \vec{r} - \omega_s t)] + c.c.$, drives the transition $|2> \leftrightarrow |4>$ and generates a non degenerate FWM signal field $\vec{E}_e = \vec{\varepsilon}_e \exp[i(\vec{k}_e \cdot \vec{r} - \omega_e t)] + c.c.$, with a wave vector $\vec{k}_e$ and frequency ω_e. The phase matching condition is given by $\vec{k}_e = \vec{k}_p - \vec{k}_c + \vec{k}_s$ where $\vec{k}_p$, $\vec{k}_c$ are the wave vectors of the probe and coupling fields respectively, and $\vec{k}_s$ is the wave vector of pump field. The spontaneous decay rates of the upper level $|4>$ to levels $|1>$ and $|2>$ are γ_{41} and γ_{42} respectively. We assume the standard EIT condition $\Omega_p << \Omega_c$ and $\Omega_e << \Omega_s$ where Ω_p $(=\mu_{31} \cdot \vec{\varepsilon}_p/\hbar)$, Ω_e $(=\mu_{41} \cdot \vec{\varepsilon}_e/\hbar)$, Ω_c $(=\mu_{32} \cdot \vec{\varepsilon}_c/\hbar)$, and Ω_s $(=\mu_{42} \cdot \vec{\varepsilon}_s/\hbar)$, are the Rabi frequencies of the probe, FWM signal, strong pump and coupler fields.

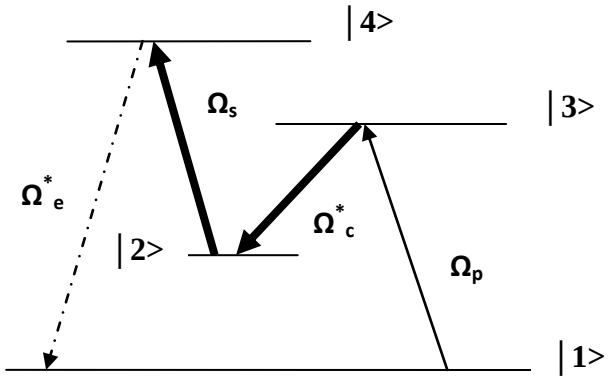

Fig.5.1: *EIT and FWM scheme in double ladder configuration. Here Ω_p , Ω_e , Ω_c and Ω_s are the Rabi frequencies of the probe, FWM signal, strong pump and coupler fields.*

5.2 a) ***Interaction Hamiltonian:***

The Hamiltonian describing interaction of the fields and system under condition of near resonant excitation is obtained in the interaction picture as

$$V^{int} = -\hbar \left[\Omega_p \exp\left[i(\vec{k}_p \cdot \vec{r} + \Delta_p t)\right] S_{31} + \Omega_c \exp\left[i(\vec{k}_c \cdot \vec{r} + \Delta_c t)\right] S_{32} + \Omega_s \exp\left[i(\vec{k}_s \cdot \vec{r} + \Delta_s t)\right] S_{42} + \Omega_e \exp\left[i(\vec{k}_e \cdot \vec{r} + \Delta_e t)\right] S_{41} + H.c.\right], \quad (5.1)$$

where $\Delta_p = (\omega_{31} - \omega_p)$, $\Delta_c = (\omega_{32} - \omega_c)$, $\Delta_s = (\omega_{42} - \omega_s)$ and $\Delta_e = (\omega_{41} - \omega_e)$ denote detuning of the probe, pump, coupling and signal field frequencies from atomic resonance frequencies ω_{31},ω_{32}, ω_{42} and ω_{41} respectively. $S_{ij} = |i\rangle\langle j|$, (i, j = 1,2,3,4) are the atomic raising or lowering operators.

5.2 ***b) Density matrix formulation:***

The equations describing time evolution of the slowly varying components of the density matrix elements $\tilde{\rho}_{ij}(v,t)$ can be obtained using Eqs.(5.1), (1.8b), (1.10), and (1.16) in Eq. (1.11). Thereafter using appropriate transformations to eliminate fast oscillating (exponential) terms together with the frequency and phase matching conditions $\Delta_e - \Delta_s = \Delta_p - \Delta_c$ and $\vec{k}_e - \vec{k}_s = \vec{k}_p - \vec{k}_c$ for the FWM process, the equations of motion for the slowly varying density matrix elements $\tilde{\rho}_{ij}(v,t)$ can be obtained.

The abovementioned derivation of density matrix elements is simplified considerably if we first consider the physical process underlying EIT and FWM. Analogous to a three level Λ case (where only a single strong field is applied) application of two strong cw (pump and coupler) fields result in rapid optical pumping of all the atomic populations into the ground state |1>. Thus before application of a probe (or generated) field, initially all the population (to zero order in probe and signal fields), $\rho_{11}^{(0)}(v)$ is in the ground level $|1\rangle$ with a thermal, i.e., Maxwell velocity (3 dimensional) distribution given by

$$\rho_{11}^{(0)}(v) = M(v) = [\ln 2/(\pi\bar{v}^2)]^{3/2} \exp(-\ln 2\, \vec{v}\cdot\vec{v}/\bar{v}^2)\,. \qquad (5.2)$$

Here $\bar{v} = \sqrt{\ln 2}\, v_{th}$ and $v_{th} = \sqrt{2k_B T/m_A}$ is the most probable velocity at temperature T of an atom of mass m_A. If the applied probe and generated signal fields are sufficiently weaker (than pump and coupler), nearly all the population continues to occupy the ground level. Under these conditions the equations of motion for the relevant slowly varying atomic variables are obtained as

$$\dot{\tilde{\rho}}_{21} = -\{\, i[(\Delta_p - \Delta_c) + (\vec{k}_p - \vec{k}_c)\cdot\vec{v}\,] + (\gamma_{21} + \Gamma_{12})\}\tilde{\rho}_{21} + i\Omega_c^*\tilde{\rho}_{31} + i\Omega_s^*\tilde{\rho}_{41} + \Gamma_{21}\, M(v)\int \tilde{\rho}_{21}(v',t)d^3v'\,, \qquad (5.3a)$$

$$\dot{\tilde{\rho}}_{31} = -\left\{i(\Delta_p + \vec{k}_p\cdot\vec{v}) + \gamma_p + \tfrac{\gamma_{31}+\gamma_{32}}{2}\right\}\tilde{\rho}_{31} + i\Omega_p\,\rho_{11}^{(0)}(v) + i\Omega_c\,\tilde{\rho}_{21}\,, \qquad (5.3b)$$

$$\dot{\tilde{\rho}}_{41} = -\left\{i\left(\Delta_e + \vec{k}_e \cdot \vec{v}\right) + \gamma_p + \frac{\gamma_{41}+\gamma_{42}}{2}\right)\right\}\tilde{\rho}_{41} + i\Omega_e\,\rho_{11}^{(0)}(v) + i\Omega_s\,\tilde{\rho}_{21} \quad . \tag{5.3c}$$

The following transformations were used in deriving the above set of equations of motion (Eq.(5.3)) for the density matrix elements :

$$\rho_{31} = \tilde{\rho}_{31}\, e^{i(\vec{k}_p\cdot\vec{r}+\Delta_p t)}\,, \tag{5.4a}$$

$$\rho_{41} = \tilde{\rho}_{41}\, e^{i(\vec{k}_e\cdot\vec{r}+\Delta_e t)}\,, \tag{5.4b}$$

$$\rho_{21} = \tilde{\rho}_{21}\, e^{i[(\vec{k}_p-\vec{k}_c)\cdot\vec{r}+(\Delta_p-\Delta_c)t]} = \tilde{\rho}_{21}\, e^{i[(\vec{k}_e-\vec{k}_s)\cdot\vec{r}+(\Delta_e-\Delta_s)t]}. \tag{5.4c}$$

The above density matrix equations for slowly varying atomic variables are written in plane-wave approximation for the probe (FWM signal) and pump (coupler) fields. In typical experimental situation a co-propagating geometry is utilized in which all the applied and generated fields are propagating along z direction. Thus the Doppler shift terms in Eq.(5.3) can henceforth be expressed as $\vec{k}_m \cdot \vec{v} = k_m v_z$, (m = p, e) and $\left(\vec{k}_p - \vec{k}_c\right)\cdot\vec{v} = (k_p - k_c)\, v_z$.

5.2 c) ***Inclusion of transit time broadening:***

The plane-wave approximation is valid and is utilized in most studies of the EIT and slow light performed using sufficiently large, well collimated probe beam diameter. For sufficiently large laser beam diameters [20] the transit time broadening effects arising from finite extent of the laser beam intensity in the transverse plane can be ignored. Eqs.(5.3) can be further generalized to include the finite beam width (in a transverse plane to propagation axis- z direction) of the probe and generated (signal) beam by replacing Ω_p and Ω_e with space-time dependent probe and signal amplitude $\Omega_p(r_\perp, t)$ and $\Omega_e(r_\perp, t)$. Consequently including space dependence in the slowly varying quantities $\tilde{\rho}_{ij}(r_\perp, t, v)$, introducing the Fourier transformation of a function as

$$f(r_\perp, t, v) = \int_{-\infty}^{+\infty} \frac{d^2 q_\perp}{(2\pi)^2}\, e^{i\vec{q}_\perp\cdot\vec{r}_\perp} \int_{-\infty}^{+\infty} \frac{d\omega}{2\pi}\, e^{-i\omega t}\, f(q_\perp, \omega, v) \tag{5.5}$$

and using equations (1.10) and (5.5) in Eq (5. 3) we get

$$\left\{i\left(\Delta_p - \omega\right) + i(k_p v_z + \vec{q}_\perp\cdot\vec{v}_\perp) + \gamma_p + \frac{\gamma_{31}+\gamma_{32}}{2}\right)\right\}\tilde{\rho}_{31}(q_\perp, \omega, v) = i\Omega_p\,\rho_{11}^{(0)}(v) + i\Omega_c\tilde{\rho}_{21}(q_\perp, \omega, v), \tag{5.6a}$$

$$\left\{i(\Delta_e - \omega) + i(k_e v_z + \vec{q}_\perp \cdot \vec{v}_\perp) + \gamma_p + \frac{\gamma_{41}+\gamma_{42}}{2})\right\}\tilde{\rho}_{41}(q_\perp, \omega, v) = i\Omega_e\, \rho_{11}^{(0)}(v) + i\Omega_s \tilde{\rho}_{21}(q_\perp, \omega, v), \quad (5.6b)$$

$$\left\{i[(\Delta_p - \Delta_c) - \omega] + i(k_p - k_e)v_z + i\,\vec{q}_\perp \cdot \vec{v}_\perp + (\gamma_{21} + \Gamma_{12})\right\}\tilde{\rho}_{21}(q_\perp, \omega, v)$$
$$= i\Omega_c^* \tilde{\rho}_{31}(q_\perp, \omega, v) + i\Omega_s^* \tilde{\rho}_{41}(q_\perp, \omega, v) + \Gamma_{21} M(v) \int \tilde{\rho}_{21}(q_\perp, \omega, v')d^3v', \quad (5.6c)$$

We now proceed to obtain, from the set of Eqs.(5.6), the one-photon coherences from which the characteristics of the probe and signal fields can be determined. For arbitrarily strong pump and coupler fields, we solve the above set of density-matrix equations to leading order in the (Rabi) amplitude of a weak probe, Ω_p and generated FWM field, Ω_e. This is done by first replacing Ω_p and Ω_e by $\lambda_p\Omega_p$ and $\lambda_e\Omega_e$ (where λ_p and λ_e are perturbation expansion parameters) and using the following expansion for the density matrix elements in Eq.(5.6):

$$\tilde{\rho}_{ij} = \lambda_e \tilde{\rho}_{ij}^{(\Omega_e)} + \lambda_p \tilde{\rho}_{ij}^{(\Omega_p)} + \ldots\ldots . \quad (5.7)$$

Here $\tilde{\rho}_{ij}^{(\Omega_p)}$ and $\tilde{\rho}_{ij}^{(\Omega_e)}$ are the one-photon coherences to first order in the Rabi amplitude Ω_p and Ω_e respectively, of the probe and signal fields. Using the above procedure we find that the relevant first order density matrix equations are:

$$A_{41}\tilde{\rho}_{41}^{(\Omega_p)}(q_\perp, \omega, v) = i\Omega_s \tilde{\rho}_{21}^{(\Omega_p)}(q_\perp, \omega, v)\,, \quad (5.8a)$$

$$A_{31}\tilde{\rho}_{31}^{(\Omega_p)}(q_\perp, \omega, v) = i\Omega_p M(v) + i\Omega_c \tilde{\rho}_{21}^{(\Omega_p)}(q_\perp, \omega, v)\,, \quad (5.8b)$$

$$A_{21}\tilde{\rho}_{21}^{(\Omega_p)}(q_\perp, \omega, v) = i\Omega_c^* \tilde{\rho}_{31}^{(\Omega_p)}(q_\perp, \omega, v) + i\Omega_s^* \tilde{\rho}_{41}^{(\Omega_p)}(q_\perp, \omega, v) + \Gamma_{21} M(v) \int \tilde{\rho}_{21}^{(\Omega_p)}(q_\perp, \omega, v')d^3v', \quad (5.8c)$$

$$A_{41}\tilde{\rho}_{41}^{(\Omega_e)}(q_\perp, \omega, v) = i\Omega_e M(v) + i\Omega_s \tilde{\rho}_{21}^{(\Omega_e)}(q_\perp, \omega, v)\,, \quad (5.8d)$$

$$A_{31}\tilde{\rho}_{31}^{(\Omega_e,)}(q_\perp, \omega, v) = i\Omega_c \tilde{\rho}_{21}^{(\Omega_e)}(q_\perp, \omega, v)\,, \quad (5.8e)$$

$$A_{21}\tilde{\rho}_{21}^{(\Omega_e)}(q_\perp, \omega, v) = i\Omega_c^* \tilde{\rho}_{31}^{(\Omega_e)}(q_\perp, \omega, v) + i\Omega_s^* \tilde{\rho}_{41}^{(\Omega_e)}(q_\perp, \omega, v) + \Gamma_{21} M(v) \int \tilde{\rho}_{21}^{(\Omega_e)}(q_\perp, \omega, v')d^3v'. \quad (5.8f)$$

Here

$$A_{41}(q_\perp,\omega,v) = \left\{ i(\Delta_e - \omega) + i(k_e v_z + \vec{q}_\perp\cdot\vec{v}_\perp) + \left(\gamma_p + \frac{\gamma_{41}+\gamma_{42}}{2}\right)\right\}, \quad (5.9a)$$

$$A_{31}(q_\perp,\omega,v) = \left\{ i\left(\Delta_p - \omega\right) + i(k_p v_z + \vec{q}_\perp\cdot\vec{v}_\perp) + \left(\gamma_p + \frac{\gamma_{31}+\gamma_{32}}{2}\right)\right\}, \quad (5.9b)$$

$$A_{21}(q_\perp,\omega,v) = \left\{ i[\left(\Delta_p - \Delta_c\right) - \omega] + i(k_p - k_e)v_z + i\,\vec{q}_\perp\cdot\vec{v}_\perp] + \left(\gamma_{21} + \Gamma_{21}\right)\right\}. \quad (5.9c)$$

Eq. (5.8) can be solved for the coherences, ρ_{jk} in the interaction picture that are related to their counterparts in the Schrodinger picture, ρ^s_{kj} through the relation $\rho_{jk} = \rho^s_{jk} e^{i\omega_{jk}t}$. Thus the *slowly varying, velocity averaged* coherences (to first order in Rabi amplitudes of the probe and signal) in the Schrodinger picture, henceforth denoted $I^{(\Omega_m)}_{jk}$ for brevity (by dropping the superscript, s) can be obtained as

$$I^{(\Omega_p)}_{31}(q_\perp,\omega) = e^{-i(\vec{k}_p\cdot\vec{r}-\omega_p t)}\int \rho^{(\Omega_p)}_{31}(q_\perp,\omega,v)\, d^3v$$

$$= i\Omega_p\left[\int \frac{(A_{21}A_{41} + |\Omega_s|^2)M(v)d^3v}{A_{31}A_{41}\xi} - \Gamma_{21}|\Omega_c|^2 \frac{\left\{\int \frac{M(v)d^3v}{A_{31}\xi}\right\}^2}{\left\{1 - \Gamma_{21}\int \frac{M(v)d^3v}{\xi}\right\}}\right], \quad (5.10a)$$

$$I^{(\Omega_e)}_{41}(q_\perp,\omega) = e^{-i(\vec{k}_e\cdot\vec{r}-\omega_e t)}\int \rho^{(\Omega_e)}_{41}(q_\perp,\omega,v)\, d^3v$$

$$= i\Omega_e\left[\int \frac{(A_{21}A_{31} + |\Omega_c|^2)M(v)d^3v}{A_{31}A_{41}\xi} - \Gamma_{21}|\Omega_s|^2 \frac{\left\{\int \frac{M(v)d^3v}{A_{41}\xi}\right\}^2}{\left\{1 - \Gamma_{21}\int \frac{M(v)d^3v}{\xi}\right\}}\right], \quad (5.10b)$$

$$I^{(\Omega_e)}_{31}(q_\perp,\omega) = e^{-i(\vec{k}_p\cdot\vec{r}-\omega_p t)}\int \rho^{(\Omega_e)}_{31}(q_\perp,\omega,v)\, d^3v$$

$$= -i\Omega_e\Omega_s^*\Omega_c\left[\int \frac{M(v)d^3v}{A_{31}A_{41}\xi} + \Gamma_{21}\frac{\left\{\int \frac{M(v)d^3v}{A_{31}\xi}\right\}\left\{\int \frac{M(v)d^3v}{A_{41}\xi}\right\}}{\left\{1 - \Gamma_{21}\int \frac{M(v)d^3v}{\xi}\right\}}\right], \quad (5.11a)$$

$$I^{(\Omega_p)}_{41}(q_\perp,\omega) = e^{-i(\vec{k}_e\cdot\vec{r}-\omega_e t)}\int \rho^{(\Omega_p)}_{41}(q_\perp,\omega,v) d^3v$$

$$= -i\Omega_p\Omega_s\Omega_c^*\left[\int \frac{M(v)d^3v}{A_{31}A_{41}\xi} + \Gamma_{21}\frac{\left\{\int \frac{M(v)d^3v}{A_{31}\xi}\right\}\left\{\int \frac{M(v)d^3v}{A_{41}\xi}\right\}}{\left\{1 - \Gamma_{21}\int \frac{M(v)d^3v}{\xi}\right\}}\right]. \quad (5.11b)$$

where

$$\xi(q_\perp,\omega,v) = A_{21}(q_\perp,\omega,v) + |\Omega_c|^2/A_{31}(q_\perp,\omega,v) + |\Omega_s|^2/A_{41}(q_\perp,\omega,v) \ . \quad (5.12)$$

An inspection of Eq.(5.10) shows that these coherences are directly proportional to either the probe or signal field Rabi frequency. Thus these are proportional to the linear polarization and hence the real and imaginary parts of Eq.(5.10) describe dispersion and absorption of probe and signal fields in the inhomogeneously broadened double lambda system. On the other hand Eq.(5.11) reveals that these coherences are proportional to the product of the Rabi frequencies of the other three fields, that is, these yield the nonlinear polarization arising due to the frequency mixing of the other three fields.

5.3 *Propagation of the signal and probe waves:*

To calculate the efficiency of the generated FWM signal we consider the propagation of the weak signal and probe waves through an extended medium composed of double (Λ) systems. In chapter 3 we have developed a formalism for propagation of a probe *pulse* through an EIT medium comprising of three level Λ systems. Although that formalism can be applied here, for the sake of simplicity and clarity, in the present case we consider the applied probe (and therefore the generated signal) pulses to be of very large duration in time, i. e., the probe (and the signal) can be approximated as nearly monochromatic, cw fields. Consequently for this case we can use steady state solutions for the coherences obtained by setting $\omega = 0$ in Eqs.(5.10) and (5.11). Propagation of a field of the form given by Eq.(1.3) is described by the Maxwell's wave equation

$$(\nabla^2 - \frac{1}{c^2}\frac{\partial^2}{\partial t^2})E_a = \frac{4\pi}{c^2}\frac{\partial^2}{\partial t^2}(P_a^L + P_a^{NL}) \ , \ (a = e, p) \quad (5.13)$$

where P_a^L and P_a^{NL} respectively, are the macroscopic linear and nonlinear polarizations associated with and aligned along the direction of the field $\vec{E}_a$. In general the macroscopic polarization P, i.e., the ensemble average of the induced dipole moment per unit volume in a medium of number density N is given by

$$P = N\,Tr(\mu < \rho >) = \sum_{j,k=1}^{4} \mu_{jk} < \rho_{kj} > = \mu_{13} < \rho_{31} > + \mu_{14} < \rho_{41} > + c.c., \quad (5.14)$$

Here angular brackets < > denote averaging over thermal velocities$< \rho_{ij} > = \int \rho_{ij}(v)dv$. The induced macroscopic linear and non linear polarization is in the medium is proportional to velocity averaged coherence (off diagonal elements) $I_{j1}^{(\Omega_e)}$, $I_{j1}^{(\Omega_p)}$ where j = 3 and 4. Thus we can write the polarization in the form (using the notation of Eqs.(5.9) and (5.10)) :

$$P_{41} = N\mu_{14}\left(I_{41}^{(\Omega_e)} + I_{41}^{(\Omega_p)}\right)e^{i(\vec{k}_e.\vec{r}-\omega_e t)} + c.c.\,, \tag{5.15a}$$

$$P_{31} = N\mu_{13}\left(I_{31}^{(\Omega_p)} + I_{31}^{(\Omega_e)}\right)e^{i(\vec{k}_p.\vec{r}-\omega_p t)} + c.c.\,, \tag{5.15b}$$

Substituting Eqs. (5.15a) and (5.15b) along with Eq. (1.3) in Eq.(5.13) and assuming the validity of the slowly-varying amplitude approximation and neglecting diffraction of the beams in the transverse plane, we get the following coupled waves equations for signal and probe field amplitudes:

$$\frac{\partial \mathcal{E}_e}{\partial z} = \frac{\alpha_e}{2}\mathcal{E}_e + \frac{\beta_e}{2}\mathcal{E}_p\,, \tag{5.16a}$$

$$\frac{\partial \mathcal{E}_p}{\partial z} = \frac{\alpha_p}{2}\mathcal{E}_p + \frac{\beta_p}{2}\mathcal{E}_e\,. \tag{5.16b}$$

The second term β_j , (j = s, p) on the right-hand side of Eqs. (5.16a) and (5.16b) essentially represents mutual coupling between the probe field and the FWM field while the first terms α_j (j = s, p) describe absorption and dispersion properties of the atomic medium. These are given by

$$\alpha_e = i\frac{8\pi^2 N|\mu_{14}|^2}{\lambda_e \hbar \gamma_D}\left(\frac{I_{41}^{(\Omega_e)}}{\Omega_e/\gamma_D}\right)\,, \tag{5.17a}$$

$$\alpha_p = i\frac{8\pi^2 N|\mu_{13}|^2}{\lambda_p \hbar \gamma_D}\left(\frac{I_{31}^{(\Omega_p)}}{\Omega_p/\gamma_D}\right)\,, \tag{5.17b}$$

$$\beta_e = i\frac{8\pi^2 N|\mu_{13}||\mu_{14}|}{\lambda_e \hbar \gamma_D}\left(\frac{I_{41}^{(\Omega_p)}}{\Omega_p/\gamma_D}\right)\,, \tag{5.17c}$$

$$\beta_p = i\frac{8\pi^2 N|\mu_{13}||\mu_{14}|}{\lambda_p \hbar \gamma_D}\left(\frac{I_{31}^{(\Omega_e)}}{\Omega_e/\gamma_D}\right) . \quad (5.17d)$$

It should be noted that since $\alpha_m \propto iI_{j1}^{(\Omega_m)}$, (m = e, p and j = 3, 4) the *real* and *imaginary* parts of α_e (α_p) respectively, describe absorption and dispersion properties of the generated signal (probe) field in the medium. The dispersion vanishes at line center since the imaginary part of α_e (α_p) is zero at exact resonance. Thus it can be shown and verified numerically that the coefficients α_m and β_m, (m = e, p) given by Eqs. (5.17) are purely real at line center. For this particular case in which all fields are on resonance, together with the boundary condition at the input $\varepsilon_p(z=0) = \varepsilon_p(0)$ and $\varepsilon_e(z=0) = 0$, we can solve the coupled Eqs.(5.16) to obtain the field amplitudes for the signal, $\varepsilon_e(z)$ and the probe wave, $\varepsilon_p(z)$ in the medium as

$$\frac{\varepsilon_e(z)}{\varepsilon_p(0)} = \frac{\beta_e}{2\Phi}\exp\left\{\left[\frac{\alpha_p+\alpha_e}{2}\right]z\right\}\sinh(\Phi z) , \quad (5.18a)$$

$$\frac{\varepsilon_p(z)}{\varepsilon_p(0)} = \exp\left\{\left[\frac{\alpha_p+\alpha_e}{2}\right]z\right\}\left(\cosh(\Phi z) + \frac{(\alpha_p-\alpha_e)}{4\Phi}\sinh(\Phi z)\right) , \quad (5.18b)$$

where $\Phi = \sqrt{\beta_e\beta_p/4 + (\alpha_p/4 - \alpha_e/4)^2}$. (5. 18c)

It is also evident that Eq.(5.16b) (and similarly (5.16a) can be obtained from the probe pulse propagation equation (3.41) developed in Chapter 3 in the steady state limit (time derivatives are zero), assuming negligible (diffraction) variation in probe pulse envelope in the transverse plane compared with that in the z direction ($i\frac{c}{2\omega_p}q_\perp^2 \ll \frac{\partial}{\partial z}$) and for nonlinear polarization component generated at wave vector $k_{nl} = k_p$ (or k_e).

5.4 *Results and discussion*:

We now present numerical results for EIT and propagation effects of the probe and generated FWM signal by applying the theory to a rubidium atomic vapor. The double lambda system can be realized, for example, by excitation of the $5S_{1/2}\rightarrow 5P_{1/2}$ transition with energy level separation wave length λ= 795 nm in a ^{87}Rb atom using (strong) pump, coupler and (weak) probe laser

fields. The tuning the field frequencies to the combination of the upper level $5P_{1/2}$ and hyperfine substructure of the ground state $5S_{1/2}$ makes the system a four-level double lambda system [7, 8]. In our numerical calculations both drive fields (pump and coupler) are fixed on resonance with their respective transitions. The dephasing rate of the two-photon coherence excited between the two (unlinked) lower states $|1\rangle$ and $|2\rangle$ is around $\gamma_{21} = 2\pi \times 200$ Hz at an atomic density, N = 2×10^{12} atoms/cm^3 of the ^{87}Rb vapor [22]. For a Ne buffer gas (of pressure p Torr) in the vapor cell, the velocity changing collision parameter is $\Gamma_{21}/2\pi$ (= p×2MHz) and the collisional dephasing parameter is given by, $\gamma_p = 2.7 \times \Gamma_{21}$. All parameters are expressed in units of the Doppler width $\gamma_D/2\pi = 270$ MHz. An optimum value of the velocity changing collision parameter, $\Gamma_{21} = 0.085\gamma_D$ (which corresponds to a fixed Ne buffer gas pressure, p = 11.5 Torr) is used in all numerical calculations.

The EIT phenomenon for both the probe and generated signal field is illustrated in Fig.5.2 by plotting the absorption characteristics as a function of the two photon detuning δ/γ_D. The pump Rabi frequency is fixed at a value $\Omega_c/\gamma_D = 0.03$ and the coupler Rabi frequency (Ω_s/γ_D) values are varied through 0, 0.01, 0.03 and 0.05. Curves **a** and **b** in Fig.5.2 (i) are the probe absorption profiles (given by the imaginary part of the coherence, $I_{31}^{(\Omega_p)}\gamma_D/\Omega_p$) in the absence of the coupler field i.e., $\Omega_s/\gamma_D = 0$. Thus curves **a** and **b** display respectively, the effect of transit time broadening and buffer gas on the typical absorption profiles of a probe beam in an isolated three level Λ system. From the absorption profile in the absence of the buffer gas (curve **a**) it is clear that substantial absorption occurs due to the transit time broadening. In contrast, the probe absorption profile in the presence of (11.5 Torr) Ne buffer gas (curve **b**) shows that velocity changing collisions give rise to perfect EIT at line center by eliminating the transit time broadening. At higher detuning values absorption is lower due to the presence of large collisional depahsing γ_p . Nonlinear generation cannot occur in the absence of the coupler field, $\Omega_s/\gamma_D = 0$. In Fig. 2(i) [2(ii)] the curves **c, d,** and **e** [**c′, d′** and **e′**] depict the probe (signal) absorption profiles in the presence of (11.5 Torr) Ne buffer gas as the value of the coupler Rabi frequency, Ω_s/γ_D is varied through 0.01, 0.03 and 0.05. Curves **c, d,** and **e** (in Fig5.2 (i)) reveal that the on-resonance probe absorption increases (or probe EIT diminishes) as one increases the strength of the coupling field amplitude Ω_s/γ_D. Simultaneously curves **c′, d′** and **e′** (in Fig.5.2(ii)) which

depict the signal absorption profiles (obtained from imaginary part of $I_{41}^{(\Omega_e)}\gamma_D/\Omega_e$) also show a similar but reverse trend. That is, initially for weak coupling field amplitudes Ω_s/γ_D , signal absorption is very high. As the coupling field amplitude increases, the line center ($\Delta_e = \Delta_p = 0$) signal absorption decreases (or EIT increases), become equal to probe absorption when both the strong driving fields are equal, $\Omega_c = \Omega_s$ and continues to decrease with further increase in coupling field amplitude. This decrease in EIT of the probe field can be attributed to creation of an additional (third) absorption channel when the coupler field is applied on the |2>→|4> transition, due to which the destructive interference that causes EIT is incomplete.

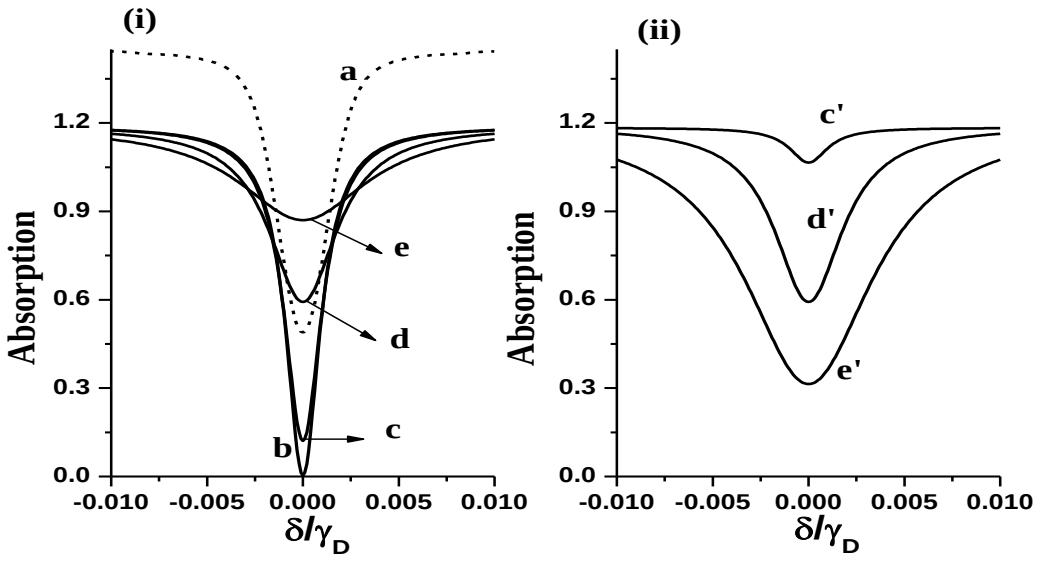

Fig.5.2: *EIT of (i) probe and (ii) generated FWM signal as a function of two photon detuning δ/γ_D for a fixed pump Rabi frequency (Ω_c/γ_D) = 0.03 and various coupling field Rabi frequencies (Ω_s/γ_D). (i) Curves **a** and **b** distinguish the effect of buffer gas collisions on typical EIT characteristics of an isolated lambda system (obtained when coupler field, $\Omega_s/\gamma_D = 0$). Curve **a** is the absorption profile in the absence of the buffer gas ($\Gamma_{21} = 0$) whereas curve **b** is that in the presence of a Ne buffer gas (of pressure **p**=11.5 Torr) corresponding to a velocity changing collision parameter $\Gamma_{21} = 0.085\gamma_D$. Curves **c, d** and **e** in (i) are the probe absorption profiles and **c′, d′** and **e′** in (ii) are those for the signal field in*

the presence of a buffer gas of pressure ***p****=11.5 Torr (* Γ_{21} *= 0.085*γ_D*). The coupler Rabi frequencies (*Ω_s/γ_D*) values for* ***c, c′*** *is 0.01,* ***d, d′*** *is 0.03 and* ***e, e′*** *is 0.05. The buffer gas dephasing parameter for Ne is,* $\gamma_p = 2.7\Gamma_{21}$.

It is well known that EIT in an (isolated) three level Λ system such as, for instance, that formed by the transitions |1>→|3>→|2> is caused by destructive interference between a one-photon (direct) probe absorption path |1>→|3> and another (indirect) three-photon path created via the transitions |1>→|3>→|2>→|3>. Now application of a third (coupler) field on the transition |2>→|4> (which generates a signal field on the transition |1>→|4>) in turn creates an additional three-photon |1>→|4>→|2>→|3> path for excitation of the level |3>, the strength of which depends upon the coupler field intensity. This can be seen from the $|\Omega_s|^2$ dependent second term in the numerator (of the first term) of Eq.(5.10a). Similar inference can be drawn for the adjacent Λ subsystem formed by the generated signal and the coupler field which through the action of the pump field Ω_s/γ_D (see the $|\Omega_c|^2$ dependent second term in the numerator (of the first term) of Eq.(5.10b)) affects the EIT of the signal field. It is clear from the above Figures that when the coupler and pump amplitudes (or intensities) become equal, the minimum EIT possible in each lambda subsystem is only 50% of that for an isolated lambda system.

Furthermore, in Fig.5.3 line center (i.e., on-resonance, $\Delta_p = \Delta_e = 0$) absorption values for probe (curves **p**) and generated FWM signal (curves **e**) are plotted as a function of the coupler field Rabi frequency Ω_s/γ_D for two distinct values of pump field Rabi frequencies, $\Omega_c/\gamma_D = 0.02$ (solid curves) and $\Omega_c/\gamma_D = 0.03$ (dashed curves). Also shown in this figure are the gain factor, obtained from the imaginary part of the nonlinear coherence, $I_{31}^{(\Omega_p)}(\frac{\gamma_D}{\Omega_p})$ [Eq.(5.11a)] or $I_{41}^{(\Omega_p)}\gamma_D/\Omega_p$ [Eq.(5.11b)] as a function of the coupler amplitude Ω_s/γ_D for a fixed pump amplitudes Ω_c/γ_D. Since the same parameters $|\mu_{13}| \cong |\mu_{14}|$, $\lambda_e \cong \lambda_p$ and N appear in the expressions for absorption and gain coefficients defined by Eq.(5.17), the absorption α_p , α_e and gain coefficients β (=β_p= β_e) as defined in Eqs.(5.17) can be obtained from the line center absorption and gain factor values depicted on y-axis of Fig.5.3 by multiplying by a factor η (= $-\frac{8\pi^2 N|\mu_{13}|^2}{\lambda_p \hbar \gamma_D}$). From Fig. 5.3(i) we find that the contributions from gain factor (for nonlinear

generation β) and absorption (loss α) to the FWM signal (and probe) field are opposite in sign and the magnitudes of these are unequal ($\alpha \neq \beta$) for the pump and coupler fields, Ω_c/γ_D= Ω_m/γ_D= 0.02 and 0.03. This is the effect of transit time broadening ($\vec{q}_\perp.\vec{v}$) due to which even when the absorption loss in both lambda subsystems becomes equal, α (= $\alpha_p = \alpha_e$) when Ω_c=Ω_s , the gain factor (nonlinear generation coeffcient β) is different from the absorption coefficient. Therefore transit time broadening ($\vec{q}.\vec{v}$) has major influence on absorption (loss α) and gain factor (generation coeffcient β) of both probe and generated FWM signals.

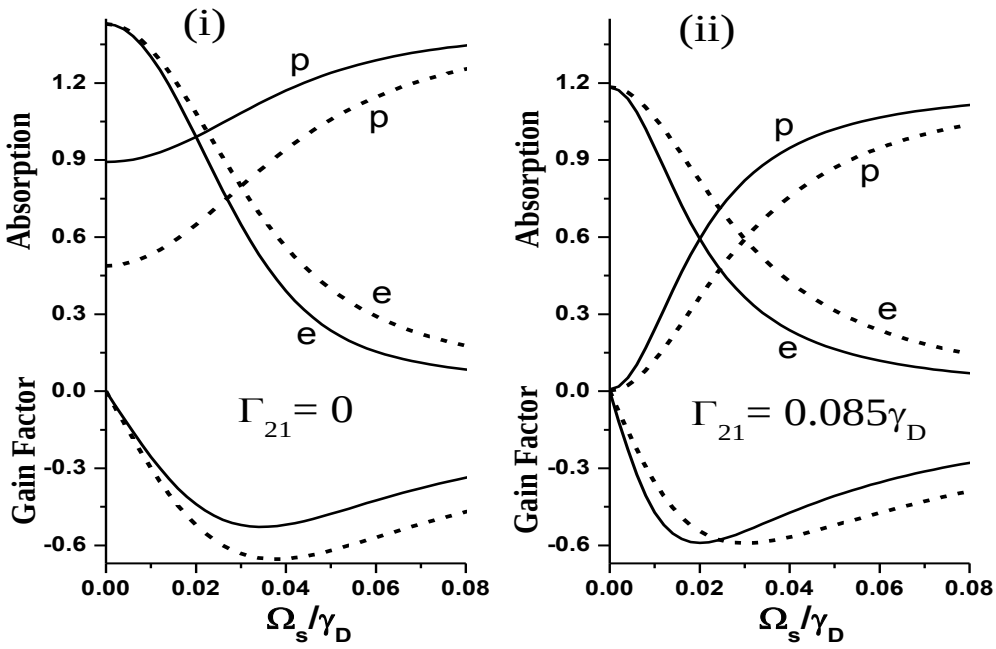

Fig.5.3: *(i) and (ii). The effect of buffer gas on absorption and gain factor values at line center (i.e., on-resonance,* $\Delta_p = \Delta_e = 0$*) for probe (curves* ***p****) and generated FWM signal (curves* ***e****) plotted as a function of the coupler field Rabi frequency* Ω_s/γ_D *for two distinct values of pump field Rabi frequencies,* $\Omega_c/\gamma_D = 0.02$ *(solid curves) and* $\Omega_c/\gamma_D = 0.03$ *(dashed curves). The gain factor is obtained from the imaginary part of the nonlinear coherence,* $I_{31}^{(\Omega_e)}\gamma_D/\Omega_p$ *[Eq.(5.11a)] and is identical in value to that obtained from* $I_{41}^{(\Omega_p)}\gamma_D/\Omega_p$ *[Eq.(5.11b)].* Since the parameters $|\mu_{13}| \cong |\mu_{14}|$ and $\lambda_e \cong \lambda_p$ *the absorption coefficients* α_p *,* α_e *and nonlinear gain parameter* β *(=*β_p*=* β_e *) as defined in Eqs.(5.17) are obtained*

respectively, by multiplying the line center absorption and gain factor values depicted on y-axis by a factor η *(*$= -\frac{8\pi^2 N|\mu_{13}|^2}{\lambda_p \hbar \gamma_D}$*).*

To overcome transit time broadening effect and to prevent the attenuation of probe and generated FWM signal fields in the medium a buffer gas is added to the system. Fig.5.3(ii) shows buffer gas effect on gain factor (nonlinear generation β) and absorption (loss coefficient α) of probe and FWM signal for pump–coupler fields, $\Omega_c/\gamma_D = \Omega_m/\gamma_D = 0.02$, and 0.03. Since other parameters appearing in the expressions Eq.(5.17) for α_e , β_e (and α_p , β_p) are the same, we find that α (= $\alpha_p = \alpha_e$) and β (= $\beta_p = \beta_e$) are nearly equal when $\Omega_c/\gamma_D = \Omega_m/\gamma_D = 0.03$ in presence of buffer gas. Thus it is expected that a balance (steady-state) will be established in the situation where the propagation loss determined by absorption coefficient α is compensated for by the effective (nonlinear) gain given by β in the medium. Whereas Fig.5.3 (i) shows that the in absence of buffer gas the balance will not be established, as the propagation loss determined by absorption coefficient α do not compensate (nonlinear) gain β in the medium.

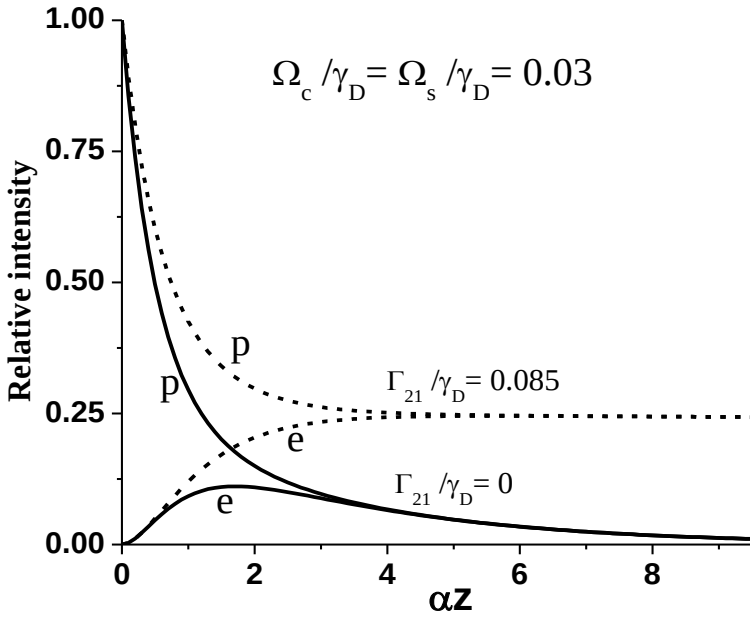

Fig.5.4: *Variation of the relative intensity of the probe (curves **p**) and generated signal (curves **e**) as a function of the dimensionless parameter **αz** where **z** is the propagation distance and*

the value of the absorption coefficient $\boldsymbol{\alpha}$ *is evaluated at line center (on-resonance). The pump and coupler Rabi frequencies are,* $\Omega_c/\gamma_D = \Omega_s/\gamma_D = 0.03$. *For this value of driving field the probe and signal propagate unattenuated through the vapor with matched intensities for* $\boldsymbol{\alpha z \geq 5}$ *in the presence of buffer gas,* $\Gamma_{21} = 0.085\gamma_D$ *(dashed curves) whereas both the fields are attenuated in the absence of the buffer gas,* $\Gamma_{21} = 0$ *(solid curves). The buffer gas collisional dephasing rate is,* $\gamma_p = 2.7\Gamma_{21}$.

We now illustrate how this competition between the absorption α and nonlinear gain β affects the propagation characteristics of the probe and signal fields by plotting in Fig.5.4 the relative signal (probe) intensity $|\frac{\varepsilon_e(z)}{\varepsilon_p(0)}|^2$ ($|\frac{\varepsilon_p(z)}{\varepsilon_p(0)}|^2$) (using Eq.(5.18)) as a function of αz . The absorption coefficient-length product, αz can be varied either by changing the atomic density or length of the vapor cell.

We observe from Fig 5.4 that initially (at the input interface) the probe has maximum value and the signal field is zero. As the fields propagate further in the medium, generation of the signal field via FWM takes place due to which the signal intensity grows at the expense of the probe fields so that the intensity of the probe decreases. However when the generated signal becomes sufficiently strong and comparable to the probe field strength, the reverse process also can occur in which the signal, coupler and the pump via FWM regenerate the probe field. In the course of propagation in the vapor, eventually these two process must reach a balance i.e., a matching of intensity (or amplitude) of the probe and the signal fields should occur. However as seen in Fig.5.2, finite absorption loss (α) causes attenuation of the fields as they propagate in the vapor. It is observed from Fig.5.4 that in the absence of the buffer gas (solid curves p and e) matching of the probe and signal field intensities does not occur and the fields are eventually attenuated for $\boldsymbol{\alpha z \geq 8}$.

On the other hand in the presence of a buffer gas (dashed curves p and e) we find that beyond a certain propagation distance characterized by the value of $\boldsymbol{\alpha z \geq 5}$ **,** the generated signal and probe intensities (or amplitudes) are matched and the probe and signal fields propagate through the medium without further dissipation. As seen in Fig. 5.3 the condition $\alpha = \beta$ is satisfied at these values of coupler and punp field Rabi frequencies $\Omega_c/\gamma_D = \Omega_s/\gamma_D = 0.03$. Hence

the propagation loss α is compensated for by the nonlinear gain β and the probe and signal fields propagate without any loss in the vapor. We further note that under these matched and no loss conditions the probe and signal amplitude are, $\varepsilon_e(z)/\varepsilon_p(0) = \varepsilon_p(z)/\varepsilon_p(0) = 1/2$ i.e., the signal (and probe) intensity relative to the incident probe intensity is 25% each. The mismatch and attenuation of the signal and probe in the absence of the buffer gas is due to fact that absorption loss α caused by transit time broadening is much larger than the nonlinear gain β as observed in Fig 5.3.

5.5 ***Conclusion:***

To summarize, we have studied the buffer gas collisions effect on EIT associated FWM signal generation in an inhomogeneous (Doppler) broadened medium. A strong collision model is considered for velocity changing collisions. Furthermore, under optimal condition of FWM generation the maximum transparency achieved for either the probe or the generated FWM field is only 50% of the one obtains in the case of an isolated 3 level (Λ) system. The forward FWM scheme is more efficient in a inhomogeous (Doppler) broadened medium than cooled (homogenous medium) system of Ref [16] provided taking care of major effect of transit time broadening and consideration of buffer gas collisions. The maximum FWM efficiency is obtained with matched coupling fields and buffer gas collisions; at higher propagation lengths the conversion efficiency reaches nearly 25%. Our results are consisted with the earlier experimental studies of Ref [16] (homogenous medium) in forward four mixing scheme.

5.5 *References*

1. S. E. Harris, J. E. Field, and A. Imamoglu, Phys. Rev. Lett. **64**, 1107 (1990).
2. P. R. Hemmer *et al.*, Opt. Lett. **20**, 982 (1995);
   M. Jain, H. Xia, G.Y. Yin, A. J . Merriam and S. E. Harris, Phys. Rev. Lett. **77**, 4326 (1996);
   Y. Q. Li and M. Xiao, Opt. Lett. **21**, 1064 (1996).
3. A. S. Zibrov, M. D. Lukin, and M. O. Scully, Phys. Rev. Lett. **83**, 4049 (1999).
4. A. J. Merriam, S. J. Sharpe, *el.* Phys. Rev. Lett. **84**, 5308(2000).
5. L. Deng M. G. Payne and W. R. Garrett, Phys. Rev. A **63**, 043811(2001);
   L. Deng and M. G. Payne , Phys. Rev. A **65**, 063806 (2002).
6. E. A. Korsunsky, T. Halfmann, J. P. Marangos and K. Bergmann, Eur. Phys. J. D **23**, 167 (2003).
7. M. Jain, H. Xia, G.Y. Yin, A. J. Merriam and S. E. Harries Phys. Rev. Lett. **77**, 4326 (1996);
Y. Q. Li and M. Xiao, Opt. Lett. **21**, 1064 (1996).
8. S. E. Harris and L.V. Hau, Phys. Rev. Lett. **82**, 4611 (1999).
9. M. D. Lukin and A. Imamoglu, Nature **413**, 273 (2001)
10. H. Schmid and Imamoglu, Opt. Lett. **21**, 1936 (1996)
11. S.E. Harris and Y. Yamamoto, Phys. Rev. Lett **81**, 3611 (1998)
12. M. D. Lukin, P. R. Hemmer, M. Loffler and M. O. Scully, Phys. Rev. Lett. **81**, 2627 (1998).
13. A. K Popov, A. S. Bayev, T. F. George, V. M. Shalaev, Eur. Phys. J. D **1**, 1(2000);
    R, Fleischhaker and J. Evers, Phys. Rev. A **77**, 043805 (2008).
14. E. A. Korsunsky, D. V. Kosachiov, Phys. Rev. A **60**, 4996 (1999).
15. Y. Wu, and X. Yang, Phys. Rev. A **70**, 053818 (2004);
    Y. Wu, and X. Yang, Phys. Rev. B **76**, 054425 (2007).
16. H. Kang, G. Hernandez, and Y. F. Zhu, Phys. Rev. A **70**, 061804(R) (2004);
    H. Kang, G Hernandez, and Y. F. Zhu, J. Mod. Opt. **52**, 2391 (2005);
    H. Kang, G Hernandez, J.P. Zhang and Y. F. Zhu, J. Opt. Soc. Am. B. **23**, 4 (2006).
17. R. M. Camacho, P. K. Vudyasetu and J. C. Howell, Nature **3**, 103 (2009).
18. G. Wang, Y. Xue, J. H. Wu, Z. H. Kang, Y. Jiang, S. S. Liu and J. Y. Gao, Opt. Lett. **35**, 3778 (2010).
19. E. Pfleghaar, J. Wurster, and S. I. Kanorsky, and A. Weis, Opt. Commun. 99, 303 (1993).

20. S. Brandt, A. Nagel, R. Wynands, and D. Meschede, Phys. Rev. A 56, R1063 (1997);
M. Erhard and H. Helm, Phys. Rev. A 63, 043813 (2001

21. C. Y. Ye and A. S. Zibrov, Phys. Rev. A **65**, 023806 (2002);
P. R. S. Carvalho, L. E. E. de Araujo, and J. W. R. Tabosa, Phys. Rev. A **70**, 063818 (2004);
C. Bolkart, D. Rostohar, and M. Weitz, Phys. Rev. A **71**, 043816 (2005).

22. M. Shuker, O. Firstenberg, Y. Sagi, A. Ben-kish, N. Davidson and A. Ron, Phys. Rev. A 78, 063818 (2008), Figure 7.

Chapter 6

Conclusions:

The phenomena of electromagnetically induced transparency (EIT), slow light in various Doppler broadened three-level (ladder, lambda and Vee) systems and EIT assisted process of four wave mixing (FWM) in a Doppler broadened four-level double lambda system were studied. Residual Doppler broadening arising from thermal motion of atoms in vapor causes broadening of EIT (absorption) and dispersion resonances. Theoretical models incorporating the velocity changing (and dephasing) collisional aspects of a buffer gas were developed to examine narrowing of various types of (residual) Doppler broadening affecting the EIT resonance. The highlight of the present work is the incorporation of transit time (or time of flight) broadening of EIT resonances in various multilevel systems. The origin of this broadening is in thermal motion of atoms across the finite intensity spread of the probe and pump lasers in transverse direction (to the direction of propagation, usually taken as z direction). Most studies till date only consider the residual broadening arising due to longitudinal velocity component v_z or a small contribution from a single transverse component v_x arising due a small angular deviation of pump and probe beams. The more general theoretical models developed here should be applicable to real experimental situation since most experiments on EIT (with or without buffer gas) are conducted using narrow diameter (of typically 2 mm) laser beams. Hence experimental data is used in most cases for numerical computations in order to make comparison with experiments. On the other hand our study of buffer gas effects on EIT in Doppler broadened three level ladder (Chapter 2) has served as a basis for a recent experimental study which confirmed our theoretical predictions.

In Chapter 2 and Chapter 4 we study EIT in Doppler broadened three level ladder (Ξ) or cascade and V systems considering thermal motion of atoms (with velocity component v_z) along the z-direction of propagation of the pump and probe waves. Chapter 2 deals with the theory of EIT and slow light in a Doppler broadened three-level ladder (Ξ) system incorporating residual Doppler broadening (arising due to pump-probe wave vector mismatch along velocity component v_z direction) and velocity-changing and dephasing collision effects of a buffer gas. Both regimes of wave-vector mismatch occurring when either the probe frequency is higher than

that of the (strong) pump field or vice versa are considered. It is found that the velocity-changing collisions in general cause narrowing of EIT resonance linewidths which, in a particular wave-vector mismatch regime, can lead to large transparency and slow light generation at relatively low control field intensities. Large collisional dephasing of two-photon coherence in a ladder system, however, tends to mask these effects. Finally we conclude that with the additions of buffer gas to the ladder system EIT resonances are broadened.

The EIT scheme in a V-type atomic system described in Chapter 4 differs from other three level lambda (Λ), ladder system (Ξ) in that the strong pump laser is connected to ground level. For this reason although the reduction of probe absorption (dip) has been experimentally reported in V-system, a certain ambiguity remains as to whether these results are consequences of EIT or a similar phenomenon known as saturation and Autler-Townes (AT) splitting. We investigate the possibility of EIT phenomenon in a three level V-type atomic system by considering both homogenous and inhomogeneously (Doppler) broadened media. The phenomenon of saturation and AT splitting has features that look very similar to those of EIT observed in the probe absorption. We demonstrate that EIT occurs in an inhomogeneous Doppler broadened medium, whereas it is not possible to observe EIT in a homogenous medium due to large dephasing (of order of spontaneous decay rate) of two photon coherence. Therefore reduced absorption of probe in a homogenous medium is mainly due to saturation and Autler-Towns splitting (AT) effect.

We address again in Chapter 3 and 5 EIT, slow light and four wave mixing (FWM) process in Doppler broadened three level lambda (Λ) and four level double lambda (Λ) systems considering three-dimensional thermal motion of atoms in the medium. Thus theoretical models in these chapters also include the transit time (or time of flight) broadening of EIT resonances arising from the transverse thermal velocities which cause atoms to move out of the finite interaction region formed by overlap of the intensities of the probe and pump lasers in transverse direction (to the direction of propagation). Most studies till date do not incorporate the transit time broadening and are restricted to residual broadening arising due to longitudinal velocity component v_z or a small contribution from a single transverse component v_x arising due to thermal motion of atoms in one direction.

In chapter 3 it is observed that in a Doppler broadened (hot vapor) medium the transit time (or time of flight) broadening affect both the width and the absorption dip of the EIT resonance. Also presented is an equation for pulse propagation in which we point out the complexity caused by the dependence of the linear susceptibility on transverse wave vector. We first, show that with increasing buffer gas buffer gas pressure p, absorption at the (collisionally shifted) line center decreases and second, the width of the EIT resonance are narrowed. Huge reduction of the group velocity also occurs under these conditions at much lower pump field intensities. The numerical and theoretical calculations which clearly demonstrate line narrowing, power broadening aspects of EIT resonances and the feasibility of attaining very slow group velocities in presence of a buffer gas are found to be in good qualitative and to some extent quantitative agreement with existing experiments of EIT and slow light propagation in hot vapors in buffer gas environment.

We further extend in chapter 5, our studies of buffer gas effect to EIT and four wave mixing (FWM) in a Doppler broadened double lambda (Λ) system. EIT of the probe and generated FWM signal and there by the generation efficiency are found to be adversely affected by the transit time broadening. The velocity changing collisions by buffer gas atoms entirely eliminate the transit time broadening and thus increase the transparency of probe and generated signals as well the forward FWM signal generation efficiency. The evolution and growth of the generated FWM signal intensity is also destroyed by the transit time broadening. We however show that, in presence of velocity changing collisions the signal intensity quickly grows to a large value even for very small values of the coupler and pump fields. The maximum FWM efficiency is obtained with matched coupling fields and buffer gas collisions; at higher propagation lengths the conversion efficiency reaches nearly 25%. The results for large buffer gas pressures almost analogous to those observed for the stationary atom ($v = 0$) case conducted in more complicated or expensive setups like cold atomic ensembles.

List of Publications:

1. M. Anil Kumar and Suneel Singh, “Electromagnetically induced transparency and slow light in three-level ladder systems: Effect of velocity-changing and dephasing collisions”, Phys. Rev. A 79, 063821(2009).
2. M. Anil Kumar and Suneel Singh, “Electromagnetically induced transparency in a V-type atomic system: Homogeneous Vs Inhomogeneous broadening”, AIP Conf. Proc. 1391, pp. 173-175(2011).